DERIVATION OF CENTURY-BASED WAVE CLIMATE AND EXTREME WAVE ANALYSIS ALONG TURKISH COASTS

A Thesis Submitted to
the Graduate School of Engineering and Sciences of
İzmir Institute of Technology
in Partial Fulfillment of the Requirements for the Degree of

MASTER OF SCIENCE

in Civil Engineering

by
Ahmet Rıza TURGUT

July 2019
İZMİR

We approve the thesis of **Ahmet Rıza TURGUT**

Examining Committee Members:

Assist. Prof. Dr. Bergüzar ÖZBAHÇECİ
Civil Engineering, İzmir Institute of Technology

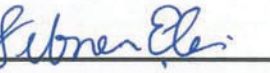

Prof. Dr. Şebnem ELÇİ
Civil Engineering, İzmir Institute of Technology

Prof. Dr. Yalçın ARISOY
Civil Engineering, Dokuz Eylül University

10 July 2019

Assist. Prof. Dr. Bergüzar ÖZBAHÇECİ
Supervisor, Civil Engineering
İzmir Institute of Technology

Prof. Dr. Şebnem ELÇİ
Head of the Department of
Civil Engineering

Prof. Dr. Aysun SOFUOĞLU
Dean of the Graduate School of
Engineering and Sciences

ACKNOWLEDGMENTS

I would like to thank my dear advisor Assist. Prof. Dr. Bergüzar Özbahçeci who guided and supported me with her valuable knowledge and experiences during my thesis. I could not have studied with better advisor.

Besides my advisor, I would like to thank Dr. Saleh Abdalla from ECMWF for his guidance.

This study was funded by the Scientific and Technological Research Council of Turkey, TUBITAK under 117M968.

My thanks also go to the European Centre for Medium-Range Weather Forecasts (ECMWF) for providing ERA-20C and CERA-20C wave data, to Prof. Dr. Erdal Özhan who was the Director of the NATO TU-WAVES for providing the buoy data at Hopa, Sinop, Bozcaada, Dalaman and Alanya, to the Turkish State Meteorological Organization for providing the buoy data at Bosphorus, Silivri, Çanakkale, Antalya and Silifke.

I also would like to thank to Ahmet Bozoklu for his help through TUBITAK Project.

Last but not the least, I would like to thank my family: my parents Esen Turgut, Tayfun Turgut and my lovely twin Çiğdem Turgut for supporting me throughout my life.

ABSTRACT

DERIVATION OF CENTURY-BASED WAVE CLIMATE AND EXTREME WAVE ANALYSIS ALONG TURKISH COASTS

Reliable and long-term wave data are essential for the design of almost all coastal and marine structures. In this study, the wave climate along the Turkish coasts was derived based on a century long data of European Centre for Medium-Range Weather Forecasts. For this purpose, firstly, the data set was calibrated and verified by using satellite and in-situ measurements. Then the design waves corresponding to different return periods were determined by extreme statistics. Therefore, a new and reliable design wave height data along the Turkish coasts have been provided for the designers and applicants. Results were compared with Wind and Deep Water Wave Atlas Along the Turkish Coasts (Ozhan and Abdalla, 2002). The comparison results indicate that the design wave heights provided by the Atlas are higher than the current study, especially in the Aegean Sea. Moreover, the effect of theoretical distribution function and the data number were investigated on the design wave height. Design wave heights were re-calculated by best fitting distribution function and it was shown that distribution function may affect the design wave height. It was also concluded that when the wave data used in extreme value analysis was less than 30 years, the error increased in the estimation of the design wave height with both 50 and 100 years return periods. Besides, by using calibrated and the verified century-long wave climate data it was shown that there was an increasing trend in the annual mean and maximum wave heights along the Turkish coasts.

ÖZET

TÜRKİYE KIYILARI İÇİN DALGA İKLİMİNİN ELDE EDİLMESİ VE EKSTREM DALGA ANALİZİ

Deniz yapılarının güvenli ve ekonomik tasarımı, en önemli yüklerden olan dalga tasarım verilerinin doğru belirlenmesine bağlıdır. Bunun için uzun dönemli dalga iklimi çalışması gereklidir. Bu çalışmada Avrupa Orta Ölçekli Hava Tahmin Ajansı (ECMWF) tarafından üretilen 110 yıllık dalga verisi uydu verileri ve yerinde ölçüm verileriyle kalibre edilmiş ve doğrulaması yapılmış ve Türkiye kıyıları için kullanılabilir hale getirilmiştir. Böylece ilk kez asırlık dalga iklimi ortaya çıkarılmıştır. Bu çalışma ile aynı zamanda ülkemizin Karadeniz, Akdeniz ve Ege kıyılarını temsil edecek noktalarda çeşitli yinelenme dönemine sahip ekstrem dalgalar belirlenmiş, tasarımcı ve uygulamacılar için tasarım dalgasının seçilmesinde güncellenmiş ve güvenilir bir kaynak sağlanmıştır. Sonuçlar NATO TU Waves Projesi kapsamında Özhan ve Abdalla (2002) tarafından hazırlanan Rüzgâr ve Derin Deniz Dalga Atlası ile karşılaştırılmış, bu çalışmada bulunan tasarım dalgalarının özellikle Ege Denizinde daha düşük olduğu görülmüştür. Çalışma kapsamında, kısa dönemli veriden dolayı şimdiye kadar ekstrem değerleri elde etmek için kullanılan en büyük değer istatistiği yönteminin sonuca etkisi araştırılmıştır. Dağılım modeli ve veri sayısının tasarım değerlerini etkilediği görülmüştür. Bu çalışma ile Türkiye kıyılarında ilk kez yüzyılı aşan bir süreçte ve bütünleşik olarak ortalama ve en yüksek dalga yüksekliğinde bir değişim eğiliminin olup olmadığı incelenmiştir. Sonuçlar kıyılarımızın önemli bir kısmında yıllık maksimum ve ortalama dalgada artma eğilimi olduğunu göstermiştir.

TABLE OF CONTENTS

LIST OF FIGURES

Figure **Page**

Figure **Page**

Figure **Page**

LIST OF TABLES

Table **Page**

CHAPTER 1

INTRODUCTION

1.1. Research Background and Problem Statement

Reliable wave data affecting a coastal region is very essential for the design of coastal structures, port planning, design of offshore wind turbines and wave energy studies. Especially for the design of the coastal structures, not only reliable but also long-term data are necessary. The sources of wave data can be divided into three main categories (Abdalla, 2013).

1. In-situ measurement
2. Remotely sensed observations
3. Numerical model estimates

The most reliable way to obtain wind and wave data is in situ measurement. However, there are lots of practical problems associated with wave measurements and their expense. Project based measurement campaigns ended between 3 months to 4 years were carried in Turkey. Therefore, those short period measurement data are generally used for verification purposes. Wave and wind data are also obtained from satellites due to the developments in space technology. Radar Altimeter (RA), Synthetic Aperture Radar (SAR) and Scatterometer are the instruments used in the satellite can provide wave height and sea surface wind speed data. Such data source has good global coverage and it is usually very reliable (Abdalla and Yilmaz, 2015). Satellites are usually designed to serve for a few years so provided data are also not enough for long term climate studies. Another source for long term wave data is numerical data derived from atmospheric and wave models. Various meteorological agencies in the world produce the models to forecast and the hindcast the wave data. One of these agencies is European Centre for

Medium-Range Weather Forecasts (ECMWF). ECMWF has been producing wave parameters for the last few decades. The ECMWF improves weather, wind and wave forecasts for operational purposes day by day with high quality models (Aarnes, Abdalla, Bidlot, & Breivik, 2015). However, it is not possible to use these operational data in wave climate studies and calculation of design wave height due to estimation errors in the past and regular changes done for the development in the prediction models (Poli et al., 2015). For this reason, the use of re-analysis model results for historical data from various meteorological agencies in the world is common. In re-analysis, modeling and measurement results are coupled. Generally, it is possible to obtain 40 years data from all these agencies (since 1979). The longest data were produced by Japan Meteorological Agency, and it contains 55 years data (Poli et al., 2016). ECMWF with the help of several international organizations started a new reanalysis Project (the ERA-CLIM Project) covering the last century (1900-2010). The analysis data called as ERA-20C assimilates surface pressure and marine wind observations. It is available at 3-hour time increments. In order to produce consistent reanalyses of the climate system, reaching back in time as far as possible given the available instrumental record. In this context, firstly, ECMWF has produced the uncoupled atmospheric reanalysis ERA-20C, which covers the period January 1901 to December 2010. ERA-20C assimilates only conventional observations of surface pressure and marine wind, obtained from well-established climate data collections. Then, as a second phase, ECMWF has completed the production of a new global 20th-century reanalysis which aims to reconstruct the past weather and climate of the Earth system including the atmosphere, ocean, land, waves and sea ice. This coupled climate reanalysis, called CERA-20C, is part of the EU-funded ERA-CLIM2 project. Both data sets are available at 3-hour time increments. Literature study shows that new century long data have started to become an attractive source for the researchers dealing with climate studies. Verification studies indicate that ERA-20C and CERA-20C may underestimate the wave height but the data is consistent and suitable to use in climate studies (Abdalla, 2013, Abdalla and Yılmaz,2015, Dafka et al., 2016, Patra and Bhaskaran,2016, Dada et al.(2016) and Kumar et al.,2016). However, ERA-20C, CERA-20C or any century long data has not been used to determine the wave climate along the Turkish coasts, yet.

1.2. Aim, Objectives and Scope of the Study

This study aims to derive the wave climate along the Turkish coasts based on a century long data of ECMWF. For this purpose, first of all, the wave height and the period data set was calibrated and verified using satellite and wave measurements together with a wave model data. Satellite missions with radar altimeter (Envisat, Jason 1, Jason2, ERS1, ERS2 and Topex), the newest dataset ERA5 of ECMWF and in-situ measurements of the State Meteorological Organization of Turkey were used for calibration. In-situ measurements within the scope of NATO TU-WAVES project were used for verification. The wave direction analysis was kept out of the scope of this study due to data lack for the calibration and verification.

Then the design wave heights corresponding to various return periods were determined along the Turkish coasts by extreme value statistics. Moreover, the effect of theoretical distribution functions and the data number on the design wave height were investigated. Gumbel, Fisher Tippet II, Log-normal and Weibull distribution function were used to find the best fitting distribution in the extreme value analysis.

Examination of a possible change in wave climate along the Turkish coasts under the scope of new century-long climate re-analyses data is another objective of the study.

1.3. The Structure of the Thesis

The structure of this thesis is as follows. A review of the literature survey is provided in Chapter 2. Data-used, calibration and verification studies are elaborated in Chapter 3, this is followed by the extreme wave statistics and the calculation of design wave heights described in Chapter 4. In Chapter 5, wave climate change along the Turkish coasts is analyzed. This thesis concludes with a discussion of the presented study in Chapter 6.

CHAPTER 2

LITERATURE REVIEW

The most important step in the design of the coastal structures is the calculating of the design wave height. The design wave is a wave that is expected to be exceeded once in a long period such as 30, 50, 100, 200 years. This period is called the return period. Therefore, to obtain long and reliable wave climate data is essential. However, since the duration of wave climate data is generally shorter than the return period the design wave height is calculated by the extreme wave statistics analysis. For this purpose, the long term climate data (generally 10-40 years) are obtained for the study region; the annual maximum data or peak values higher than a threshold wave height are determined; the cumulative probability distributions of the data are obtained; fitted to some theoretical distribution function, extrapolation is performed to estimate the design wave height corresponding to the low probability of occurrence that is once in a given return period. Although the result may contain a certain error due to assumptions and the methods, this is the only method to apply since the wave data are limited. Even in this method, at least N/3 years wave data are necessary to determine the design wave with N-year return period.

The most reliable way to obtain wave data is in-situ wave measurement. However, the continuous measurements along the coasts of Turkey began in 2015. The continuous measurement campaigns started in Istanbul, Antalya, Çanakkale, Mersin and Samsun have been carried out by the State Meteorological Organization of Turkey. In addition, project-based measurements are available. These are Hopa, Sinop, Tekirdağ, Bozcaada, Dalaman and Alanya measurements within the scope of NATO TU-WAVES project (Özhan & Abdalla, 1999). Filyos, Çandarlı and Karaburun measurements that were conducted by Ministry of Transport (Bilyay, Ozbahceci, & Yalciner, 2011) and İstanbul – Karaburun measurements that were done by Yıldız Technical University (Ar Güner, Yüksel, & Özkan Çevik, 2013). Unfortunately, the measurements were ended in 3 months to 4 years. These measurement data are generally used for verification purposes.

The wave data can be obtained from satellites due to the developments in space technology. The use of satellite observations for climate studies began with the acquisition of this data for the last 10-20 years (Young, Zieger, & Babanin, 2011). There are lots of satellite tools related with wave studies. Especially, Scatterometer, Synthetic Aperture Radar (SAR) and Radar Altimeter (RA) have a great importance. Radar Altimeter (RA) is an active microwave device that is the lowest level.??? This device transmits a signal and analyze the signal that is reflected from the sea surface. Travel duration, shape and magnitude of returned signal are used to suggest Hs. Generally, RA takes 20 records in one second (20 Hz). Mean of these 20 values is used to produce one value in one second. The satellite missions with the radar altimeter and their measurement periods are given in Figure 1.

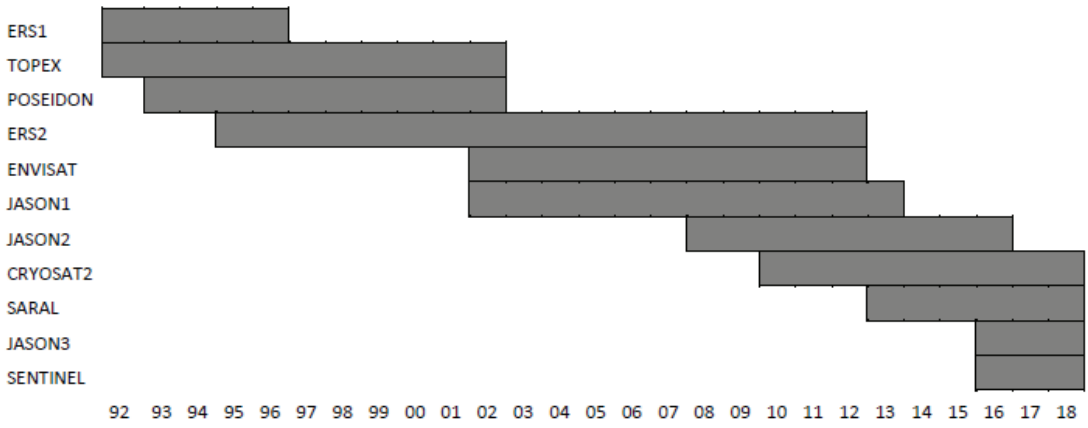

Figure 1. Satellite missions with RA measurement and their measurement period

RA provides data in a certain track, so it cannot provide a globally covered data as numerical models do. Instead of that, RA measurements follow a track like a mesh as it is shown in Figure 2. Repeat cycle defines a time period that is necessary to measure the same area again. Jason satellite family (TOPEX / Poseidon / Jason 1 and Jason 2) have 10 days repeat cycle and they follow the route as it is shown in Figure 2-a (track space 250 km). In addition, ENVISAT satellite family (SARAL, ERS-1, ERS-2 and ENVISAT) have 35 days repeat cycle and they follow the root in Figure 2-b (track space 70 km)(Abdalla, 2013).

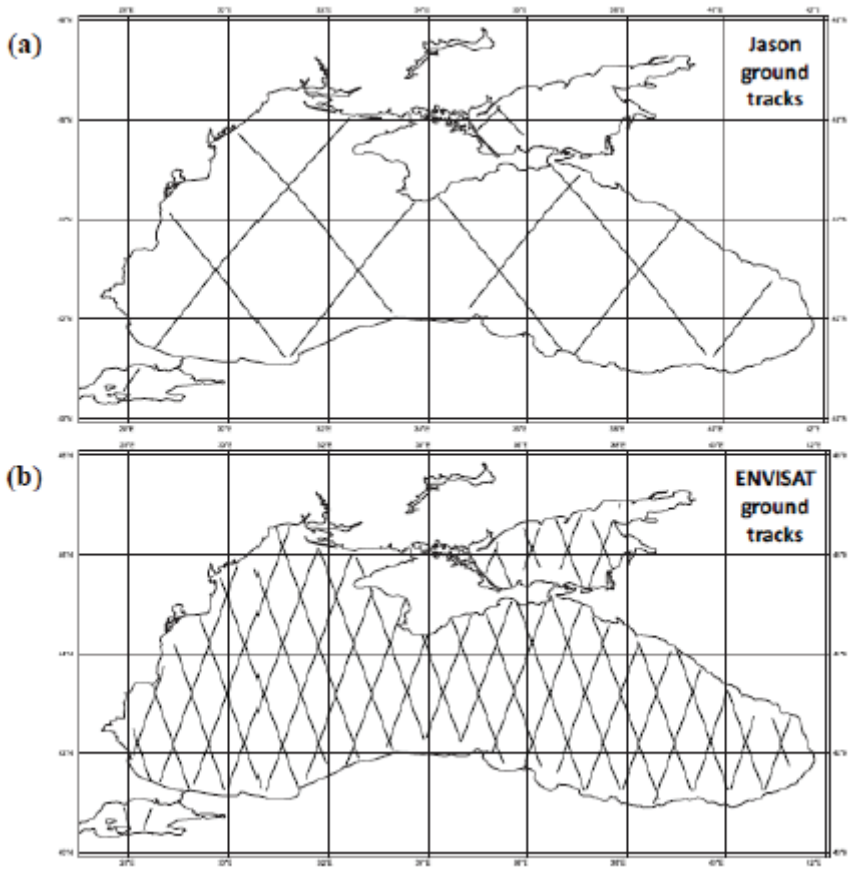

Figure 2. Ground Tracks of Jason Satellite Family (a) and ENVISAT Satellite Family (b) (Abdalla, 2013)

Radar Altimeter (RA), Synthetic Aperture Radar (SAR) and Scatterometer placed on satellites can be used to obtain wind and wave data on the sea surface. These global data that are generally quite reliable cannot be used as a long – term data because of that mission of satellite is usually in use between 3 – 7 years.

Thus, there are two ways for a designer who wants to find a design wave height along the Turkish Coasts.

1. Wind and Deep-Water Wave Atlas of the Turkish Coast

Wind and Deep-Water Wave Atlas Along the Turkish Coasts was prepared within the scope of NATO TU-Waves Project (Özhan & Abdalla, 2002). The Atlas has been an important guidebook that provides the valuable information about wind and deep-water wave climate for Turkish Coasts. The Atlas is also an important resource for selecting the design wave height by giving extreme wave statistics of the annual maximum significant wave heights. While the annual maximum significant wave height data of 20 years were

used for Black Sea those of 17 years were used for Aegean Sea and Mediterranean Sea. Synoptic maps provided by the General Directorate of Meteorology were used to obtain the maximum annual significant wave height data . Although the number of data may be sufficient to predict a design wave with up to 50-year return period, reliability for longer return periods is questionable. Furthermore, when we consider the improvements in models and data in the last 20 years, it may be necessary to produce a new version of the Atlas .

2. Wave Modeling

Waves can be estimated by using wind and bathymetry data with the help of numerical wave models. Land based wind measurement campaigns have been organized at many points by the Turkish State Meteorological Organization. Approximately 40-50 years of data are available. However, those land-based measurements may be questionable to use to predict waves on the sea because of some stations are far away from the coasts and have been covered with buildings and trees as time passed. For this reason, the production of re-analysis model data for hindcasting purposes from various meteorological agencies in the world is becoming widespread. In the re-analysis model, modeling and measurement results are blended. One of these agencies producing re-analysis data is the ECMWF (European Centre for Medium-Range Weather Forecasts). The ECMWF improves weather, wind and wave forecasts for operational purposes day by day with high quality models (Aarnes et al., 2015). It is not possible to use these operational data in wave climate studies and calculation of design wave height due to estimation errors in the past and regular changes are done for development in the prediction models (Poli et al., 2015). A database is called ERA-INTERIM was produced to find the hindcast data by using the re-analysis method (Dee et al., 2011). ERA-INTERIM has wind and wave data from 1979 until today. Data that are obtained from ERA-INTERIM are in 6 hours periods. Another data source is the CFSR-Climate Forecast System Reanalysis data that was published by the National Centers for Environmental Prediction NCEP. Another wind and wave re-analysis data also were published by the Japanese Meteorological Agency (JMA) and NASA. Generally, it is possible to obtain 40 years data from all these agencies (since 1979). The longest data were produced by JMA, and it contains 55 years data (Poli et al., 2016).

The first 20th century re-analysis data set 20CR was generated to obtain century-based data by NOAA (National Oceanic and Atmospheric Administration) (Compo et al., 2011). In NOAA-20CR only surface pressure observations are used. Data can be obtained since 1871. A new re-analysis data set that is called as ERA-20C was generated by ECMWF in scope of ERA-CLIM Project. It is possible to obtain wave data from 1901 to 2010. The ERA-20C has daily, invariant and monthly mean data that resolution is approximately 165 km for the wave model. Unlike ERA-Interim and NOAA-20CR, it is aimed to generate a homogeneous and consistent data set by using surface pressure measurements as well as wind measurements on the sea. The time interval between the data was also reduced from 6 hours to 3 hours. However, the resolution of data is lower than ERA-Interim. The grid spaces 110 km at ERA-Interim and 165km at ERA-20C. However, the resolution is higher than NOAA-20CR in both horizontal and vertical. Dada et al., (2016) say that ERA-20C has a higher performance than NOAA-20CR. At the beginning of this study, ECMWF presented another climate data: CERA-20C. CERA-20C is the final version of century-based reanalysis data sets that are developed by ECMWF. It consists of 110 years reanalysis model data that are in three-hour steps from 1901 to 2010. The CERA–20C has 165 km resolution for wave model same as ERA-20C. Coupled climate reanalysis, CERA-20C is part of the EU-funded ERA-CLIM2 project, which builds on the ERA-CLIM project. aims to reconstruct the past weather and climate of the Earth system including the atmosphere, ocean, land, waves and sea ice. The latter produced ERA-20C, a 20th-century reanalysis for the atmosphere, land and waves only (Poli et al., 2016).

(Abdalla, 2013) compared ERA-20C and ERA-Interim with satellite data for Black Sea for whole 2006. Comparison results show that ERA-Interim is generally more accurate than ERA-20C. However, the results of ERA-20C were very close to ERA-Interim and satellite data from 1979 until today. Abdalla & Yilmaz (2015) investigated the suitability of ERA-20C data for wind and wave climate studies in Black Sea and they say that ERA-20C can be suitable data set for wave climate and design wave studies when length and consistency are considered. (Patra & Bhaskaran, 2017) compared satellite RA (1992 – 2012), ERA-Interim (1992 – 2012) and ERA-20C (1992 – 2012) wave data with WAVEWATCH III model data in Bay of Bengal. Results of their study showed that ERA-20C had lower significant wave height despite high correlation, and ERA-20C had better wave period result than NOAA-20R. Dada et al. (2016) estimated wave data by using

ERA-20C wind data in SWAN model, then they used TOPEX/POSEIDON RA data (2008 – 2010) for verification. Significant wave heights that were calculated by SWAN model were smaller than the satellite data especially in case of Hs<0.5m and these wave heights were ignored in the calibration. Kumar, Min, Weller, Lee, & Wang (2016) preferred ERA-Interim (1980 – 2014) and ERA-20C (1952 – 2010) data sets to investigate the effect of climate change on the extreme wave height in ocean. In the comparison, both data sets were generally consistent, and ERA-Interim had a higher result than ERA-20C. They decided that difference between two data sets was based on data sets' time period.

There is a commercial software that was developed by Prof. Dr. Lale Balas to determine the wave climate and the design waves for Turkish coasts. Its name is HYDROTAM-3D and it is allowed to use freely for research purposes by DLTM R&D Company (Balas, n.d.). In the program, the user only needs to select the area to work on the map. The program gives long term and the extreme wave statistics by using the fetch distances calculated by the program, and wind data of the nearest station. The option to use ECMWF wind data is also being developed. In Turkey, wave climate studies have also been done to derive wave energy potential. Aydoğan, Ayat, & Yüksel (2013) showed that wave energy decreased from west to east in Black Sea by using ECMWF wind data of Black Sea (1996 – 2009). Akpinar & Kömürcü (2013) also studied wave energy potential with 15 years ERA-Interim wind data (1995 – 2009) for Black Sea by using SWAN. Ayat (2013) did similar wave energy study for the Aegean Sea and the East Mediterranean. In their study, 15 years ECMWF wind data (1992 – 2009) were used and wave results that were obtained in the study were compared with the in-situ measurements. Akpınar & Bingölbali (2016) investigated the change in the wave height and the wind speed in Black Sea with 31 years ERA-Interim wind data. This was the longest period data used for the study in Turkey. Moreover, Akpinar & Ponce de León, (2016) modeled a storm occurred in 2003 by using re-analysis wind data run by SWAN wave model. Then, the model result was compared with satellite and in-situ measurement data. The comparison results show that more accurate results were obtained when ECMWF wind data were used. Kutupoğlu, Akpınar, Bingölbali, & Çakmak, (2018) calculated the extreme wave height with 100 years return period in Marmara Sea as approximately 3 m by using SWAN wave model run with CFSR wind data.

Turkey can be affected from sea level, wave and storm surge changes because of that it is surrounded by water on three sides. Although seaside cities are lower than 5%

of all cities of Turkey, approximately half of population of Turkey live in these cities (Karaca & Nicholls, 2008). There are more than 400 major coastal structures in the coasts of Turkey. These are not only pier but also breakwater that consists of several pieces. New ports and marinas are planned to construct when the increase in international cargo volume, tourism and fishing activities are considered (*Ulaştırma Kıyı Yapıları Master Plan Çalışması*, 2010). Therefore, possible long-term changes in wind and wave climate are important as much as sea level increase in Turkish coasts. Studies for climate changes in coastal areas of Turkey, have mostly done on rising of sea level and vulnerability. EROL, (1990) and (1991) investigated rising of sea level in Turkish coasts and their effect. He considered property and geomorphology of coasts in his studies. Karaca & Nicholls, (2008) did not make an inference about rising of sea level because of short term measurement in Aegean Sea and Mediterranean. They said that rising of sea level was 1 – 3 mm/year in Black Sea. Alpar, (2009) stated that rising of sea level 8.8, 6.2, 4.6 and 7.9 mm for Erdek, Menteş, Bodrum and Antalya, respectively. Özyurt & Ergin(2009) investigated effect of sea level in coastal by considering geologic properties of land. Then, this effect was modelled for Amasra, Göcek and Göksu. According to model results, delta of Göksu was unsafe, Göcek was neutral and Amasra was safe.Özyurt, Ergin, & Baykal, (2010) updated their model. They considered not only geologic properties but also human effect in the new model and gave separate coefficient for each effect. Simav, Şeker, & Gazioğlu, (2013) stated that rising of sea level in East Mediterranean had a positive tendency by using multi purposes satellite data, and they predicted that rising is 3.4 ± 0.1 mm/year. Doğan, Ciioglu, Sanli, & Ulke, (2015) investigated data of 4 tide stations near Aegean Sea and Mediterranean. Then, relation between sea level change, North Atlantic Oscillation (NAO) and water temperature was shown. There has been no nationwide study covering all coasts. In addition, there has been no study on the long-term changes in the waves.

According to the results of all this literature study:

1. Century based wind and wave re-analysis data sets produced by ECMWF have been used worldwide by researchers who investigate wind and wave climate, changes and extreme storms. This data set gives good result in verifications. In addition, although it gives a little bit lower wave height, researchers report that the century-based data set is consistent and valuable.

2. Generally, wind and wave climate studies have been performed for the Turkish coasts, are on wave energy potential. These studies are generally performed with 13 – 15 years data. There is only one study used 31 years data. Therefore, there is not any wave climate study that was performed with century-based data for Black Sea, Aegean Sea and Mediterranean coasts.

3. The most practical way to find the design wave height along the Turkish coasts has been to use the Wave Atlas (Ozhan and Abdalla, 20002) t When we consider developments in the data in hand and improvements in modelling, it may be necessary to produce a new version of the Wave Atlas. So, designers need a new and more reliable source to find the design wave height.

4. The question of whether there is a change of wind and wave climate along the Turkish coasts or not has not been answered yet. The studies in the literature are based on specific regions with short-term data.

CHAPTER 3

RESEARCH METHODOLOGY: DATA, CALIBRATION AND VERIFICATION STUDIES

3.1. ERA–20C and CERA–20C Wave Data

At the beginning of the study, there was only one century-based reanalysis model of European Centre for Medium – Range Weather Forecasts (ECMWF), ERA-20C. Then ECMWF produced CERA-20C model data. The details of those models were explained in Chapter 2. In order to decide which century-based data set is appropriate to use in the study, a comparative study was performed.

Both ERA-20C and CERA-20C data can be downloaded from ECMWF Public Datasets web interface as an example case is shown in Figure 3. As it can be seen in Figure3, it is possible to download different kind of wind, wave, wave spectra parameters. In this study, the significant wave height (Hs), the mean wave period (Tm) and the mean wave direction data were downloaded from ECMWF. Hs is the average of the one-third of the highest waves in a storm. It is also represented as $H_{1/3}$.

In order to download the database automatically and quickly, instead of using web interface, a script was written in python and the data for each region were downloaded in monthly base.

It is possible to download the data with finer spatial resolutions however, in this study default grid points are chosen in order to avoid having possible errors due to interpolation issues in finer resolutions. Therefore 40 default grid points were specified along The Turkish coasts for the study and they are shown in Figure 4.

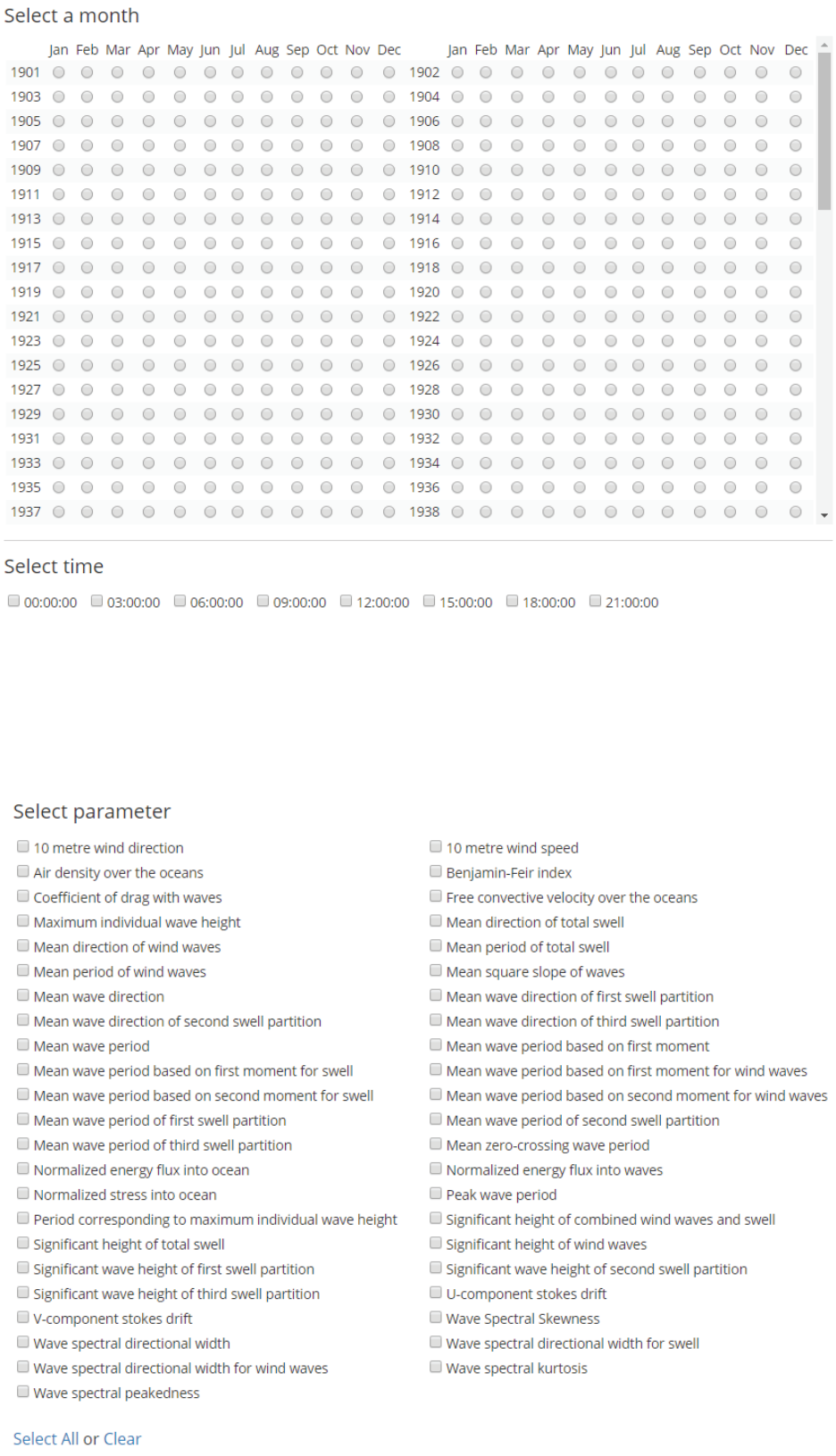

Figure 3. ECMWF Public Datasets web interface

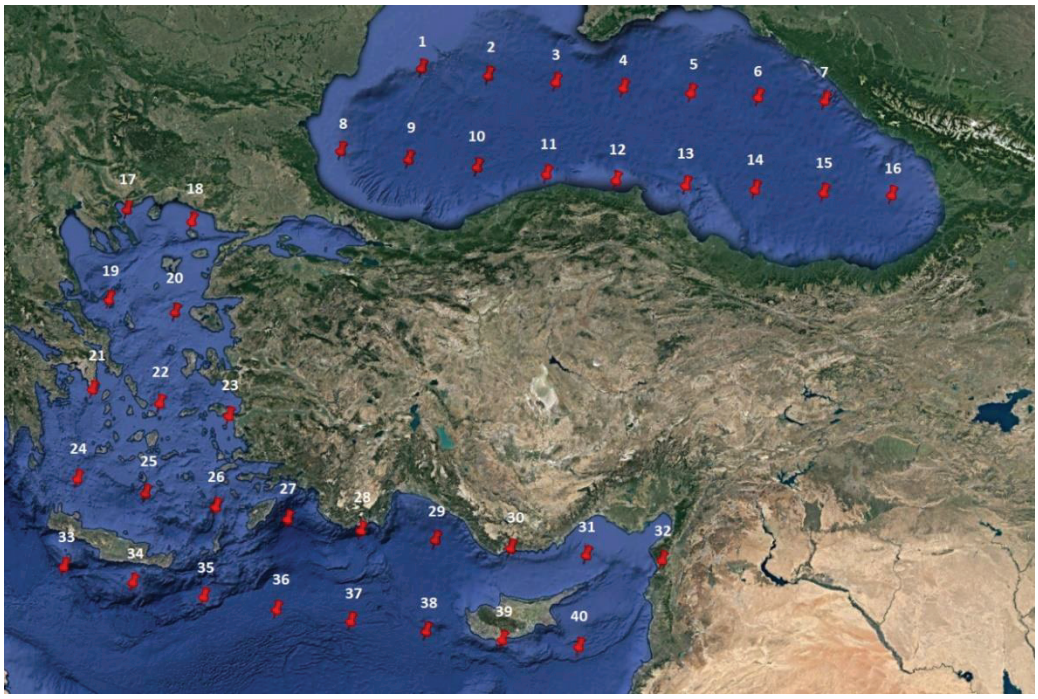

Figure 4. ERA-20C and CERA-20C Wave Data Default Grid Points

3.1.1. Comparison of ERA-20C and CERA-20C Wave Height Data

In order to decide which century-based data set is appropriate to use in the study, both ERA-20C and CERA-20C were compared with ENVISAT data over the whole Black Sea for 2007-2008 as a pilot study. 17 default grid points of ERA-20C and CERA-20C in Black Sea were determined for the comparison study. The Significant Wave Height (Hs) that is one of the most frequently used in the engineering applications was selected as a wave height.

Several error parameters were calculated in the comparison study. These are:

1. Root Mean Square Error (RMSE)

RMSE is square root of mean of difference between predicted and observed values. In this formula, P_i refers to predicted values, and O_i refers to observed values.

$$RMSE = \left[\frac{1}{N}\sum_{i=1}^{N}(P_i - O_i)^2\right]^{\frac{1}{2}} \quad (1)$$

2. Scatter Index (SI)

SI is given in Eq. 2. RMSE and SI parameters should be as near 0 as possible for the best model performance. In Eq. 2, $\overline{O}$ refers to mean of observations.

$$SI = \frac{RMSE}{\overline{O}} \quad (2)$$

3. Mean of Predict Error Parameter (Bias)

Bias is mean of difference between predicted and observed value. When bias is 0 it is named as objectivity.

$$Bias = \sum_{i=1}^{N} \frac{1}{N} (P_i - O_i) \quad (3)$$

- Correlation Coefficient (R)

  The correlation coefficient is a statistical measure that calculates the strength of the relationship between two variables.

- Standard Deviation

  It is a measure used to summarize the propagation of data values.

$$\sigma = \sqrt{\frac{1}{N-1} \sum_{i=1}^{n} (x_i - \bar{x})^2} \quad (4)$$

- Regression Coefficient

  The Regression Coefficient is the constant ‘b’ in the regression equation that tells about the change in the value of dependent variable corresponding to the unit change in the independent variable.

Error parameters are given in Table 1. When Table 1 is analyzed, it can be seen that CERA-20C is more compatible with satellite data as well as it is difficult to define exact result. Because of that reason, CERA-20C data set were used in the rest of the study.

Table 1. Comparison of ERA-20 and CERA-20C with Satellite

		ERA-20C			CERA-20C		
Latitude	Longitude	R^2	Bias (Satellite - Model)	St Dev. (Satellite - Model)	R^2	Bias (Satellite - Model)	St Dev. (Satellite - Model)
43.5	28.5	0.741135	0.329733	0.351016	0.707193	0.250296	0.371639
43.5	30	0.719385	0.177949	0.396969	0.692174	0.129815	0.425562
43.5	31.5	0.867310	0.302825	0.369003	0.818534	0.249711	0.349067
43.5	33	0.685992	0.363611	0.444969	0.789895	0.338784	0.391357
43.5	34.5	0.721322	0.280416	0.437311	0.665491	0.340708	0.467658
43.5	36	0.729833	0.245897	0.392571	0.730918	0.301736	0.391248
43.5	37.5	0.700138	0.349504	0.363949	0.750030	0.363660	0.337918
43.5	39	0.166335	0.449048	0.419720	0.116051	0.502853	0.430644
42	28.5	0.685252	0.208033	0.378926	0.704008	0.136661	0.381599
42	30	0.600954	0.313349	0.483260	0.649088	0.295654	0.453906
42	31.5	0.549178	0.414730	0.483355	0.660032	0.352737	0.431488
42	33	0.642118	0.498337	0.426233	0.677581	0.525957	0.421147
42	34.5	0.541253	0.465423	0.405887	0.582687	0.444144	0.388780
42	36	0.734388	0.465259	0.380786	0.732261	0.493593	0.394870
42	37.5	0.790189	0.444463	0.406280	0.829545	0.449947	0.386774
42	39	0.618865	0.441126	0.324170	0.589620	0.476717	0.340103
42	40.5	0.724387	0.446872	0.403617	0.745201	0.474463	0.422458

3.1.2. Comparison of CERA-20C and In-situ Measurements

After deciding to use the CERA-20C data in the rest of the study, the CERA20C data were compared with in-situ measurements to decide whether calibration was necessary or not. The comparison study was performed for the significant wave height, Hs, the mean period, Tm and the mean wave angle, θm.

3.1.2.1. Significant Wave Height(Hs)

Buoy data that were measured in Hopa, Sinop, Tekirdağ, Bozcaada, Dalaman and Alanya within the scope of NATO TU-WAVES Project (Özhan & Abdalla, 1999) were used to compare with CERA-20C data. Information about measurement stations is given in Table 2.

Table 2. Information About Measurement Stations

Station	Latitude	Longitude	Depth(m.)	Offshore Distance (m.)	Measurement Duration (YDM)
Alanya	36° 32' 30" N	31° 58' 30" E	100	1,400	19941101-19960208
Dalaman	36° 41' 30" N	28° 45' 18" E	100	1,000	19941121-19960729
Bozcaada	39° 42' 14" N	26° 02' 57" E	62	13,200	19941128-19950926
Sinop	42° 07' 24" N	35° 05' 12" E	100	11,600	19941201-19960614
Hopa	41° 25' 24" N	41° 23' 00" E	100	4,600	19941227-19990426

The comparison is performed by Quantile-Quantile plots (Q-Q plots) because the agreement between the CERA-20C and the buoy data in terms of probability distributions may become more important than the agreement in terms of time series and scatter plots from the climate and extreme value analysis of view. In order to calculate the quantiles, CERA-20C default grid point closest to the measurement location is determined. Then the data of CERA-20C and the buoy are collocated and the quantiles corresponding to same non-exceedance probabilities are calculated. As a result, Q-Q plots are graphed by plotting their quantiles against each other. Q-Q plots of buoy Hs data measured in Hopa, Sinop, Bozcaada,Dalaman and Antalya versus CERA-20C Hs data together with the line y= x are shown in Figure 5.

As it can be seen in Figure 5, while Hs values of CERA-20C are lower than the buoy Hs in Hopa and Sinop, they are higher in Bozcaada and Alanya measurements. Therefore, Hs data of CERA-20C should be calibrated.

3.1.2.2. Mean Wave Period (Tm)

Mean wave period, Tm data of CERA-20C were compared with the Tm data of the buoys and the results are indicated in Figure 6. CERA-20C Tm data have much better agreement with the buoy Tm data compared with the agreement in CERA-20C and the buoy for Hs, as it can be noticed in Figure 6. Nevertheless, Tm values of CERA-20C are greater than the buoy data in Bozcaada. Therefore, Tm also should be calibrated.

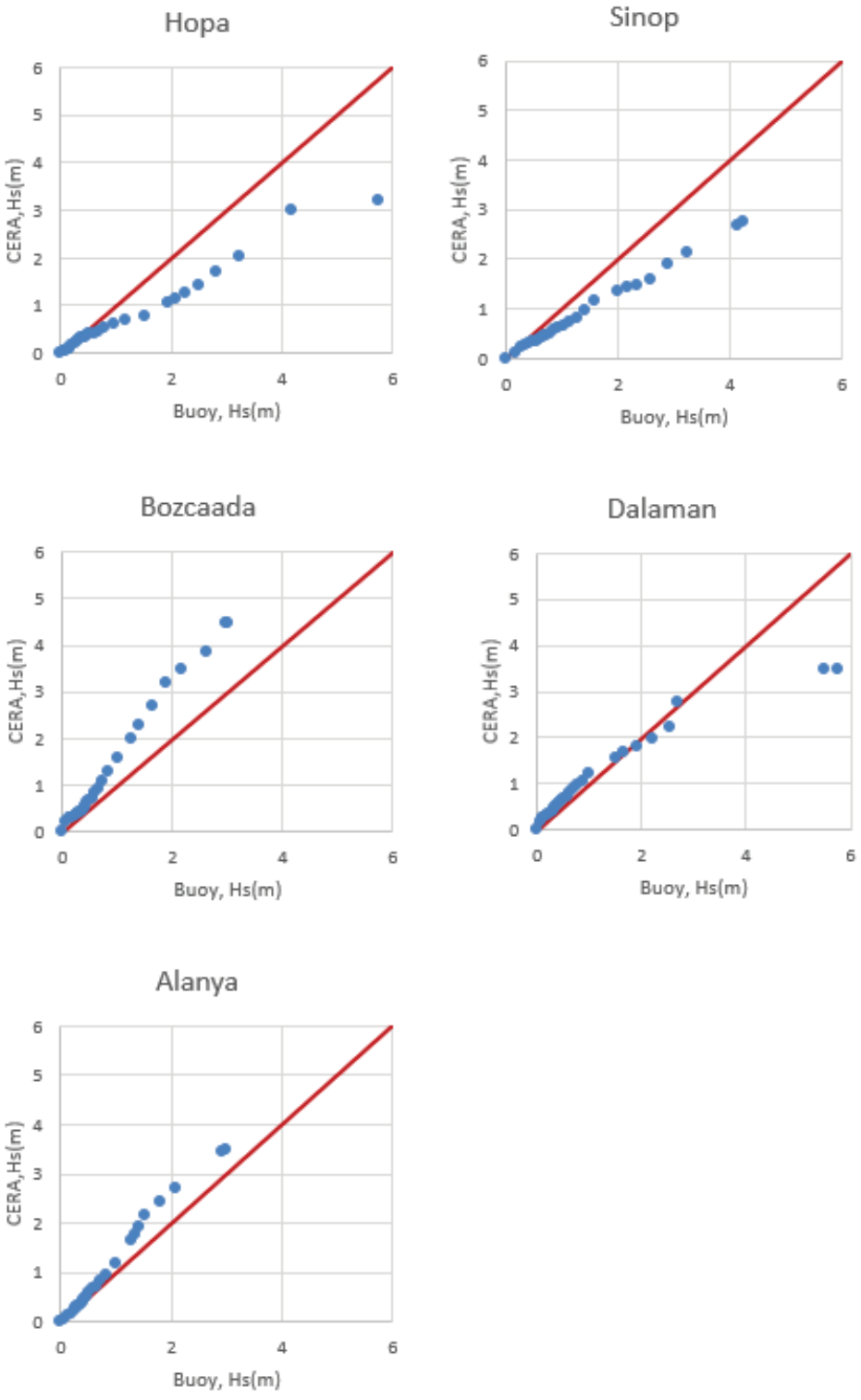

Figure 5. Comparison between Hs of CERA-20C and Hs of Buoy by Q-Q plots

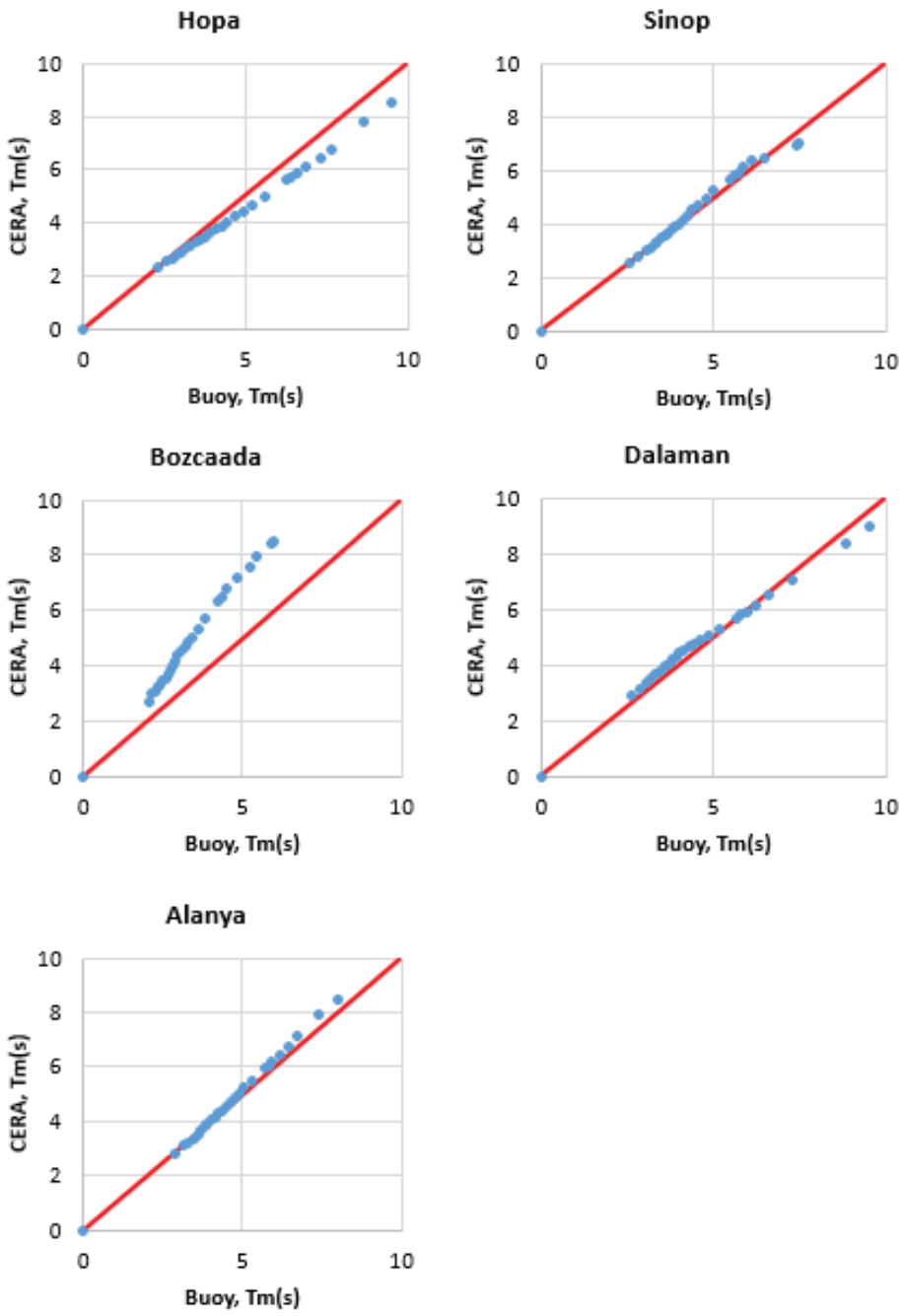

Figure 6. Comparison of CERA-20C Tm data and Buoy Tm data

3.1.2.3. Mean Wave Direction, θm

The mean wave direction data of the CERA-20C were compared with the buoy data and the comparison is shown in Figure 7 and Figure 8. Although there is not any one-to-one correspondence , effective directions seem similar.

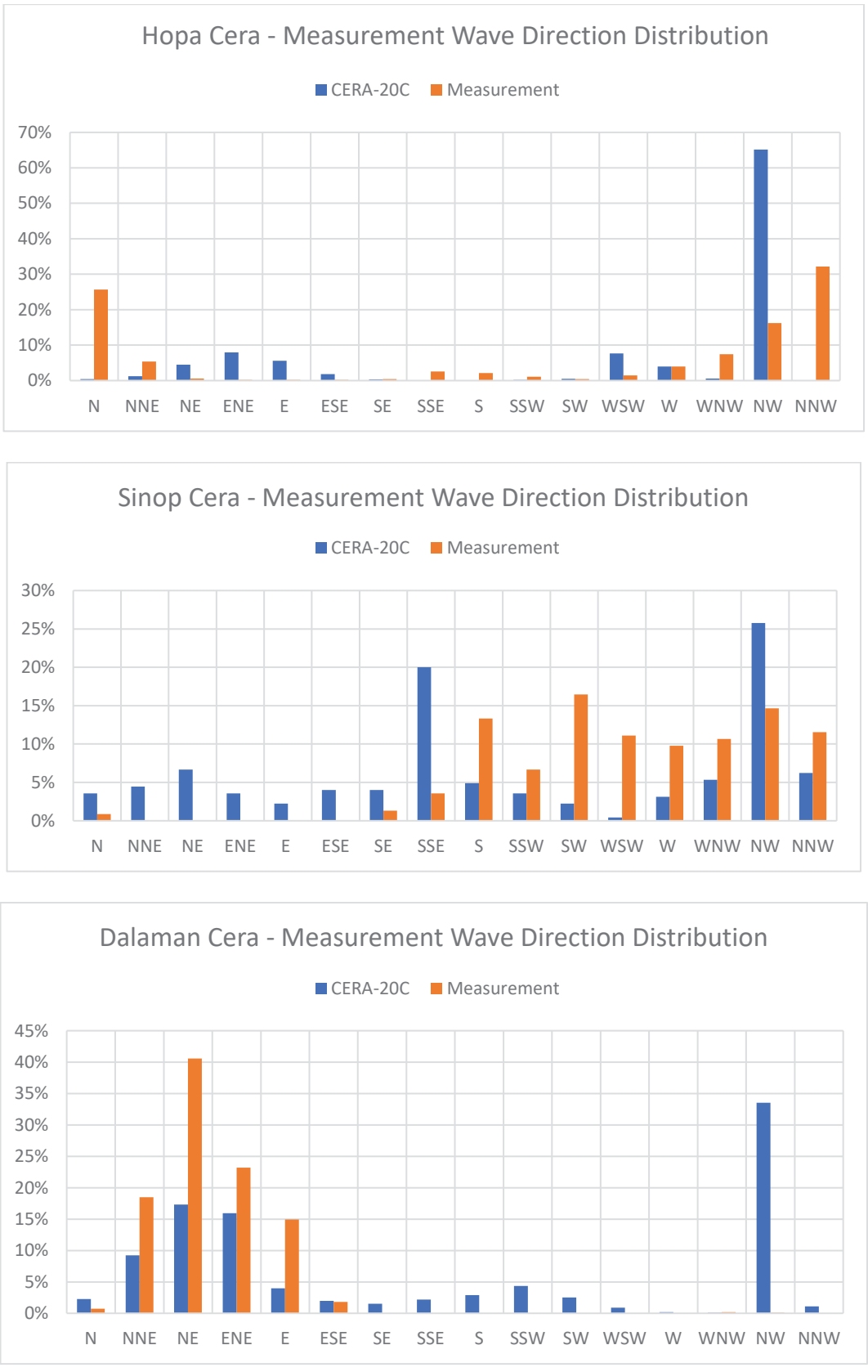

Figure 7. Comparison of CERA-20C and measurement mean wave directions for Hopa, Sinop and Dalaman

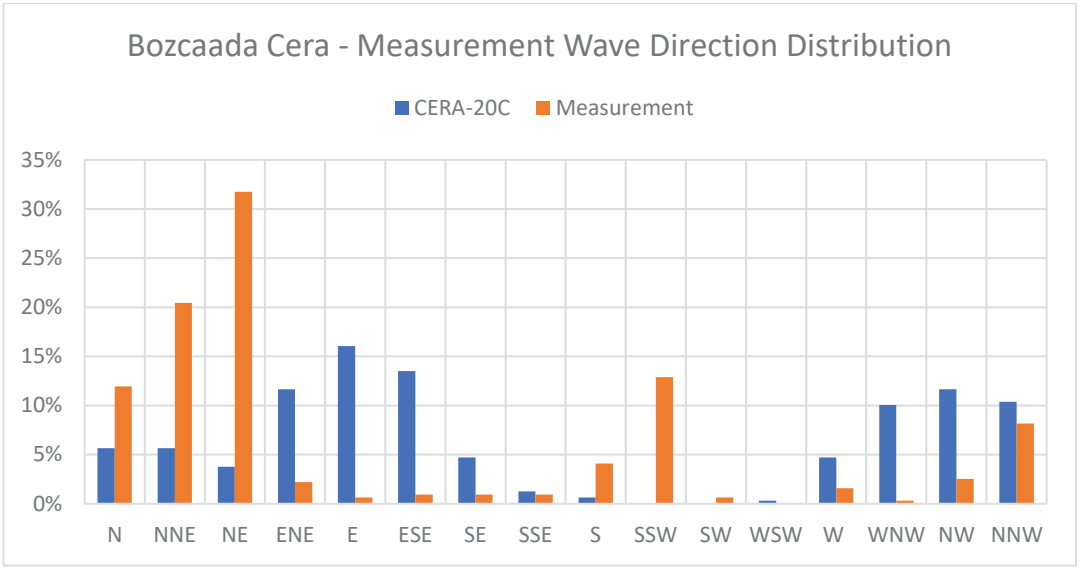

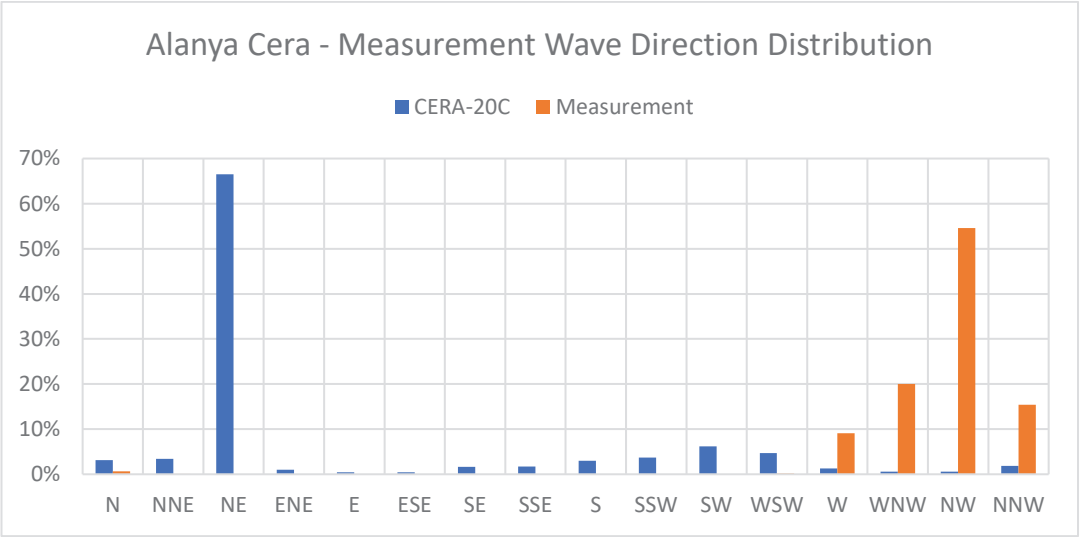

Figure 8. Comparison of CERA-20C and measurement mean wave directions for Bozcaada and Alanya

The comparison study indicates that CERA-20C data should be calibrated before they are used for the wave climate analysis along the Turkish coasts. Since NATO-TU-WAVES buoy measurement stations are only five and the data are limited (between 1994-1999), they are reserved for the verification. Therefore, it is decided to use the satellite data for the calibration of CERA-20C data.

3.2. Satellite Data

Radar altimeter can record the significant wave height and the wind speed. It is commonly used for the wind and wave measurements. The satellites with the radar altimeter and their measurement periods are given in Figure 1 in Chapter 2. In this study satellite data were obtained from RADS (Radar Altimeter Database System) that was firstly developed by Delft University of Technology. Nowadays, RADS is supported by NOAA (Scharroo et al., 2013).

3.2.1. Filtering of Satellite Data

Although Hs data downloaded from RADS have already been checked, it was noticed that there would be some errors and inconsistencies like too high values or negative and NAN values. In order to remove those errors, filtering was done before data were used. For filtering, Ku and C band back scatter coefficients, standard deviation of Hs and standard deviation of Ku band range were also downloaded. The data are removed if one of the following conditions occur: standard deviation of Hs >1.0, backscatter coefficient is NAN, standard deviation of Ku band range> 0.15 An example of satellite data is given in Figure 8. In the Figure 8, first column is track time, second column is latitude, third column is longitude, 4^{th} column is Ku band Hs, 5^{th} column is Ku band backscatter coefficient, 6^{th} column is C band backscatter coefficient, 7^{th} column is U_{10} (wind speed at 10m elevation above sea surface), 8^{th} column is standard deviation of Ku band range and 9^{th} column is standard deviation of Hs.

Those data belong to a satellite mission Jason2 measured in 7^{th} August of 2015 at 8:36:10. In order to filter the satellite data, the following steps were followed: The data with NAN values were removed. The data with the standard deviation of Hs>1 and Ku band range standard deviation > 0.15 were removed. In addition, inconsistent data were removed by checking the differences of two succeeding Hs and u10 data. For example, the data with Hs=0.466m were removed. Because, it was inconsistent with the rest of the data i.e. the mean of them >1.5m . If the difference between two successive Hs>1m, the datum was removed.

```
# RADS_ASC
# Satellite = JASON-2
# Phase     = a
# Cycle     = 261
# Pass      = 0109
# Equ_time  =  965550969.908000 (07-Aug-2015 08:36:10)
# Equ_lon   =  369.220000
# Original  = JA2_GPN_2PdP261_109_20150807_080803_20150807_090416.nc (V5.3)
# Col  1    = time rel. to equator passage [s]
# Col  2    = latitude [degrees_north]
# Col  3    = longitude [degrees_east]
# Col  4    = Ku-band significant wave height [m]
# Col  5    = Ku-band backscatter coefficient [dB]
# Col  6    = C-band backscatter coefficient [dB]
# Col  7    = altimeter wind speed [m/s]
# Col  8    = std dev of Ku-band range [m]
# Col  9    = std dev of Ku-band significant wave height [m]
  856.267458  41.002311   28.221900  0.468 11.52 14.99   5.56 0.0599 0.545
  857.287612  41.048273   28.256293    NaN   NaN   NaN    NaN    NaN   NaN
  858.307765  41.094221   28.290739    NaN   NaN   NaN    NaN    NaN   NaN
  859.327920  41.140156   28.325240    NaN   NaN   NaN  24.54    NaN   NaN
  860.348073  41.186078   28.359794  1.797   NaN   NaN  16.26    NaN   NaN
  861.832155  41.252858   28.410159    NaN   NaN   NaN    NaN    NaN   NaN
  862.252113  41.316727   28.458455    NaN   NaN   NaN    NaN    NaN   NaN
  863.840400  41.343180   28.478496    NaN   NaN   NaN    NaN    NaN   NaN
  864.860556  41.389042   28.513291    NaN   NaN   NaN    NaN    NaN   NaN
  865.880708  41.434889   28.548140  1.536 11.07 14.25   4.00 0.0646 0.531
  866.900864  41.480724   28.583045  1.478 10.82 14.06   9.00 0.0749 0.632
  867.921016  41.526544   28.618005  1.673 10.75 14.06   8.34 0.0749 0.422
  868.941171  41.572351   28.653020  1.473 10.75 14.05   7.89 0.0472 0.314
  869.961323  41.618144   28.688090  1.773 10.77 14.09   9.37 0.0530 0.477
  870.981478  41.663923   28.723217  1.322 10.78 14.07   8.48 0.0766 0.634
  872.001633  41.709688   28.758398  1.398 10.76 14.01   8.50 0.0586 0.797
  873.021786  41.755439   28.793636  1.689 10.77 14.14   8.82 0.0591 0.600
  874.041939  41.801177   28.828930  1.779 10.80 14.14   8.52 0.0530 0.505
  875.062093  41.846900   28.864280  1.589 10.76 14.06   8.28 0.1010 0.738
  876.082247  41.892609   28.899686  1.596 10.74 14.06   8.63 0.0622 0.589
  877.102401  41.938304   28.935149  1.730 10.69 14.07   9.45 0.0764 0.689
  878.122554  41.983985   28.970668  1.633 10.67 13.98   8.79 0.0696 0.427
```

Figure 9. Sample Satellite Data (Jason2, 7 August 2015, 8:36:10)

3.2.2. Comparison of Satellite and In-situ Significant Wave Height Measurements

Although there are lots of study showing that the satellite data are reliable (Abdalla et al. (2011), etc), any comparison study has not been done for Turkish coasts yet. Therefore, in this study, firstly they are compared with in-situ data before using them for the calibration of CERA-20C data.

In 2013, State Meteorological Organization of Turkey (SMO) started to permanent offshore wind and wave measurements in Silivri. Then, it was followed by the measurements in Bogaz, Canakkale, Antalya and Silifke began in 2015. Hourly data are

provided. Locations, deployment depths, distance from the shore and measurement periods of the buoys of SMO are summarized in Table 3. It should be noted that the measurement periods given in Table 3 cover the many time intervals without any measurements.

Table 3. Locations, deployment depths, distance from the shore and measurement periods of the buoys of SMO

Station	Latitude	Longitude	Water depth (m.)	Distance from shore (km.)	Measurement Period (YMD)
Silivri	40.9742	28.2487	50	4	2013-2018
Bogaz	41.2922	29.1656	75	8	2015-2018
Canakkale	40.0483	26.0356	70	11	2015-2018
Antalya	36.7167	31.0167	330	13	2015-2018
Silifke	36.0800	33.8300	180	14	2015-2018

Figure 10. Silivri Station

A SEAWATCH Midi 185 Buoy equipped with an ultrasonic anemometer is used to collect the wind and wave data. The station in Silivri (Marmara Sea) is shown in Figure 10.

To compare the radar altimeter and in-situ measurement data, ideally, it is desirable to collocate the altimeter and buoy observations at no spatial or temporal difference (Abdalla, Janssen, & Bidlot, 2011). However, then, it would be possible to find only very few collocations. Therefore, matchup areas shown in Figure 11 were selected for SMO buoys in Bogaz, Silivri, Canakkale, Antalya and Silifke such that buoy and satellite data separated by no more than 0.5 deg in latitude/longitude as recommended by (Young et al., 2011). The matchup time was determined as 30 minutes. Jason2, Saral, Cryosat2, Jason3 and Sentinel 3 are the satellite missions with available significant wave height data for the measurement periods of in-situ data given in Table 3. In order to increase the collocation number, all the altimeter data (Jason2, cryostat, Saral, Jason3, Sentinel) were combined and one satellite database was obtained for each buoy location.

Figure 11. Locations of the measurement stations and matchup area

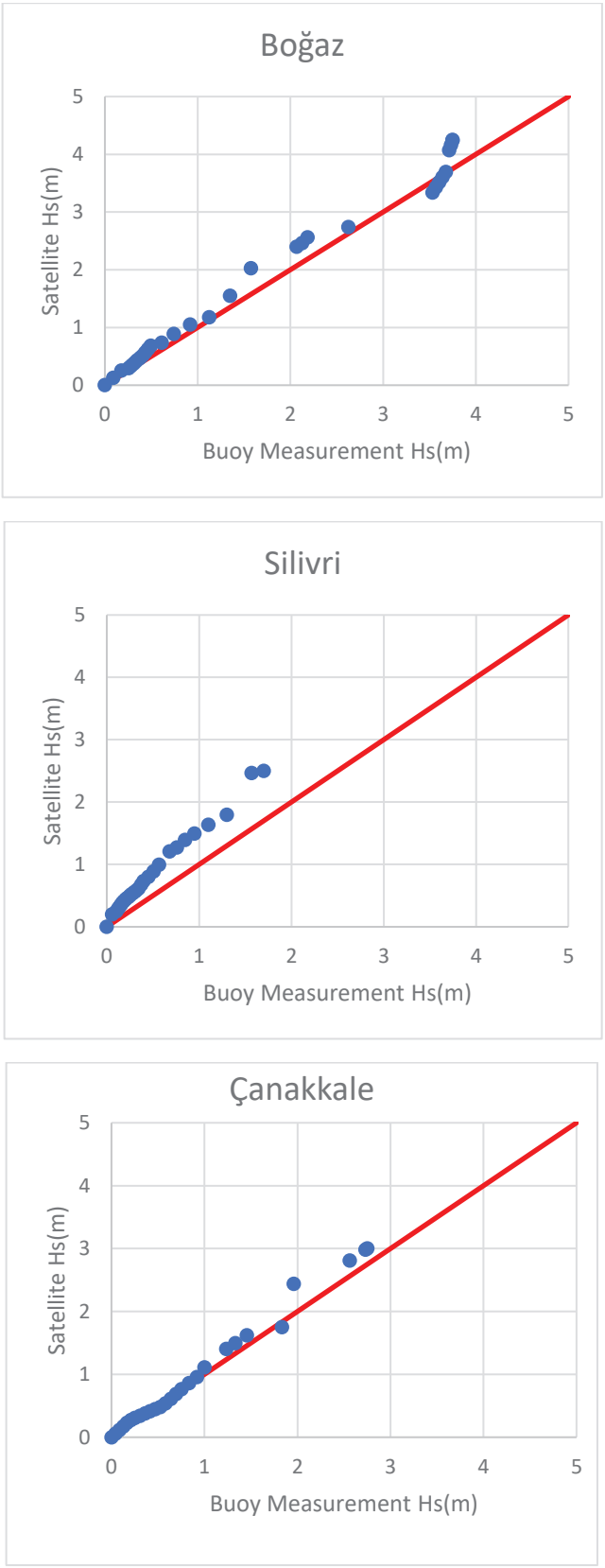

Figure 12. Q-Q plots of Hs measured by the buoys versus Hs measured by the satellites for Boğaz, Silivri and Çanakkale

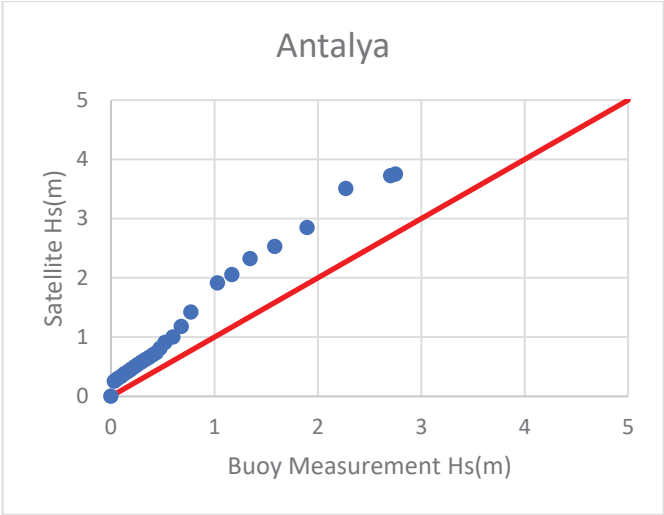

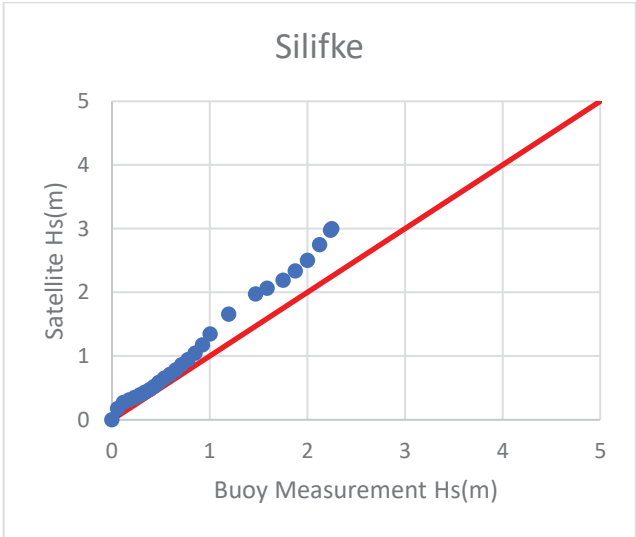

Figure 13. Q-Q plots of Hs measured by the buoys versus Hs measured by the satellites for Antalya and Silifke

For the error assessment, RMSE (root mean square error), SI (scattered Index), Bias, symmetric slope, A (y=Ax) and the correlation coefficient ,R, are calculated and the results are presented together with the data numbers and the mean values of altimeter and buoy wind speeds in Table 4.

Figure12, Figure 13 and Table 4 show that especially the error in Silivri and Antalya seem high. The reason may be the data number. Table 4 indicates that collocated data of the buoy and the satellite are limited due to both limited satellite data in the match area and the limited duration of the wave measurement as given in Table 3.

Table 4. Error assessment for Hs of combined of satellite RA against the buoy measurements

Buoy Location	Data No	RMSE	SI	Bias	A	R	RA Mean	Buoy Mean
Silivri	603	0.3799	1.2134	0.2724	1.5510	0.57630	0.5855	0.3131
Antalya	383	0.4823	1.1677	0.3433	1.6086	0.80310	0.7564	0.4131
Boğaz	72	0.2378	0.2799	0.1482	1.1098	0.98170	0.9977	0.8496
Silifke	176	0.3029	0.4419	0.1273	1.1929	0.88300	0.8127	0.6855
Çanakkale	147	0.3230	0.5821	0.0065	0.9319	0.72290	0.5613	0.5548

Considering the results of the comparison study between the satellite RA data and the buoy data, it was decided to use another data source together with the satellite data for the calibration of CERA-20C. It is the recent and the newest data of ECMWF: ERA5.

A first segment of the ERA5 dataset is now available for public use (1979 to within 3 months of real time). ERA5 provides hourly estimates of a large number of atmospheric, land and oceanic climate variables. The data cover the Earth on a 30km grid space (ECMWF, n.d.).

A similar comparison study was carried out for the Hs of the buoys and the ERA5. Q-Q plots are given in Figure14, Figure 15 and Figure 16.

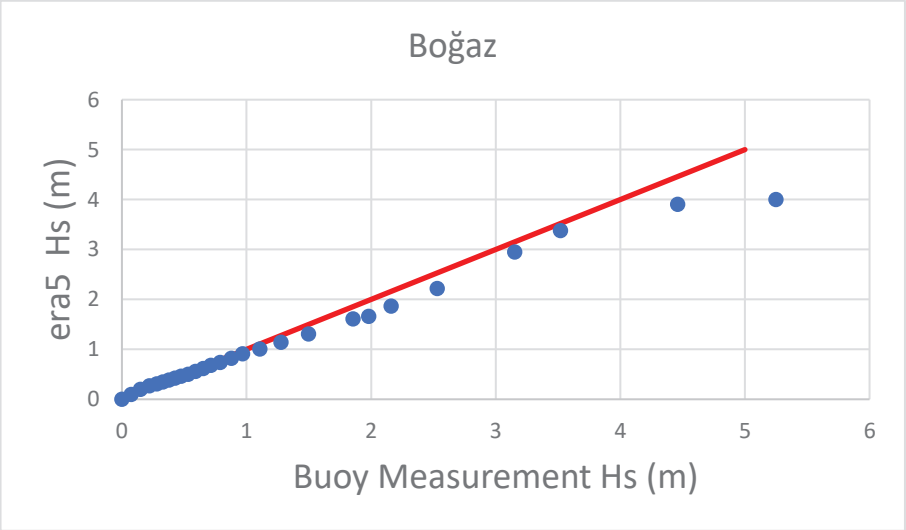

Figure 14. Q-Q plots of Hs measured by the buoys versus Hs data of ERA5 for Boğaz

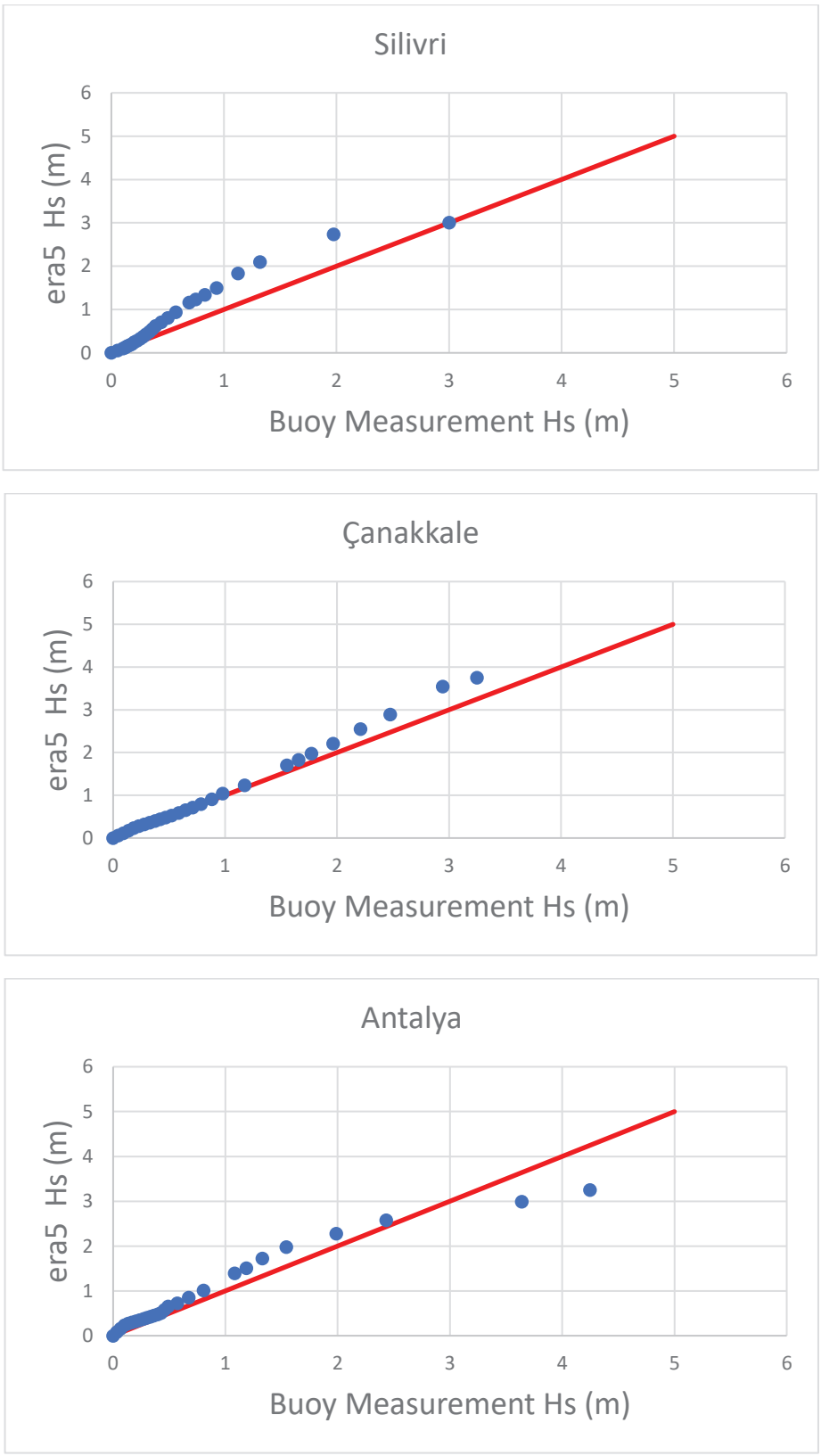

Figure 15. Q-Q plots of Hs measured by the buoys versus Hs data of ERA5 for Silivri, Çanakkale and Antalya

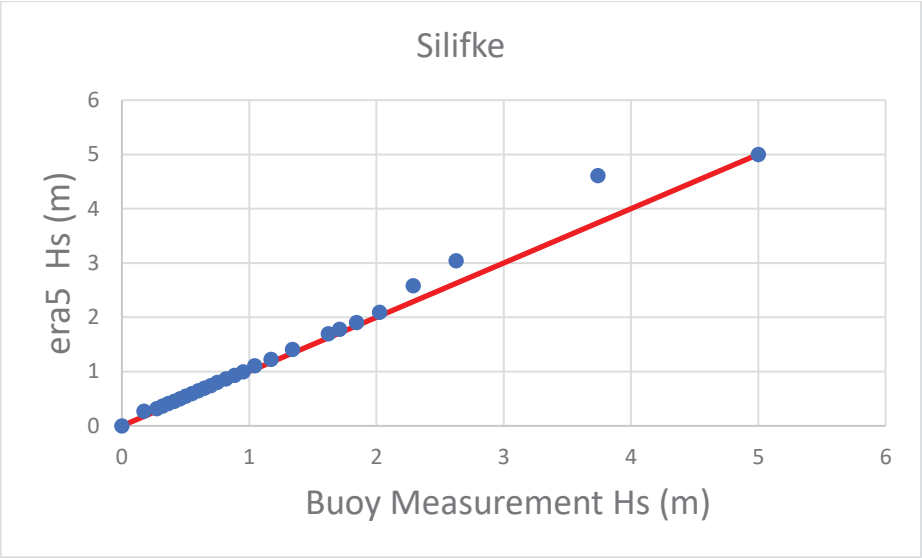

Figure 16. Q-Q plots of Hs measured by the buoys versus Hs data of ERA5 for Silifke

For the error assessment, RMSE (root mean square error), SI (scattered Index), Bias, symmetric slope, A (y=Ax) and the correlation coefficient ,R, are calculated and the results are presented together with the data numbers and the mean values of altimeter and buoy wind speeds in Table 5.

Table 5. Error assessment for Hs of ERA5 data against the buoy measurements

Buoy Location	Data No	RMSE	SI	Bias	A	R	RA Mean	Buoy Mean
Silivri	36811	0.3231	1.0466	0.1304	1.3029	0.62420	0.4391	0.3087
Boğaz	10460	0.2165	0.2903	-0.0535	0.8844	0.93860	0.6925	0.7460
Silifke	14481	0.2762	0.3704	0.0497	1.0187	0.83460	0.7953	0.7456
Çanakkale	8237	0.2578	0.4398	0.0346	1.0188	0.86420	0.6209	0.5863
Antalya	13520	0.2495	0.5962	0.1227	1.1512	0.84920	0.5412	0.4185

Figure14, Figure 15, Figure 16 and Table 5 shows that the error is less compared to the satellite and the buoy comparison. The reason may be the data number. Table 5 shows that it is possible to find ERA5 data corresponding to each hourly measurement by the buoys. Therefore, it was decided to use ERA5 data together with satellite data in the calibration study of CERA20C.

3.3. Calibration of CERA-20C Wave Data

In generally, satellites are designed to work for several years (3 – 7). Although this period can be doubled, it is not enough for climate studies and calibration of CERA-20C data. In order to extend the duration of the RA data record, different satellite measurements can be spliced. However, the characteristics of the measurements of various altimeters are different. Therefore, any attempt to carry out climate computations from a spliced radar altimeter must include an inter-calibration exercise (Abdalla, 2013). In order to be able to calibrate CERA-20C data, radar altimeters with available data before 2010 are checked. It is noticed that the Jason family of satellites (TOPEX/Poseidon, Jason-1 and 2) and ENVISAT family of satellites (ERS-1, ERS-2 and ENVISAT) have the data before 2010 in the study area. Measurement periods of these family satellites are given in Figure17. As it can be seen in Figure17, measurement period of one satellite mission overlaps the next. In this study collocated records in overlap periods are used for inter-calibration of the satellites.

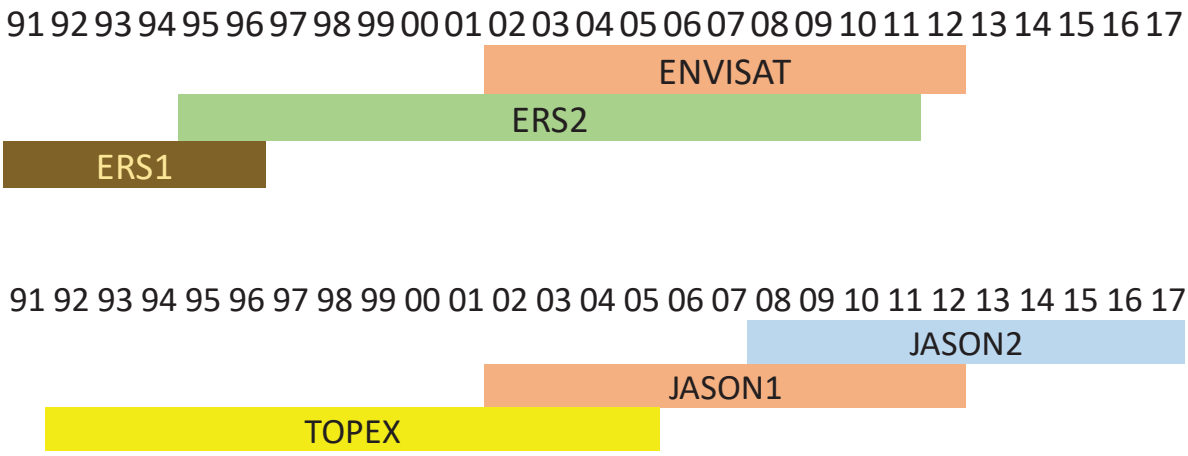

Figure 17. Measurement and the overlap periods of ENVISAT and JASON family satellites

For the inter-calibration of the satellites by using the overlap periods, first of all, the satellite data were retrieved from RADS website by defining the matchup area for each of the 40 default grid points of CERA-20C given in Figure 4. The latitude and the longitude of each default grid point and the boundaries of the matchup area were tabulated in Table 6.

Table 6. Default grid points of CERA20C data and the boundaries of the corresponding matchup area

Area	Latitude	Longitude	South	North	West	East
A1	43.50	30.00	42.75	44.25	29.25	30.75
A2	43.50	31.50	42.75	44.25	30.75	32.25
A3	43.50	33.00	42.75	44.25	32.25	33.75
A4	43.50	34.50	42.75	44.25	33.75	35.25
A5	43.50	36.00	42.75	44.25	35.25	36.75
A6	43.50	37.50	42.75	44.25	36.75	38.25
A7	43.50	39.00	42.75	44.25	38.25	39.75
A8	42.00	28.50	41.25	42.75	27.75	29.25
A9	42.00	30.00	41.25	42.75	29.25	30.75
A10	42.00	31.50	41.25	42.75	30.75	32.25
A11	42.00	33.00	42.00	43.50	32.25	33.75
A12	42.00	34.50	42.00	43.50	33.75	35.25
A13	42.00	36.00	41.25	42.75	35.25	36.75
A14	42.00	37.50	41.25	42.75	36.75	38.25
A15	42.00	39.00	41.25	42.75	38.25	39.75
A16	42.00	40.50	41.25	42.75	39.75	41.25
A17	40.50	24.00	39.75	41.25	23.25	24.75
A18	40.50	25.50	39.75	41.25	24.75	26.25
A19	39.00	24.00	38.25	39.75	24.00	25.50
A20	39.00	25.50	38.25	39.75	24.75	26.25
A21	37.50	24.00	36.75	38.25	23.25	24.75
A22	37.50	25.50	36.75	38.25	24.75	26.25
A23	37.50	27.00	36.75	38.25	26.25	27.75
A24	36.00	24.00	35.25	36.75	23.25	24.75
A25	36.00	25.50	35.25	36.75	24.75	26.25
A26	36.00	27.00	35.25	36.75	26.25	27.75
A27	36.00	28.50	35.25	36.75	27.75	29.25
A28	36.00	30.00	35.25	36.75	29.25	30.75
A29	36.00	31.50	34.50	36.00	30.75	32.25
A30	36.00	33.00	35.25	36.75	32.25	33.75
A31	36.00	34.50	35.25	36.75	33.75	35.25
A32	36.00	36.00	35.25	36.75	35.25	36.75
A33	34.50	24.00	33.75	35.25	23.25	24.75
A34	34.50	25.50	33.25	34.75	24.75	26.25
A35	34.50	27.00	33.75	35.25	26.25	27.75
A36	34.50	28.50	33.75	35.25	27.75	29.25
A37	34.50	30.00	33.75	35.25	29.25	30.75
A38	34.50	31.50	33.75	35.25	30.75	32.25
A39	34.50	33.00	33.00	34.50	32.25	33.75
A40	34.50	34.50	33.75	35.25	33.75	35.25

As an example, calibration study of 16th region at Eastern Black Sea near Hopa is given. After all the satellite data were retrieved and filtered, Hs of Jason2 data from Jason satellite family and Hs of Envisat data from Envisat satellite family were compared with ERA5 Hs data. Q-Q plots of the comparison are demonstrated in Figure 18. Figure 18 shows that Envisat Hs has better agreement with the ERA5 Hs. Therefore, Envisat satellite family (Envisat, ERs2, Ers1) was selected for the calibration of CERA-20C data at 16th grid.

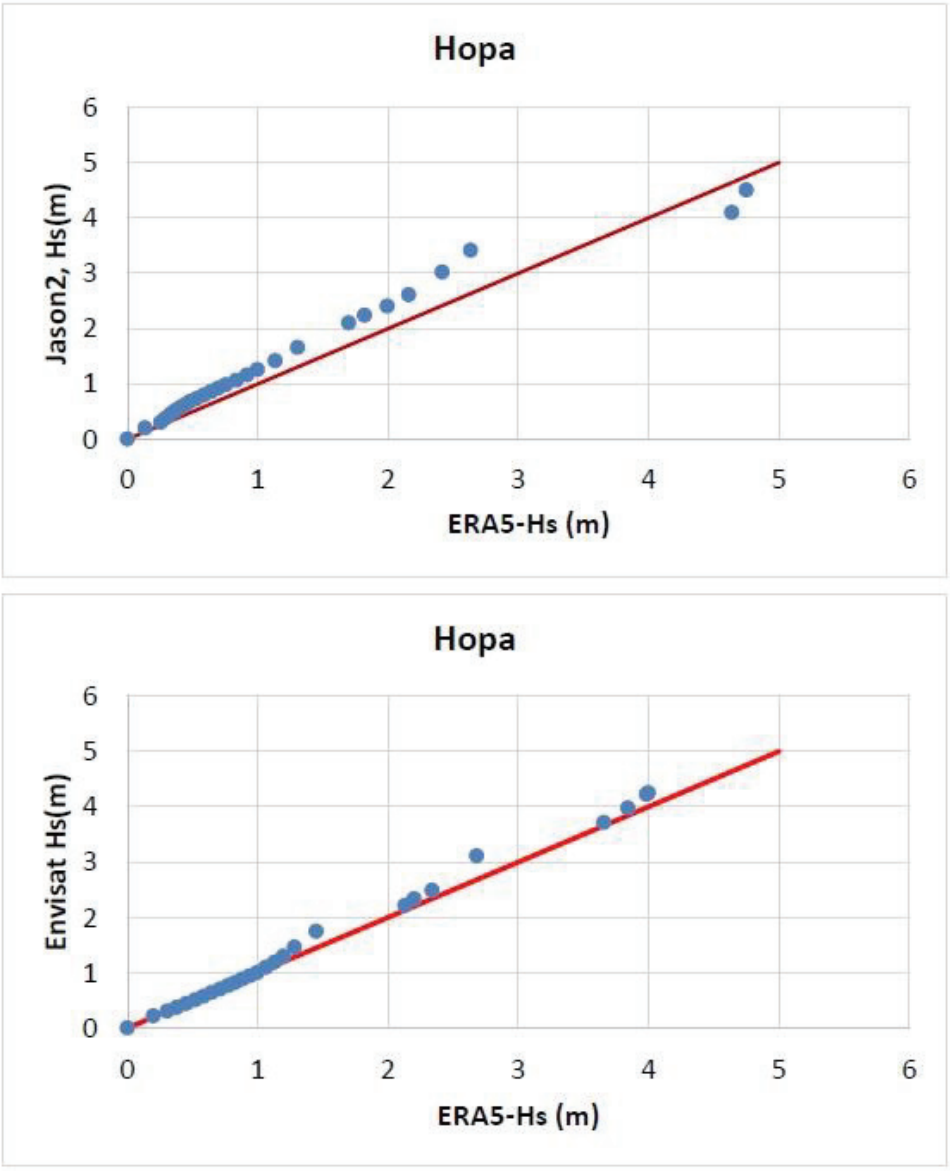

Figure 18. Q-Q plots for Hs of ERA5 versus Envisat and Jason2

Then, ERS2 was inter-calibrated with respect to Envisat data by using overlapped measurement period shown in Figure 17. Inter-calibration means that the comparison of the overlapped data of two different satellites. If the agreement is not good, previous data set is calibrated with respect to the recent dataset. In the example, ERS2 and the Envisat data were compared and since the agreement is good then ERS2 was not calibrated with respect to Envisat data. Figure 19 shows the Q-Q plots of the comparison.

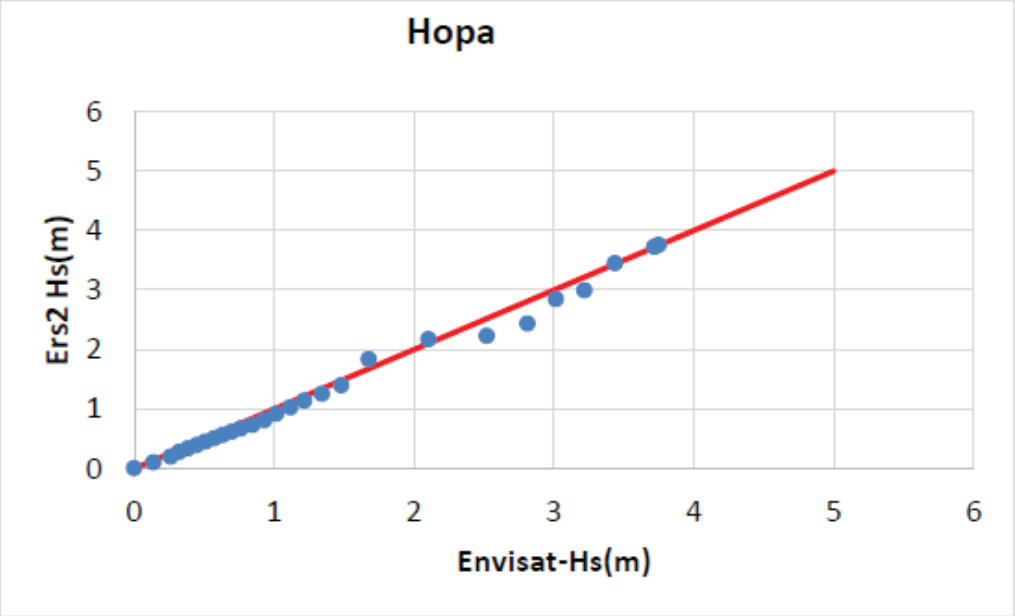

Figure 19. Comparison for Hs of ERS2 and Envisat

Although there are overlap periods between ERS2 and ERS1 as it is indicated in Figure 17, it could not be possible to find ERS1 data recorded in the matchup area for the same period of ERS2. Therefore, through inter-calibration procedure it was possible to combine Envisat and ERS2 data and to obtain satellite data with a total duration of 18 years (1995-2012). Then, inter-calibrated and the combined ERS2 and Envisat satellite data were used to calibrate CERA-20C.

When combined satellite Hs data were compared with Hs of CERA-20C by Q-Q plot as it is shown in Fig 20, it seems that Hs of CERA-20C is lower than the Hs of the combined ERS2-Envisat satellites. It means that CERA20C Hs should be calibrated and Figure 20 shows the good agreement between CERA-20C and the satellite data after the calibration.

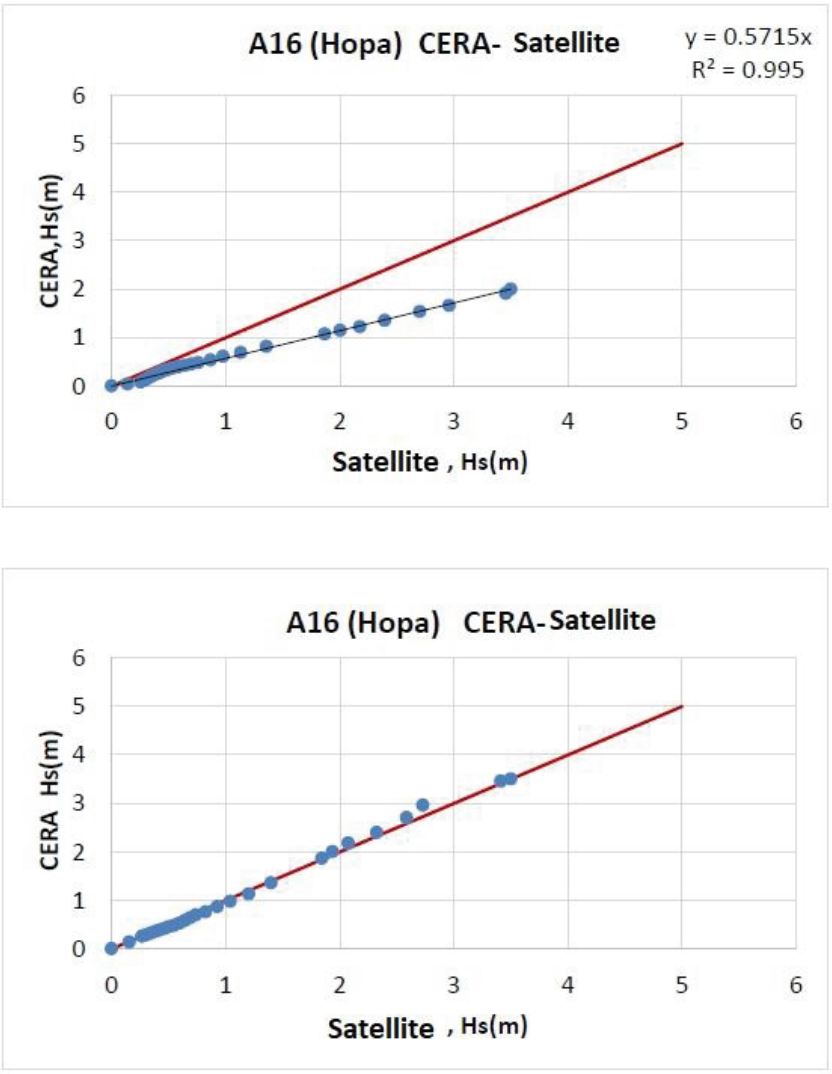

Figure 20. CERA-20C Hs Data Before Calibration (upper) and After Calibration (below)

Jason Family satellite (jason2 – jason1 – Topex) resulted a better agreement with ERA5 data in some default grid points. Point A13 is given as an example in Figure 21.

During the inter-calibration procedure, it was observed some cases that agreement between the overlap period data of two satellites were good as it is given in Figure 21 and 19. However at some points, the agreement was not good as it is shown in Figure 22 for the points A15 and A26. In those cases, they were calibrated by the recent satellite data and After then satellite data were combined and the duration was extended to 26 years (1992-2017)

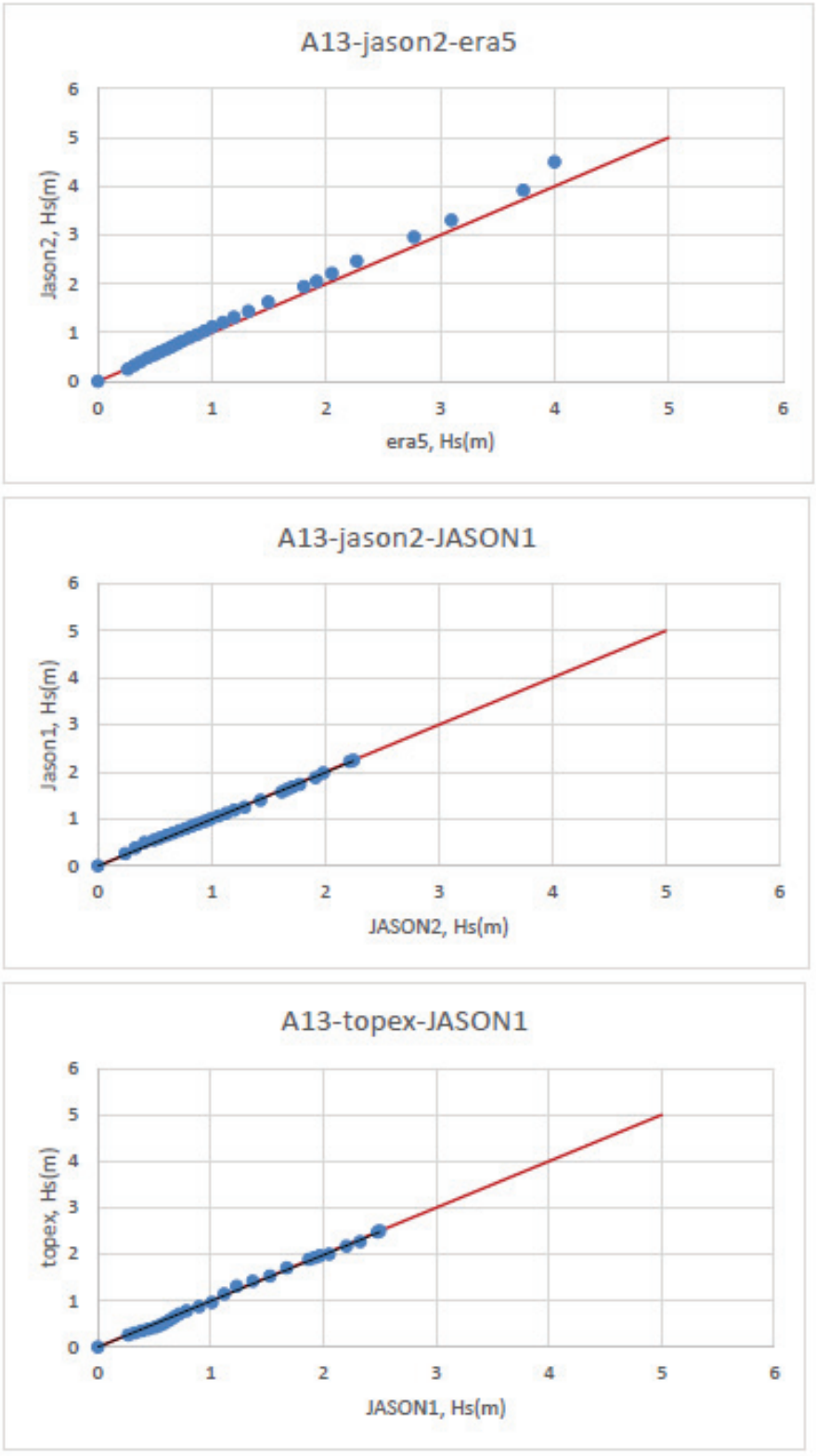

Figure 21. Comparison of Jason2 Satellite Data with ERA5and inter-calibration of Jason1 and Topex data

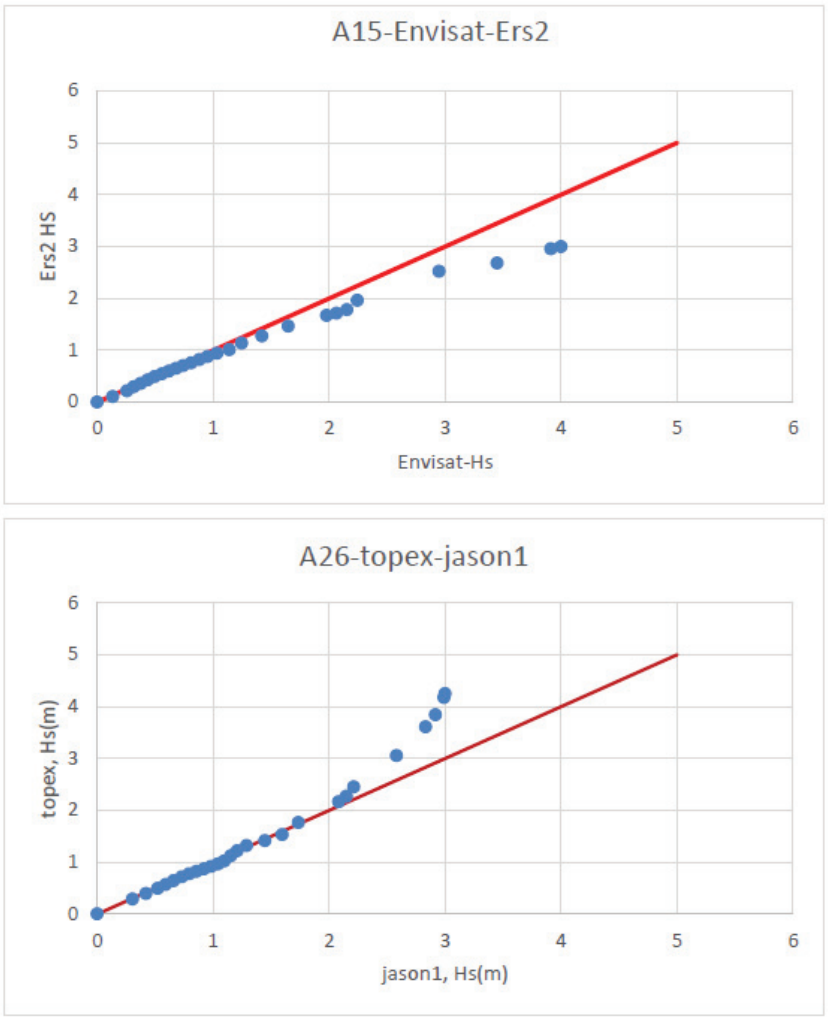

Figure 22. Examples that the agreement in the overlapped duration data of two satellites are not good

3.4. Estimation of the Wave Period from Satellite Records

The satellite scatterometer, Synthetic Aperture Radar (SAR) and radar altimeter (RA) measure the wave height (Hs)and the wind speed (u10). The wave period cannot be obtained directly because it is not possible to record by RA, SAR or scatterometer. However, the wave period can be derived from the satellite data by using several methods. (Gommenginger, Srokosz, Challenor, & Cotton, 2003) proposed a simple empirical formula with a significant wave height and back-scatter coefficient to find the wave period. (Quilfen, Chapron, Collard, & Serre, 2004) used the artificial neural network method. (Mackay, Retzler, Challenor, & Gommenginger, 2008) derived a new empirical

formula for the back-scatter coefficient>0.13, since the period does not depend on this coefficient. (Badulin, 2014) created a physical model using wave height and positional derivative without using back-scatter coefficient and calculated the wave period.

In this study, Artificial Neural Networks (ANN) method which is trained by using the significant wave height and back scattering coefficients (σKu and σC) which can be obtained from the satellite was used. In order to train artificial neural network model, the significant wave height, σKu and σC measured by Jason3 satellite during the year 2017, were used as input; ECMWF model data for the same year were used as output. The feed forward artificial neural network model was used to estimate the wave period values. Because, Advanced Propagation ANN, which uses Back Propagation Algorithm from consulted learning methods is the most commonly used method in modeling and estimating time series. It also makes successful predictions in the modeling of both linear and nonlinear structures ("Neural Network Concepts," n.d.). Levenberg-Marquardt (LM) algorithm was used in the education of the network. In this study, 3 input neurons, 10 hidden layer neurons and 1 output neuron were used in the ANN model design. The model design is shown in Figure 23.

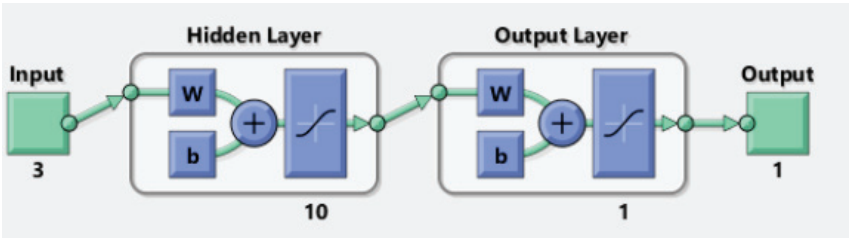

Figure 23. Design of Artificial Neural Network

Since iterative prediction method is adopted in developed ANN, the number of output neurons is one. In the same way, single-secret layer is generally used in feed-forward ANNs developed in the literature. For this reason, it is considered appropriate to use single-layer in the ANN model developed in the study. The tanjantsigmoid transfer function is used between the input layer and the hidden layer, and the linear transfer function is used between the hidden layer and the output layer. The Mean Squared Error (MSE) method was used to determine the accuracy of the ANN. After neural network created with the data to be collected from all over the world in 2017 by Jason3 satellite,

training and testing were performed in 4 different parts as World, Mediterranean, Turkish Coasts and Black Sea. 70% of the data were used for training, 15% for verification and 15% for testing. The square of the correlation coefficient (R2) obtained from the test results are given in Table 7.

Table 7. Artificial Neural Network Model Training and Test Results (R2)

		Test			
		World	**Mediterranean**	**Turkey Coast**	**Black Sea**
Train	**World**	0.7541	0.7591	0.6803	0.7078
	Mediterranean	0.6368	0.8340	0.7211	0.7956
	Turkey Coast	0.6320	0.8293	0.7325	0.7919
	Black Sea	0.5955	0.8217	0.7161	0.8017

Table 7 shows that, when the model was trained with global data, good results were obtained globally. However, the results obtained for the Mediterranean and Black Sea, which are enclosed seas, were not good. When the model was trained with regional data, then the test results were significantly better for the enclosed seas and the Turkish coasts. The mean wave periods obtained with ANN were compared with the measurements, and the Q-Q plots are given in Figure 24, Figure 25 and Figure 26.

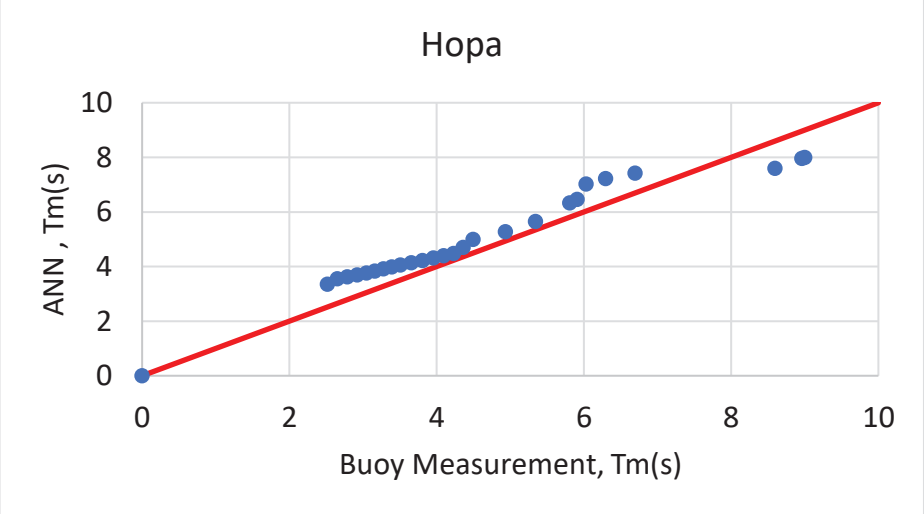

Figure 24. Q-Q plots for Tm of of ANN versus Measurement for Hopa

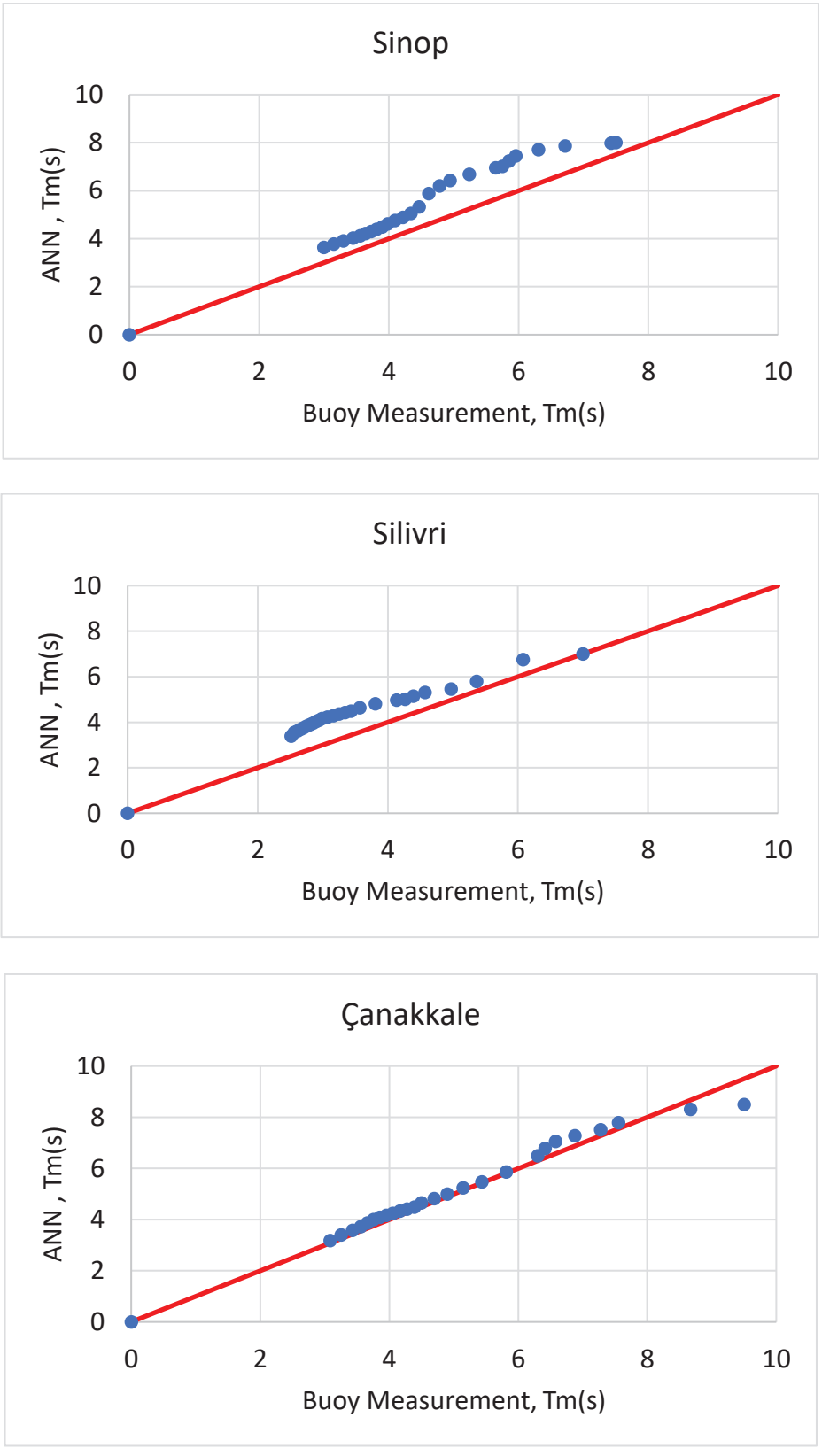

Figure 25. Q-Q plots for Tm of of ANN versus Measurement for Sinop, Silivri and Çanakkale

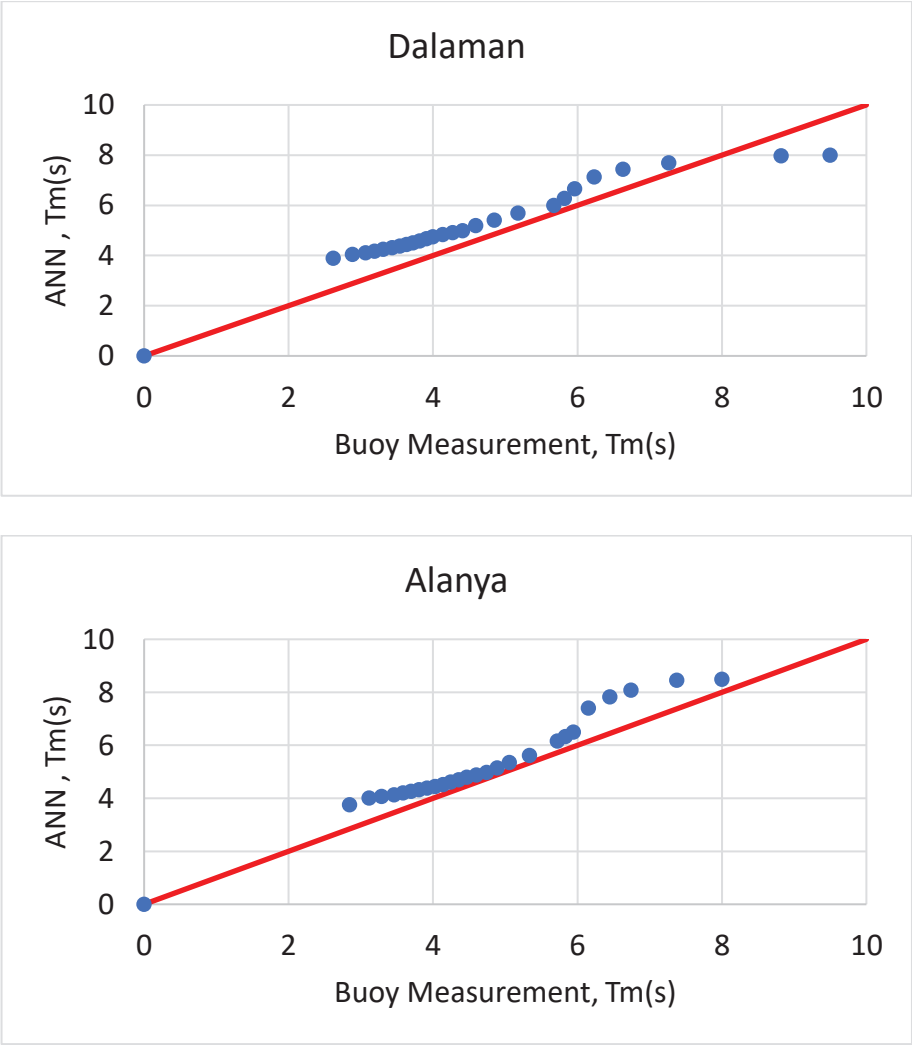

Figure 26. Q-Q plots for Tm of of ANN versus Measurement for Dalaman and Alanya

3.5. Calibration of CERA-20C Wave Period Data

Original CERA-20C periods have a better agreement with the measurement compared to the case of Hs as shown in Figure 27. However, it was observed that there are extremely high period results especially in Bozcaada. Therefore, it is decided to calibrate CERA-20C period for Bozcada with respect to satellite derived wave period. For this purpose, the period from the satellite data was derived by using the neural networks model as explained above. Then the CERA-20C period data was calibrated with respect to the derived period by ANN. Figure 27 shows the comparison of measurement and CERA-20C wave period data before the calibration by the derived period from the satellite by ANN and after the calibration .

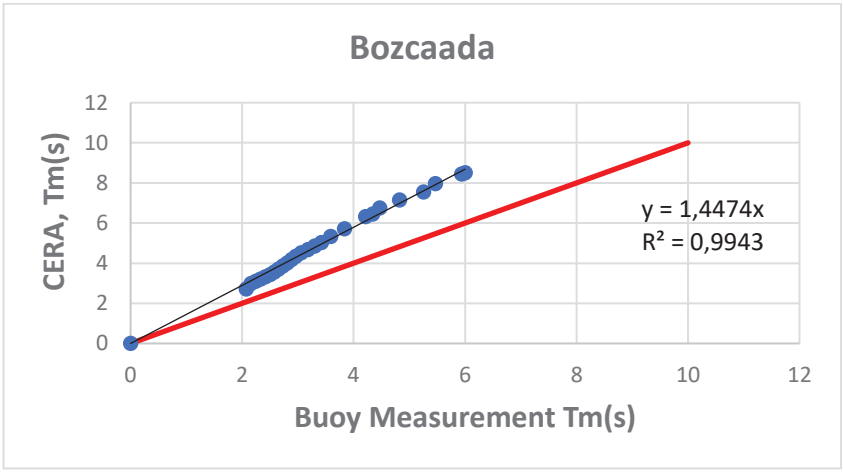

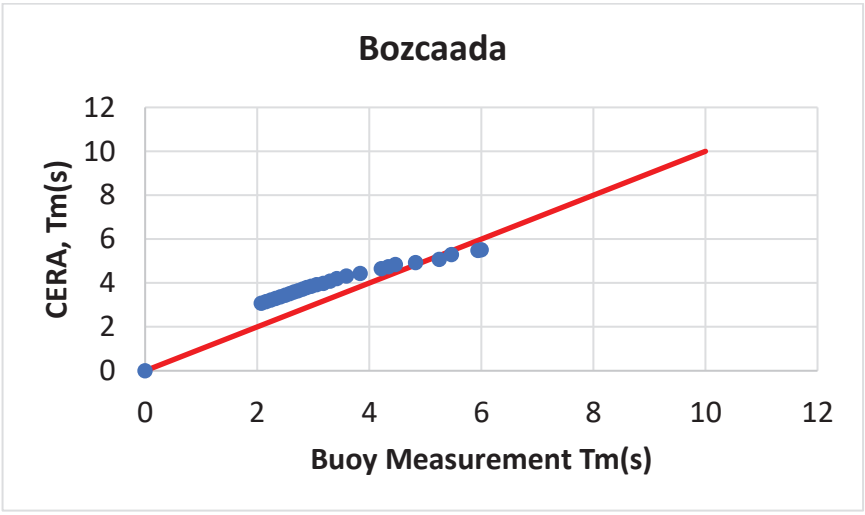

Figure 27. Comparison of CERA-20C periods before the calibration(above) and after the calibration(below)

In Figure 27, it is seen that the CERA-20C periods become more compatible with the measurements after the calibration study was performed.

3.6. Verification of CERA-20C Wave Data

After the extensive calibration study, the CERA-20C wave height data was compared with the NATO-TU Waves measurements for the verification. The results are given in Figure 28 and Figure 29.

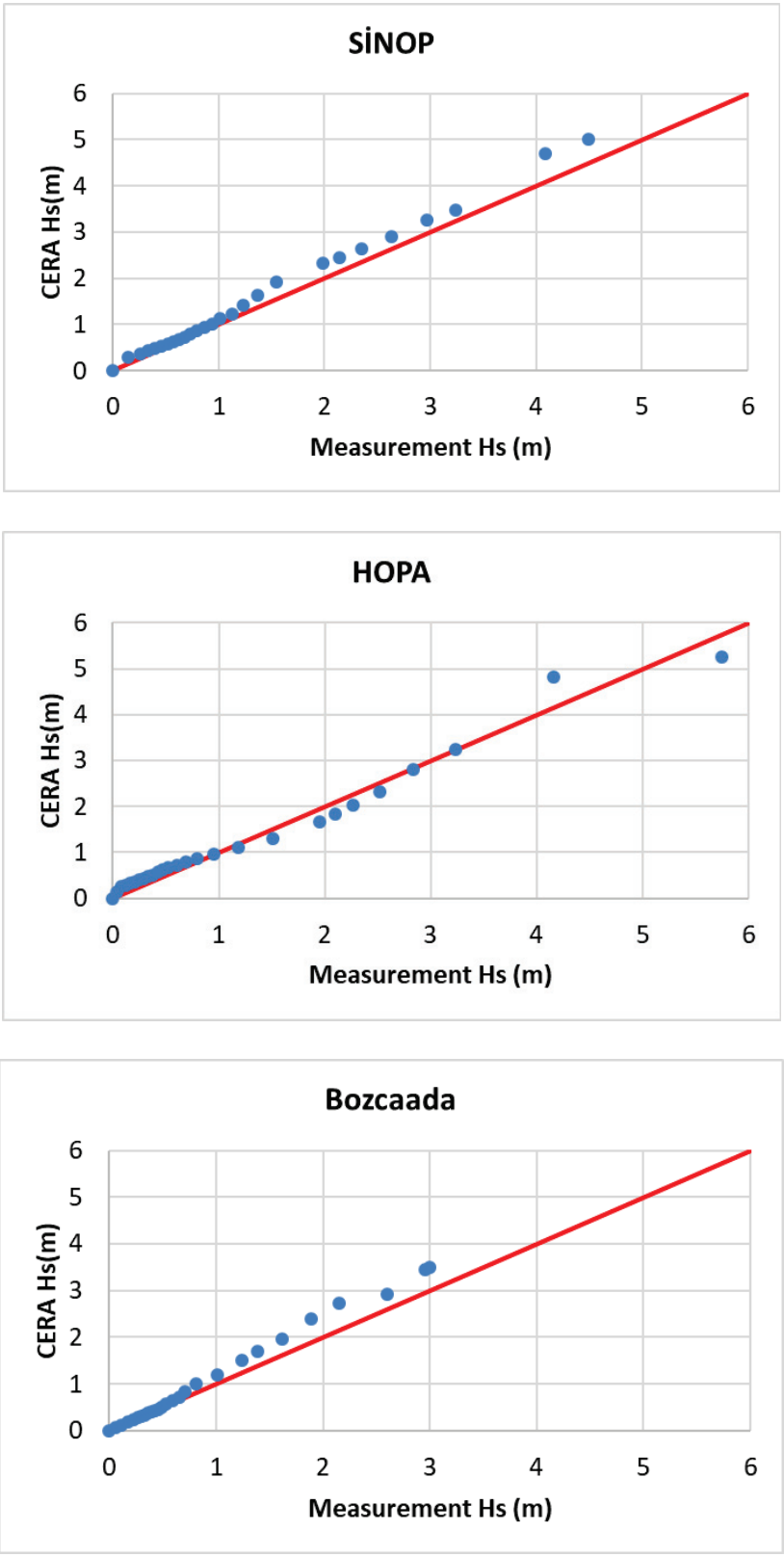

Figure 28. Comparison of CERA-20C Hs Data with in-situ On-Site Measurements after the extensive calibration study for Sinop, Hopa and Bozcaada

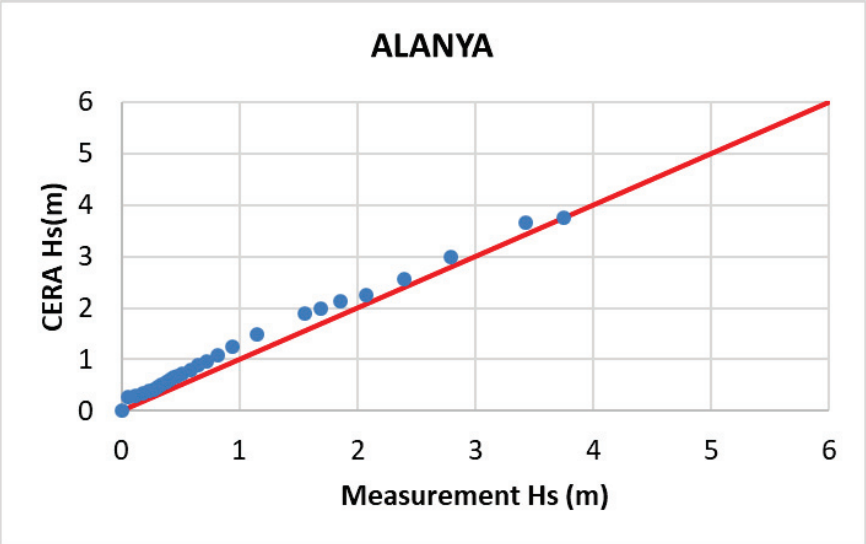

Figure 29. Comparison of CERA-20C Hs Data with in-situ On-Site Measurements after the extensive calibration study for Alanya

Figure 29 represents that, the CERA-20C wave heights are very compatible with the measurement data. Considering the pre-calibration comparisons given in Figure 28, the effect of calibration is quite remarkable. So, it can be said that CERA-20C data became appropriate, to determine the wave climate and design wave heights along the Turkish coasts.

CHAPTER 4

EXTREME WAVE ANALYSIS

4.1. Extreme Wave Statistics and Design Wave Heights

The design wave is an extreme wave that is expected to be exceeded once in a long period such as 30, 50, 100, 200 years. The design wave height is calculated by the extreme wave statistics analysis. For this purpose, the long term climate data are obtained for the study region; the annual maximum data or peak values higher than a threshold wave height are determined; the cumulative probability distributions of the data are obtained; fitted to some theoretical distribution function, extrapolation is performed to estimate the design wave height corresponding to the low probability of occurrence that is once in a given return period .

After the calibration and validation analysis explained in the 3rd Chapter , 110 years of significant wave height data with three hours interval were obtained at the designated points along the Turkish coasts as given in Figure 4. Therefore, unlike the usual design wave estimation which is generally performed with data sets less than 40 years by extrapolation as mentioned above, in this study, design wave heights with a return period of less than 200 years were estimated by interpolation.

In order to estimate the design wave heights with different return periods, first of all, annual maximum significant wave heights were determined for 110 years. Those 110 annual maximum data were arranged in the descending order. It is called as ordered statistics and is used to calculate the nonexceedance probability. Here the order number is expressed with (Goda, 2000). The best-known formula to calculate the nonexceedance probability (plotting position formula) is the Weibull formula given in Eq.5 (Goda, 2000).

$$P(Hs < Hs^*) = 1 - \frac{m}{N+1} \tag{5}$$

where; Hs is the significant wave height, Hs* is any specified value, P (Hs<Hs*) is the probability of nonexceedance, m= order number, N=data number

(Goda & Kobune, 1990) show that Eq.5 may produce a positive bias in the estimation of the design wave height. Therefore, another formula providing unbiased results is used in this study. It is given in Eq. 6

$$P(Hs < Hs^*) = 1 - \frac{m-\alpha}{N+\beta} \quad (6)$$

where; a and b are the coefficients changing according to the used theoretical distribution function. The coefficients are given in Table 5 for different distribution functions that are frequently used.

Table 8. The coefficient α and β for frequently used distributions (Goda, 2000)

	Gumbel	FT-II	Weibull	Log-Normal
α	0.44	0.44+0.52/k	0.2+0.27/√k	0.375
β	0.12	0.12-0.11/k	0.2+0.23/√k	0.25

Then Fisher Tippet I (Gumble) distribution, which is widely used in the extreme value analysis, was selected to fit the nonexceedance probabilities calculated by Eq.6 as a theoretical distribution function. Gumble distribution function is given in Eq.7 (Goda, 2000):

$$P(Hs < Hs^*) = exp\left[-exp\left(-\frac{Hs-B}{A}\right)\right] \quad : -\infty < Hs < \infty \quad (7)$$

where; A and B are the scale and the location parameters, respectively. Fitting the calculated nonexceedance probabilities to a distribution function is performed by obtaining the A and B parameters. There are different methods to obtain A and B parameters like least square, method of moments and maximum likelihood method. In this study, the least squares method was used. It is possible to re-write the Eq 7 as given below:

$$Hs=[-\ln(-\ln(P(Hs<Hs^*))]*A+B \quad (8)$$

-ln(-ln(P(Hs<Hs*) values calculated by Eq.6 versus Hs were plotted and the line best fitting to the points were obtained by the least square method. The parameters A and B in Eq. (7) and (8) are calculated from the slope and the intercept, respectively.

As an example, fitting the 110 annual maximum significant wave data of the point A1 to the Gumbel distribution function is given in Figure 30 together with 95% confidence limits. The plots for the other grid points are given in the Appendix.

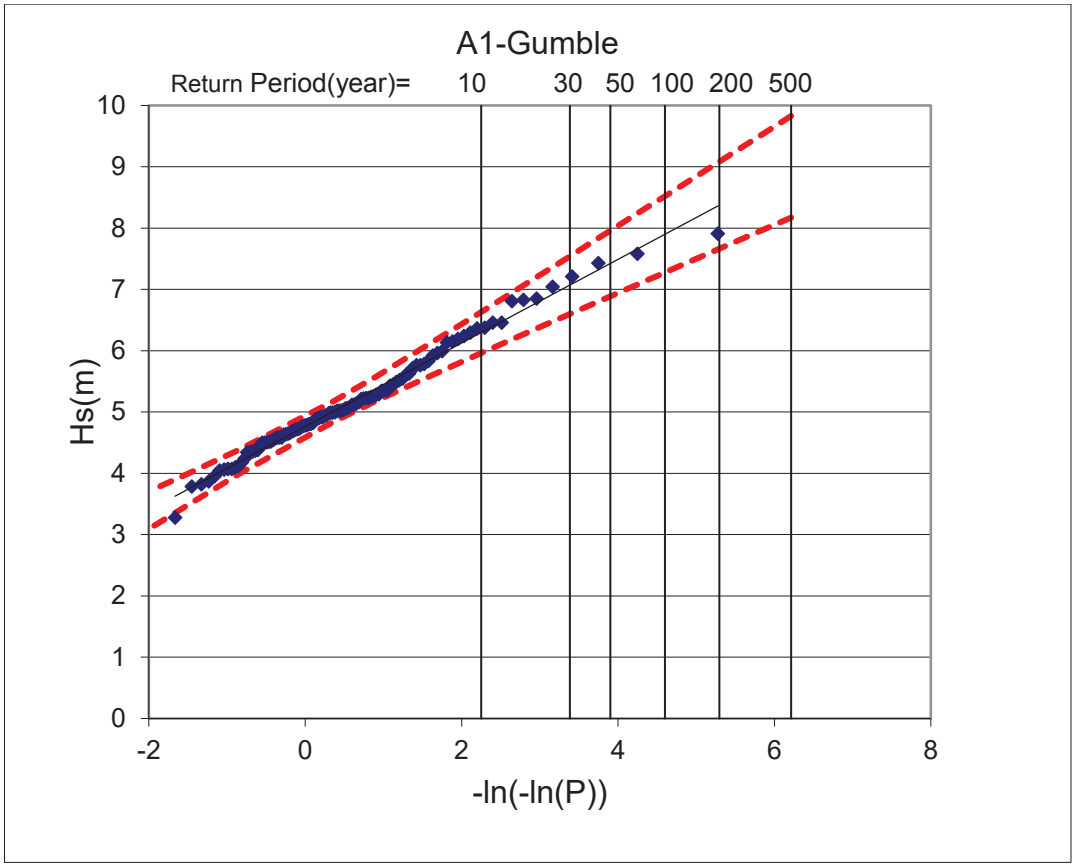

Figure 30. Fitting to Gumbel distribution function by the least square method for the point A1

Figure 30 shows that the data remains in the 95% confidence limits. It is possible to find the design significant wave height (Hs) corresponding to the return periods (Rp) given in the upper axis of the graph. The design Hs values that are corresponding to the 50 and 100 years return periods are the most commonly used design wave heights in the coastal and marine activities. Therefore, the design wave heights for Rp=50 and 100 years for 40 points along the Turkish coasts were calculated and displayed on the map in Figure 31.

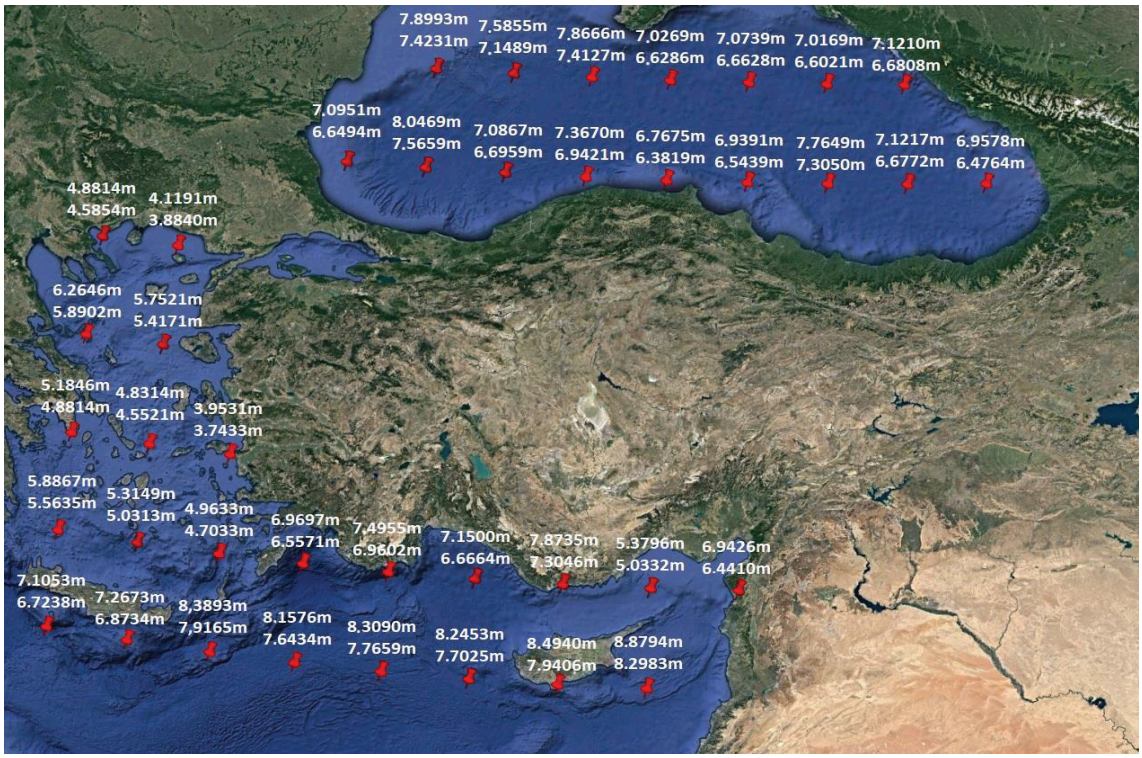

Figure 31. Hs values corresponding to the return periods of 50 and 100 years (lower value is for 50 years)

Figure 31 shows that, the highest design wave in the Black Sea is in the Western Black Sea with H_{50} = 7.57 m, H_{100} = 8.05 m. Moreover, design waves are higher in the Western Black Sea than Eastern Black Sea.

In the Aegean Sea, the highest design wave was calculated in the North Aegean Sea with, H50 = 5.89m, H100 = 6.26m. 50 year design wave height reduces to almost 4m in Turkish coasts of Aegean Sea.

In the Mediterranean, higher design waves were observed in the offshore region compared to regions close to coastal area as expected. The highest design wave was calculated in Antalya Mersin line with H50 = 7.3m and H100 = 7.87m.

After the design wave heights for Rp=50 and 100 years for 40 points along the Turkish coasts were calculated, they were compared with the results given in The Wind and Deep water Wave Atlas Along The Turkish Coasts (Özhan & Abdalla, 2002) which has been widely used by Turkish designers and researchers. For the extreme analysis, the maximum annual wave data covering 20 years for Black Sea and 17 years for Mediterranean and Aegean Seas were fitted to Gumbel distribution. The Wave Atlas

results are given in a resolution of 0.3 degrees in longitude and 0.25 degrees in latitude. Comparison results are summarized as the latitude and the longitude of the points, design wave heights calculated by the current study and the Wave Atlas for Rp=50 years in Table 9. The lower and upper confidence limits of the design wave heights, H50 corresponding to 99% confidence level are also presented in Table 9. Table 10 gives the similar summary for the design wave heights with Rp= 100 years.

As it can be seen in Table 9 and Table 10, it was not possible to find the results of offshore points in the Atlas because offshore points are out of the scope of the Atlas study. For the points other than the offshore region, results with closer coordinates were selected from the Atlas and the results were compared. Table 9 and Table 10 indicate that design waves obtained in the current research are lower than the results provided by Atlas. Figure 32 also shows the H50 comparison of the Wave Atlas results and the results of the current study together with the confidence intervals. As can be seen in Figure 32, while the agreement is better in the eastern Black Sea, the difference between the Atlas and current study is high in the Aegean Sea (areas between 18-26). Kutupoğlu et al. (2018) also state that the Atlas overestimates the design values in Marmara Sea and Aegean Sea. Considering the fact that the maximum annual wave data covering 20 years for Black Sea and 17 years for Mediterranean and Aegean Seas were for the extreme analysis of the Atlas, the current research with 110 years of data has an important advantage considering the reliability of the results.

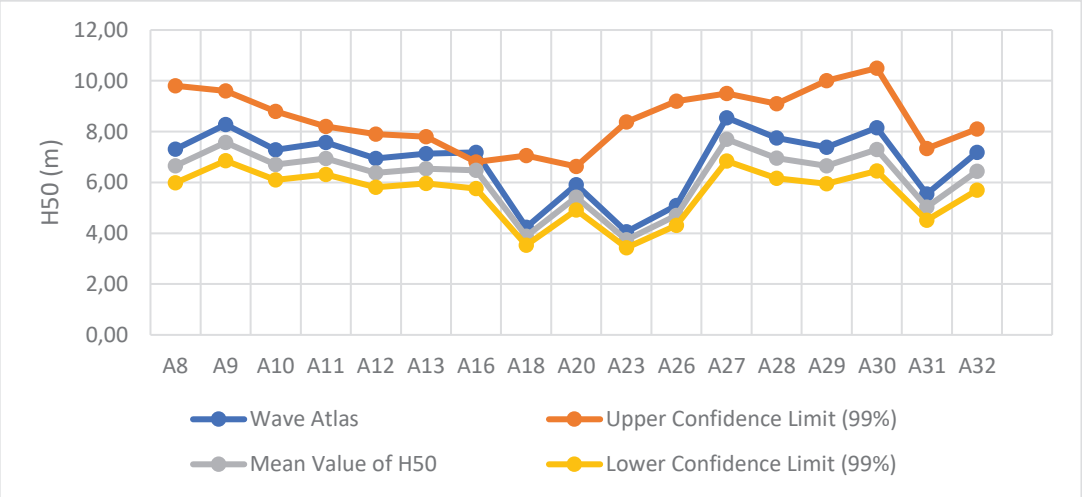

Figure 32. The comparison for H50 of the Wave Atlas and the current study

Table 9. Comparison of Hs50 results with Wave Atlas (Özhan and Abdalla, 2002)

Point	Lat.	Long.	Hs50 99% Lower Confidence Limit (m)	Mean Value Hs50 (m)	Hs50 99% Upper Confidence Limit (m)	Wave Atlas Hs (50yrs)
A1	43.50	30.00	6.72	7.42	8.13	x
A2	43.50	31.50	6.50	7.15	7.80	x
A3	43.50	33.00	6.74	7.41	8.09	x
A4	43.50	34.50	5.51	6.63	6.46	x
A5	43.50	36.00	6.05	6.66	7.28	x
A6	43.50	37.50	5.99	6.60	7.22	x
A7	43.50	39.00	6.03	6.68	7.33	x
A8	42.00	28.50	5.99	6.65	7.31	9.8
A9	42.00	30.00	6.85	7.57	8.28	9.6
A10	42.00	31.50	6.10	6.70	7.29	8.8
A11	42.00	33.00	6.31	6.94	7.57	8.2
A12	42.00	34.50	5.81	6.38	6.95	7.9
A13	42.00	36.00	5.96	6.54	7.13	7.8
A14	42.00	37.50	6.62	7.31	7.99	x
A15	42.00	39.00	6.01	6.68	7.34	x
A16	42.00	40.50	5.76	6.48	7.19	6.8
A17	40.50	24.00	4.14	4.59	5.03	x
A18	40.50	25.50	3.54	3.88	4.23	7.06
A19	39.00	24.00	5.33	5.89	6.45	x
A20	39.00	25.50	4.92	5.42	5.91	6.63
A21	37.50	24.00	4.43	4.88	5.34	x
A22	37.50	25.50	5.22	5.75	6.27	x
A23	37.50	27.00	3.43	3.74	4.06	8.38
A24	36.00	24.00	5.09	5.56	6.04	x
A25	36.00	25.50	4.61	5.03	5.45	x
A26	36.00	27.00	4.32	4.70	5.09	9.2
A27	36.00	28.50	6.85	7.70	8.55	9.5
A28	36.00	30.00	6.17	6.96	7.75	9.1
A29	36.00	31.50	5.95	6.66	7.39	10
A30	36.00	33.00	6.46	7.30	8.15	10.5
A31	36.00	34.50	4.51	5.03	5.55	7.33
A32	36.00	36.00	5.69	6.44	7.19	8.1
A33	34.50	24.00	6.16	6.72	7.29	x
A34	34.50	25.50	6.28	6.87	7.46	x
A35	34.50	27.00	7.21	7.92	8.62	x
A36	34.50	28.50	6.88	7.64	8.41	x
A37	34.50	30.00	6.96	7.77	8.57	x
A38	34.50	31.50	6.90	7.70	8.51	x
A39	34.50	33.00	7.12	7.94	8.76	x
A40	34.50	34.50	7.44	8.30	9.16	x

Table 10. Comparison of Hs100 results with Wave Atlas (Özhan and Abdalla, 2002)

Point	Lat.	Long.	Hs100 99% Lower Confidence Limit (m)	Mean Value Hs100 (m)	Hs100 99% Upper Confidence Limit (m)	Wave Atlas Hs (100yrs)
A1	43.50	30.00	7.08	7.90	8.72	x
A2	43.50	31.50	6.83	7.59	8.34	x
A3	43.50	33.00	7.08	7.87	8.65	x
A4	43.50	34.50	5.78	7.03	7.04	x
A5	43.50	36.00	6.36	7.07	7.79	x
A6	43.50	37.50	6.30	7.02	7.73	x
A7	43.50	39.00	6.36	7.12	7.88	x
A8	42.00	28.50	6.33	7.10	7.86	11
A9	42.00	30.00	7.22	8.05	8.87	10
A10	42.00	31.50	6.40	7.09	7.78	9.5
A11	42.00	33.00	6.63	7.37	8.10	8.7
A12	42.00	34.50	6.10	6.77	7.43	8.6
A13	42.00	36.00	6.25	6.94	7.62	8.5
A14	42.00	37.50	6.97	7.76	8.56	x
A15	42.00	39.00	6.35	7.12	7.90	x
A16	42.00	40.50	6.13	6.96	7.79	7.4
A17	40.50	24.00	4.37	4.88	5.40	x
A18	40.50	25.50	3.71	4.12	4.52	7.63
A19	39.00	24.00	5.61	6.26	6.92	x
A20	39.00	25.50	5.17	5.75	6.33	7.06
A21	37.50	24.00	4.66	5.18	5.71	x
A22	37.50	25.50	5.49	6.10	6.70	x
A23	37.50	27.00	3.59	3.95	4.32	9.13
A24	36.00	24.00	5.33	5.89	6.44	x
A25	36.00	25.50	4.83	5.31	5.80	x
A26	36.00	27.00	4.51	4.96	5.41	10
A27	36.00	28.50	7.28	8.27	9.26	10.5
A28	36.00	30.00	6.57	7.50	8.42	10.2
A29	36.00	31.50	6.31	7.15	7.98	11
A30	36.00	33.00	6.89	7.87	8.86	11.75
A31	36.00	34.50	4.78	5.38	5.98	8
A32	36.00	36.00	6.07	6.94	7.81	9.1
A33	34.50	24.00	6.45	7.11	7.76	x
A34	34.50	25.50	6.58	7.27	7.95	x
A35	34.50	27.00	7.57	8.39	9.21	x
A36	34.50	28.50	7.27	8.16	9.04	x
A37	34.50	30.00	7.37	8.31	9.25	x
A38	34.50	31.50	7.31	8.25	9.18	x
A39	34.50	33.00	7.53	8.49	9.45	x
A40	34.50	34.50	7.88	8.88	9.88	x

4.2. Effect of Theoretical Distribution Functions on The Design Wave Height

As described in Section 4.1, the design wave heights were calculated by fitting the nonexceedance probability of the data to Gumble distribution function. Because the assumption that the nonexceedance probability of annual maximum data is obeying to the Gumble distribution function is common in extreme value analysis. However, there are other distribution functions different than Gumble, and the different functions may change the design wave height. Therefore, the best fitting distribution function should be used. Therefore, the design wave heights were also calculated by using the best-fitting function. In order to examine the best fitting distribution, in this study three frequently used functions rather than Gumbel were used as candidate distribution functions. Those are Fisher Tippet II, Log-normal and Weibull distribution functions. Their equations are given below:

Fisher Tippet II

$$P(Hs < Hs^*) = exp\left[-\left(1 + \frac{Hs-B}{kA}\right)^{-k}\right] \qquad : \text{B-kA} < Hs < \infty \tag{9}$$

Weibull

$$P(Hs < Hs^*) = 1 - exp\left[-\left(\frac{Hs-B}{A}\right)^{k}\right] \qquad : \text{B} < Hs < \infty \tag{10}$$

Lognormal

$$F(Hs < Hs^*) = \int_{-\infty}^{x} f(t)\, dt \qquad : 0 < Hs < \infty$$

$$f(Hs) = \frac{1}{\sqrt{2\pi}AHs} exp\left[-\frac{(lnHs-B)^2}{2A^2}\right] \qquad : 0 < Hs < \infty \tag{11}$$

As it can be seen in Eq.(7) and (11) the functions have two variables 'A' and 'B', while Eq.(9) and (10) have three variables 'A', 'B' and 'k'. Variable k is the shape variable because it determines the shape of the distribution. In this study, Gumbel, Log-normal, Fisher Tippet II (k = 2.5, 3.33, 5.0 and 10.0) and Weibull (k = 0.75, 1.0, 1.4, and 2.0) distributions were used to examine the best fitting distribution function.

4.2.1. Fitting of Data to a Distribution Function

Similar fitting analysis done for the Gumbel distribution as explained in Section 4.1 was performed for the other three distribution functions: 110 annual maximum data were arranged in the descending order. Probabilities of the exceedance were calculated by using Eq.6. Plotting position method was used and the line was estimated by the least squares method. The parameters A and B were determined. The four different value were chosen for the parameter k. They were k = 2.5, 3.33, 5.0 10.0 for Fisher Tippet II and k = 0.75, 1.0, 1.4, and 2.0for Weibull distributions.

4.2.2. Examination of the Best Fitting Distribution Function

After the exceedance probabilities of the 110 data of the annual maximum significant heights were fitted to the theoretical distribution functions given in Eq. 7,9,10 and 11. Then, the best fitted distribution function was examined by considering the following criteria:

1. Correlation coefficient, R: Gives a relation between Hs and its reduced variate changing according to the distribution function When the correlation coefficient R is near to 1, the fitting becomes better.

2. Minimum Ratio of Residual Correlation Coefficient (MIR): Residue of Correlation Coefficient is defined as $\Delta r=1 - R$. (Goda & Kobune, 1990) proposed a test to examine the best fitting by using the residue of correlation coefficient. . In their study, probability distribution curves are obtained by using 10,000 numerical simulations for each distribution. Then they derived an empirical formula to estimate mean residue Δr_{mean} given in Eq.(12):

$$\Delta r_{mean} = exp(a + b \ln N + c(\ln N)^2) \quad (12)$$

N refers the number of data. The a, b and c are the empirical coefficients given in Goda (2010). To test the goodness of fit, $\Delta r/\ \Delta r_{mean}$ is calculated. The lower the $\Delta r/\ \Delta r_{mean}$, the better the fitting is.

3. Deviation of Outlier (DOL): Sometimes, the greatest value of the data is much larger than the rest of the data and it is far above the line of fitted distribution curve when the data are plotted. Such a data is called as outlier. In another case, the difference between the largest data and the second largest may be very small and it causes the largest data to remain far below the fitted line. This is also an outlier (Goda, 2010). (Goda & Kobune, 1990) proposed a criterion that can be used to eliminate distributions with outliers. . It is called as deviation of outlier (DOL) criterion. To calculate DOL criterion, the dimensionless deviation is calculated firstly as it is given below:

$$\zeta = \frac{(H_1 - \bar{H})}{s} \tag{13}$$

H_1= highest data;

$\bar{H}$ = The average of significant waves;

S = Standard deviation.

Then, the cumulative distribution curves of ζ were obtained by using 10000 numerical simulation data for each distribution function. If the data's ζ meets the condition of $\zeta_{\%5} < \zeta_{\ data} < \zeta_{\%95}$ then the distribution function is accepted, otherwise it is rejected. $\zeta_{\%5}$ and $\zeta_{\%95}$ correspond to the exceedance probabilities of 0.05 and 0.95, respectively. They are calculated by using Eq. (14).

$$\zeta_{\%95} \text{ and } \zeta_{\%5} = exp(a + b \ln N + c(\ln N)^2) \tag{14}$$

The coefficients a, b, c for both $\zeta_{\%5}$ and $\zeta_{\%95}$are given in Goda (2010).

4. REC (Residue of Correlation coefficient): Goda and Kobune (1990) have also proposed a rejection criterion using the residue of correlation coefficient. In this criterion, residue of Correlation Coefficient is calculated as $\Delta r=1 - R$. If Δr is higher than $\Delta r_{\%95}$ it

is rejected. $\Delta r_{\%95}$ means the residue with exceedance probability of 0.95. The rejection value $\Delta r_{\%95}$ is defined as in Eq. (15):

$$\Delta r_{\%95} = exp(a + b \ln N + c(\ln N)^2) \quad (15)$$

After fitting procedure was completed for 10 candidates of distribution functions used in this study (Gumbel, Log-normal, Fisher Tippet II (k = 2.5, 3.33, 5.0 and 10.0) and Weibull (k = 0.75, 1.0, 1.4, and 2.0)), the criteria for the rejection (REC and DOL) and for the goodness of fitting (R and MIR) were calculated for each candidate. A scoring system was created to decide which distribution function is the best fit according to the results of criteria calculations. In the scoring system, the candidate distribution gets '0' score when it is rejected according to REC or DOL criteria.

However, if it is accepted, , candidate distribution gets '10'. In addition, the candidates are sorted in descending order according to R and MIR values. While the candidate with the highest R is getting '10', the lowest is getting '0'. Oppositely, while the candidate with low MIR value is getting the score '10', the highest is getting '0'. Then all the scores are sum up and the candidate distribution with the highest score is evaluated as the best fitting distribution. It should be noted that in this scoring system, the highest score is 40.

Table 11 shows the best fitting distribution function for each study point along the Turkish coasts together with the design wave height values corresponding to 50 and 100 years return periods. Table 11 indicates that Gumble distribution mostly fits better. especially, in Mediterranean Sea. Both Gumble and Log-normal are better in Black Sea. Moreover, Log-normal is much better in the Aegean Sea. Table 9 and Table 10 also shows the design wave height results of Gumble distribution and it is seen that the design wave height calculated by Gumble distribution is higher than the other distributions.

Example plots of the design wave heights calculated by Weibull and Log-normal distributions which are the best fits for the points A22 and A6 are given in Figure 33 and Figure 34. 95% confidence limits are also shown in the Figures.

Table 11. The Best Matching Distributions and Design Waves

Gumble			Best Fitting Distribution		
Grid no	**Hs50 (m)**	**Hs100 (m)**	**Best Fitting Distribution**	**Hs50 (m)**	**Hs100 (m)**
1	7.42	7.90	Gumbel	7.42	7.90
2	7.15	7.59	Weibull (k4=2.0)	6.96	7.25
3	7.41	7.87	LogNormal	7.15	7.47
4	6.63	7.03	LogNormal	5.85	6.10
5	6.66	7.07	LogNormal	6.48	6.78
6	6.60	7.02	LogNormal	6.38	6.67
7	6.68	7.12	Weibull (k4=2.0)	6.49	6.79
8	6.65	7.10	Gumbel	6.65	7.10
9	7.57	8.05	Weibull (k4=2.0)	7.35	7.67
10	6.70	7.09	LogNormal	6.55	6.83
11	6.02	6.38	LogNormal	5.80	6.05
12	6.98	7.40	Gumbel	6.98	7.40
13	6.54	6.94	LogNormal	6.35	6.63
14	7.31	7.76	Gumbel	7.31	7.76
15	6.68	7.12	Gumbel	6.68	7.12
16	6.48	6.96	Gumbel	6.48	6.96
17	4.59	4.88	Weibull (k4=2.0)	4.45	4.65
18	3.88	4.12	LogNormal	3.75	3.91
19	5.89	6.26	LogNormal	5.78	6.06
20	5.42	5.75	LogNormal	5.24	5.48
21	4.88	5.18	Gumbel	4.88	5.18
22	4.55	4.83	Weibull (k4=2.0)	5.59	5.83
23	3.74	3.95	Gumbel	3.74	3.95
24	5.56	5.89	Gumbel	5.56	5.89
25	5.03	5.31	Gumbel	5.03	5.31
26	4.70	4.96	Weibull (k4=2.0)	4.59	4.77
27	7.70	8.27	LogNormal	7.48	7.93
28	6.96	7.50	Gumbel	6.96	7.50
29	6.03	6.47	Gumbel	6.03	6.47
30	7.30	7.87	Gumbel	7.30	7.87
31	5.03	5.38	Gumbel	5.03	5.38
32	6.44	6.94	Gumbel	6.44	6.94
33	6.72	7.11	Gumbel	6.72	7.11
34	5.92	6.26	Gumbel	3.92	4.14
35	7.92	8.39	Gumbel	7.92	8.39
36	7.64	8.16	Gumbel	5.19	5.53
37	7.77	8.31	Gumbel	7.77	8.31
38	7.70	8.25	Gumbel	7.70	8.25
39	6.79	7.26	Gumbel	6.79	7.26
40	8.30	8.88	Gumbel	8.30	8.88

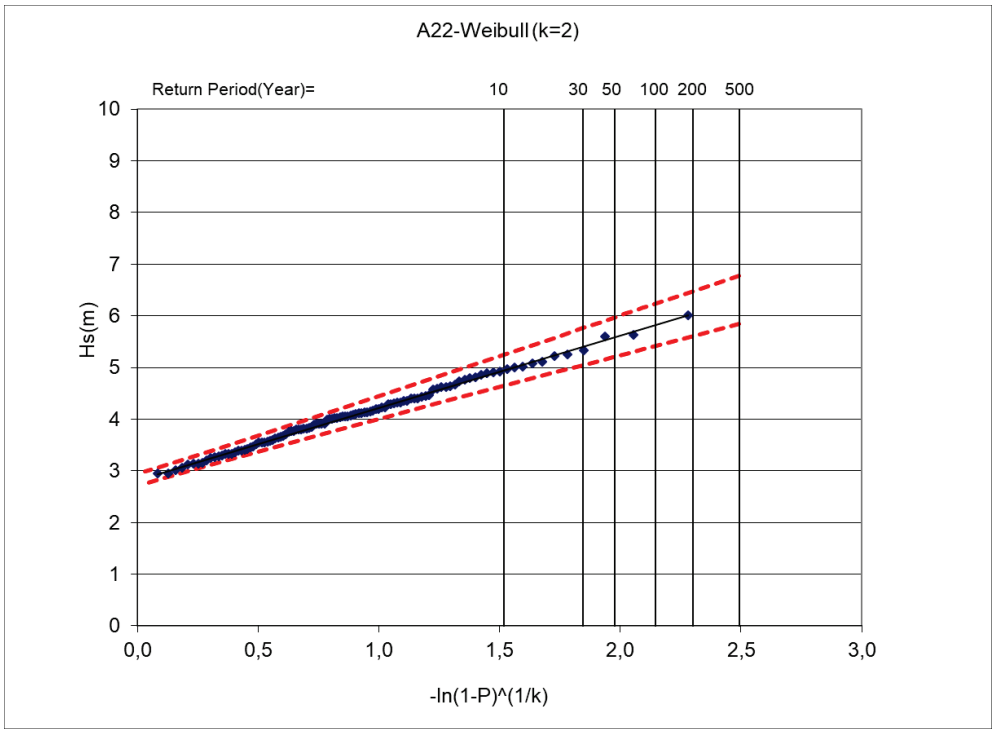

Figure 33. The design wave heights by Weibull distribution function which is the best fit for the point A22

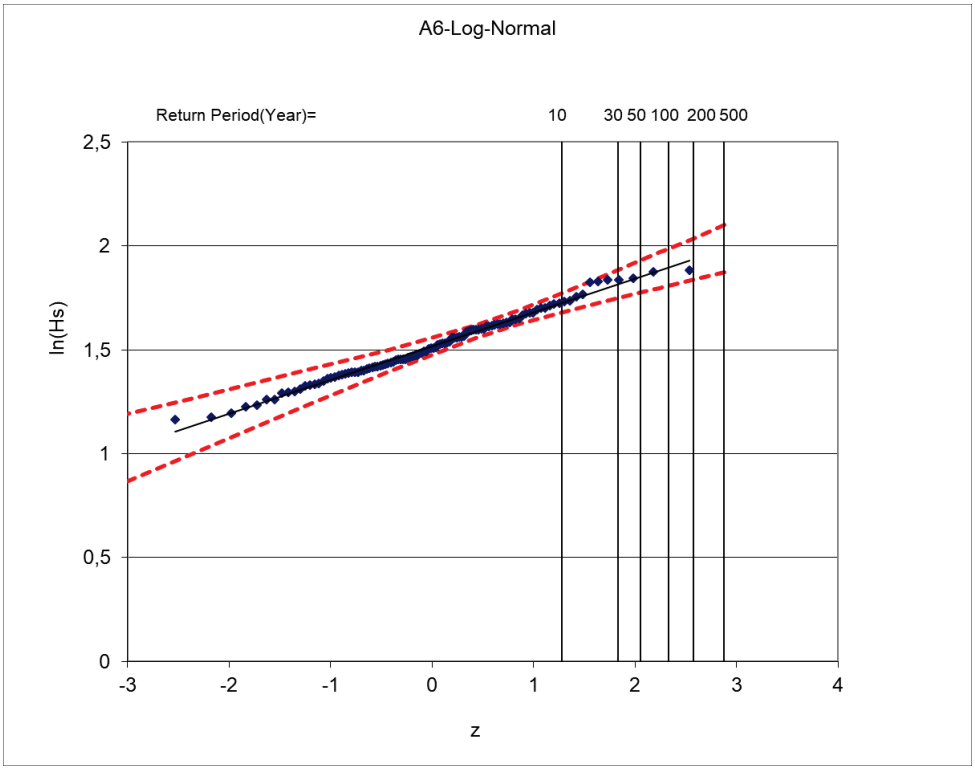

Figure 34. The design wave heights by Log-normal distribution function which is the best fit for the point A6

4.3. Effect of Data Number on the Design Wave Height

The number of data used in the extreme value statistics analysis is also an important parameter that may affect the design wave height. In order to investigate the effect of the number of data, the extreme value analysis was performed for the data of the recent 10 (2001-2010), 20 (1991-2010), 30 (1981-2010), 40 (1971-2010), 50 (1961-2010), 60(1951-2010), 70(1941-2010), 80 (1931-2010), 90(1921-2010), 100(1911-2010) and 110 (1901-2010) years. The design wave heights with the 50 and 100 years return periods were calculated in each analysis. The example comparison is given in Figure 35.

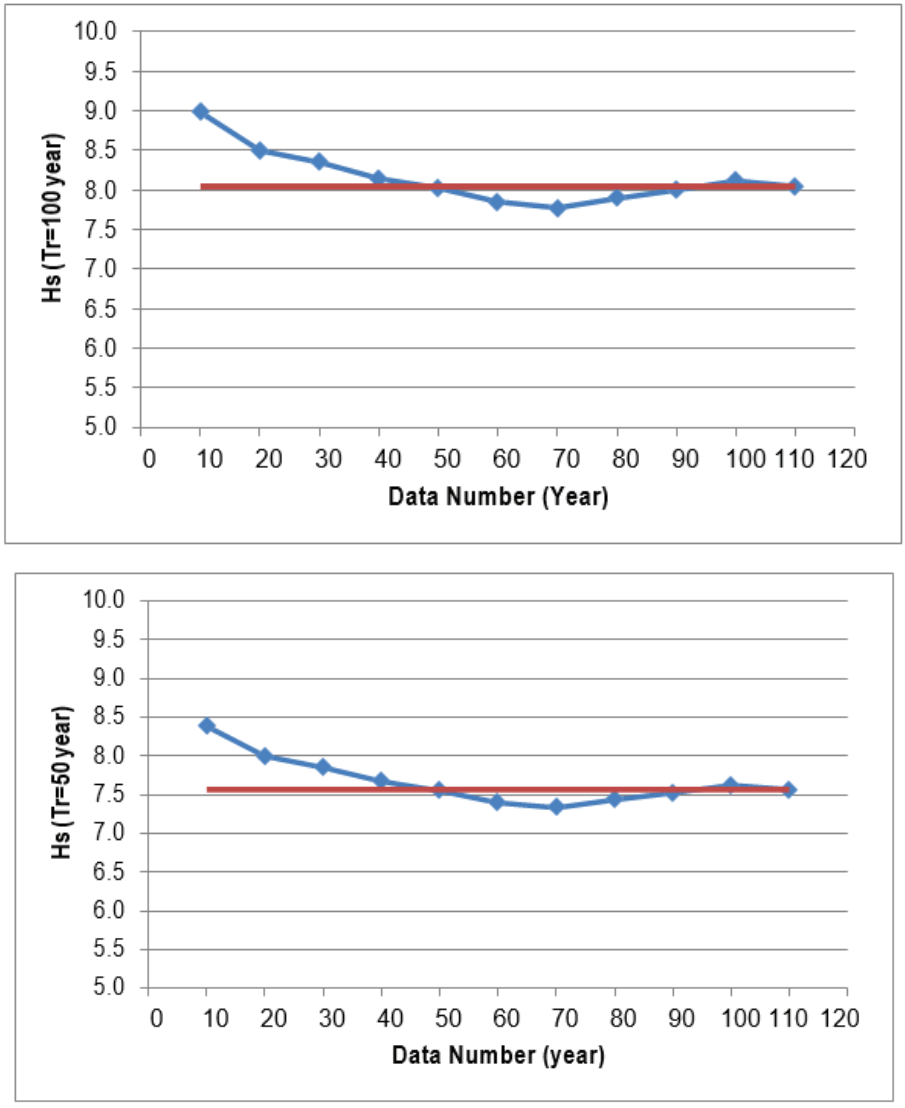

Figure 35. Effect of Data Number on Design Wave Height

Figure 27, when the number of data is less than 30 year, the error increases in the estimation of the design wave height with both 50-year and 100-year return period. The error reaches up to 10%. For example, cube of design wave height is taken in the design of the rubble-mound breakwaters. Although the 10% error does not seem too large, 10% difference in wave height causes an error of 33% in stone weight. This can affect both economy and stability.

CHAPER 5

CLIMATE CHANGE ANALYSIS

The change of annual mean and the maximum wave heights in the past 110 years duration was analyzed for each grid point. The least square method was used to determine the trend. Slopes of the trendline for each grid are given in Table 12. As it can be seen in Table 12, there is a general tendency that both mean and maximum wave heights increase. The maximum increase in the annual maximum wave is in 27th grid which is at the Southwestern part of Turkey. Trendline is given in Figure 36. For the mean wave height, the maximum increase is in the Eastern Black Sea. Trendline is also given in Figure 36.

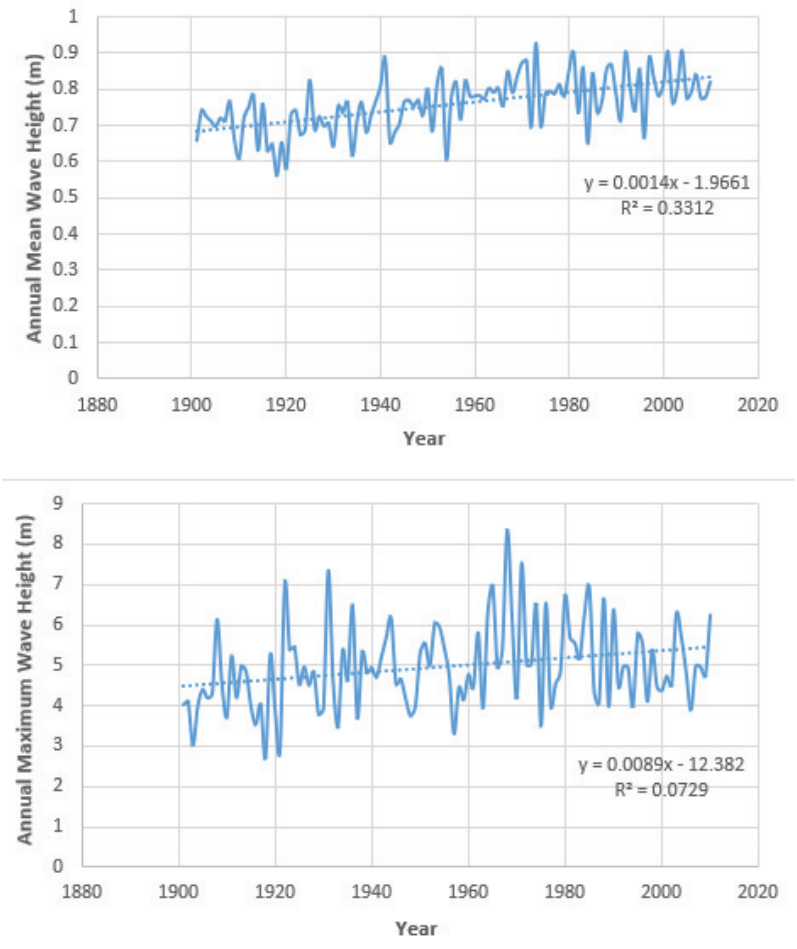

Figure 36. Annual Mean and Maximum Wave Height

Table 12 Changes in the Annual Maximum and Mean Wave Heights

Grid Points	**Annual Maximum (m/year)**	**Annual Mean (m/year)**
1	0.002507	0.000277
2	0.002971	0.000407
3	0.006646	0.000790
4	0.007544	0.000896
5	0.007959	0.001134
6	0.006998	0.001242
7	0.006474	0.001394
8	0.003833	0.000171
9	-0.000140	0.000049
10	0.001845	0.000282
11	0.004500	0.000594
12	0.004900	0.000993
13	0.004131	0.001036
14	0.003005	0.000502
15	0.003755	0.001271
16	0.004877	0.001323
17	0.004769	0.000199
18	0.003471	0.000051
19	0.003413	0.000097
20	0.001039	0.000076
21	0.001048	0.000087
22	-0.000018	0.000134
23	0.001141	0.000277
24	0.000437	0.000205
25	0.000957	0.000298
26	0.003396	0.000654
27	0.008867	0.000894
28	0.006060	0.000721
29	0.007300	0.000672
30	0.004902	0.000646
31	0.004481	0.000552
32	0.004631	0.000664
33	0.000790	0.000374
34	0.001800	0.000506
35	0.004884	0.001066
36	0.004095	0.000277
37	0.003573	0.000871
38	0.003376	0.000885
39	0.002700	0.000732
40	0.004088	0.000909

CHAPTER 6

CONCLUSIONS

In this study, the wave climate along the Turkish coasts was derived based on a century long data of European Centre for Medium-Range Weather Forecasts. For this purpose, firstly, the data set was calibrated and verified by using satellite and in-situ measurements. Then the design waves corresponding to different return periods were determined by extreme statistics. Moreover, the effect of theoretical distribution function and the data number were investigated on the design wave height. Besides, by using calibrated and the verified century-long wave climate data, the wave climate change was investigated. As a result, the following conclusions are derived:

Since European Centre for Medium – Range Weather Forecasts (ECMWF) has produced two century-based reanalysis wave data ERA-20C and CERA-20C , both dataset were compared with ENVISAT data over the whole Black Sea for 2007-2008 as a pilot study in order to decide which century-based data set is appropriate to use in the study. Both data give similar results. However, CERA-20C data is better from the significant wave height view. **Therefore CERA-20C wave data were used in the rest of the study.**

40 default grid points were specified along The Turkish coasts for the study and they are shown in Figure 4. 16 points are in the Black Sea and 24 points in Aegean and Mediterranean Sea. Since there is not any CERA-20C data in the Sea of Marmara, Marmara sea coasts are out of the scope of this study.

After deciding to use the CERA-20C data in the rest of the study, the CERA20C data were compared with in-situ measurements to decide whether calibration was necessary or not. The comparison study was performed for the significant wave height, Hs, the mean period, Tm and the mean wave angle, θm. The comparison was performed by Quantile-Quantile plots (Q-Q plots). Hs values of CERA-20C were lower than the buoy Hs in Hopa and Sinop, they were higher in Bozcaada and Alanya measurements. Tm values of CERA-20C were greater than the buoy data in Bozcaada. There was not

any one-to-one correspondence for mean wave direction. Therefore, the comparison study indicated that **CERA-20C data should be calibrated before they are used for the wave climate analysis along the Turkish coasts.**

Satellite data were used for the calibration. Since any comparison study has not been done for Turkish coasts yet, firstly they were compared with in-situ data before using them for the calibration of CERA-20C data. Considering the results of the comparison study between the satellite RA data and the buoy data, it was decided to use another data source together with the satellite data for the calibration of CERA-20C. It is the recent and the newest data of ECMWF: ERA5. A similar comparison study was carried out for the Hs of the buoys and the ERA5. The error was less compared to the satellite and the buoy comparison. Therefore, **ERA5 data were used together with satellite data in the calibration study of CERA20C.**

In order to be able to calibrate CERA-20C data, the Jason family of satellites (TOPEX/Poseidon, Jason-1 and 2) and ENVISAT family of satellites (ERS-1, ERS-2 and ENVISAT) with data before 2010 in the study area were used. Overlap periods of the satellites were used for inter-calibration of the satellites. **After inter-calibration procedure, data were combined and the satellite wave data with a total duration of 18 years (1995-2012) for Envisat family and 26 years (1992-2017) for Jason family were obtained to calibrate CERA-20C.**

In order to estimate the wave period from satellite records, Artificial Neural Networks (ANN) method was used. In order to train artificial neural network model, the significant wave height, σKu and σC measured by Jason3 satellite during the year 2017, were used as input; ECMWF model data for the same year were used as output. When the model was trained with global data, good results were obtained globally. However, the results obtained for the Mediterranean and Black Sea, which are enclosed seas, were not good. **When the model was trained with regional data, then the test results were significantly better for the enclosed seas and the Turkish coasts.**

Original CERA-20C periods had a better agreement with the measurement compared to the case of Hs. However, it was observed that there were extremely high period results especially in Bozcaada. Therefore, it was decided to calibrate CERA-20C period for Bozcaada with respect to satellite derived wave period. For this purpose, the period from the satellite data was derived by using the neural networks model. Then the

CERA-20C period data was calibrated with respect to the derived period by ANN. **The CERA-20C periods become more compatible with the measurements after the calibration study was performed.**

After the extensive calibration study, the CERA-20C wave height data were compared with the NATO-TU Waves measurements in Hopa, Sinop, Bozcada, Dalaman and Alanya for the verification. As a result, the CERA-20C wave heights agree well to the measurement data. Considering the pre-calibration comparisons, the effect of calibration was quite remarkable. So, it can be said that **CERA-20C data became appropriate to determine the wave climate and design wave heights along the Turkish coasts.**

The design wave heights corresponding to 50 and 100 years return periods calculated by extreme statistical analysis are given in Figure 31. For Black Sea, the highest design wave is H_{50} = 7.57m, H_{100} = 8.05m and it was calculated in the Western Black Sea. Design wave heights in Western Black Sea are higher than the Eastern part. In the Aegean Sea, the highest design wave was calculated in the North Aegean Sea with, H_{50} = 5.89m, H_{100} = 6.26m. 50-year design wave height reduces to almost 4m in Turkish coasts of Aegean Sea. In the Mediterranean, higher design waves were observed in the offshore region compared to regions close to coastal area as expected. The highest design wave was calculated in Antalya Mersin line with H_{50} = 7.3m and H_{100} = 7.87m.

After the design wave heights for Rp=50 and 100 years for 40 points along the Turkish coasts were calculated together with the 99% confidence limits, they were compared with the results given in The Wind and Deep Water Wave Atlas Along The Turkish Coasts (Özhan & Abdalla, 2002) which has been widely used by Turkish designers and researchers. Comparison results indicate that design waves obtained in the current research are lower than the results provided by Atlas. Especially , the difference is high in the Aegean Sea. Kutupoğlu et al. (2018) also state that the Atlas overestimates the design values in Marmara Sea and Aegean Sea. Considering the fact that the maximum annual wave data covering 20 years for Black Sea and 17 years for Mediterranean and Aegean Seas were for the extreme analysis of the Atlas, the current research with 110 years of data has an important advantage considering the reliability of the results.

The effect of the distribution function on the design wave height was also investigated. Gumbel, Log-normal, Fisher Tippet II (k = 2.5, 3.33, 5.0 and 10.0) and Weibull (k = 0.75, 1.0, 1.4, and 2.0) distributions were used to examine the best fitting distribution function. The examination results indicate that Gumble distribution mostly fits better, especially, in Mediterranean Sea. Both Gumble and Log-normal are better in Black Sea. In fact, Log-normal is much better in the Aegean Sea. Table 9 and Table 10 also shows the design wave height results of Gumble distribution and it is seen that the design wave height calculated by Gumble distribution is higher than the other distributions.

The change of annual mean and the maximum wave heights in the past 110 years duration was analyzed for each grid point. The least square method was used to determine the trend. Results show that **there is a general tendency that both mean and maximum wave heights increase along the Turkish coasts.** While the maximum increase in the annual maximum wave height is determined at the Southwestern part of Turkey, the maximum increase is in the Eastern Black Sea for the mean wave height. Effect of climate change on the coastal structures may be very important. Therefore, **to develop a reliability-based design method to adapt coastal structures design to climate change effect is recommended as a future study.**

REFERENCES

Aarnes, O. J., Abdalla, S., Bidlot, J. R., & Breivik, Ø. (2015). Marine wind and wave height trends at different ERA-interim forecast ranges. *Journal of Climate*, *28*(2), 819–837. https://doi.org/10.1175/JCLI-D-14-00470.1

Abdalla, S. (2013). Wind and wave data selection for climate studies in enclosed seas. *Proceedings of the 10th Global Congress on ICM: Lessons Learned to Address New Challenges, EMECS 2013 - MEDCOAST 2013 Joint Conference*, *2*(November).

Abdalla, S., Janssen, P. A. E. M., & Bidlot, J.-R. (2011). On the accuracy of surface wind and wind-wave data. *Proceedings of the 10th International Conference on the Mediterranean Coastal Environment, MEDCOAST 2011*, *2*(January 2011).

Abdalla, S., & Yilmaz, N. (2015). Suitability of ECMWF ERA-20C for wind and wave climate in the Black Sea. *12th International Conference on the Mediterranean Coastal Environment, MEDCOAST 2015*, *2*(October), 6–10.

Akpinar, A., & Kömürcü, M. I. hsa. (2013). Assessment of wave energy resource of the Black Sea based on 15-year numerical hindcast data. *Applied Energy*, *101*, 502–512. https://doi.org/10.1016/j.apenergy.2012.06.005

Akpinar, A., & Ponce de León, S. (2016). An assessment of the wind re-analyses in the modelling of an extreme sea state in the Black Sea. *Dynamics of Atmospheres and Oceans*, *73*, 61–75. https://doi.org/10.1016/j.dynatmoce.2015.12.002

Akpınar, A., & Bingölbali, B. (2016). Long-term variations of wind and wave conditions in the coastal regions of the Black Sea. *Natural Hazards*, *84*(1), 69–92. https://doi.org/10.1007/s11069-016-2407-9

Alpar, B. (2009). Vulnerability of Turkish coasts to accelerated sea-level rise. *Geomorphology*, *107*(1–2), 58–63. https://doi.org/10.1016/j.geomorph.2007.05.021

Ar Güner, H. A., Yüksel, Y., & Özkan Çevik, E. (2013). Estimation of wave parameters based on nearshore wind-wave correlations. *Ocean Engineering*, *63*, 52–62. https://doi.org/10.1016/j.oceaneng.2013.01.023

Ayat, B. (2013). Wave power atlas of Eastern Mediterranean and Aegean Seas. *Energy*, *54*, 251–262. https://doi.org/10.1016/j.energy.2013.02.060

Aydoĝan, B., Ayat, B., & Yüksel, Y. (2013). Black Sea wave energy atlas from 13 years hindcasted wave data. *Renewable Energy*, *57*, 436–447. https://doi.org/10.1016/j.renene.2013.01.047

Badulin, S. I. (2014). A physical model of sea wave period from altimeter data. *Journal of Geophysical Research: Oceans*, *119*(2).

Balas, L. (n.d.). HYDROTAM-3D Dalga İklimi Modelleme. Retrieved from HYDROTAM-3D Dalga İklimi Modelleme

Bilyay, E., Ozbahceci, B. O., & Yalciner, A. C. (2011). Extreme waves at filyos, southern black sea. *Natural Hazards and Earth System Science*, *11*(3), 659–666. https://doi.org/10.5194/nhess-11-659-2011

Compo, G. P., Whitaker, J. S., Sardeshmukh, P. D., Matsui, N., Allan, R. J., Yin, X., … Worley, S. J. (2011). The Twentieth Century Reanalysis Project. *Quarterly Journal of the Royal Meteorological Society*, *137*(654), 1–28. https://doi.org/10.1002/qj.776

Dada, O. A., Li, G., Qiao, L., Ma, Y., Ding, D., Xu, J., … Yang, J. (2016). Response of waves and coastline evolution to climate variability off the Niger Delta coast during the past 110 years. *Journal of Marine Systems*, *160*, 64–80. https://doi.org/10.1016/j.jmarsys.2016.04.005

Dee, D. P., Uppala, S. M., Simmons, A. J., Berrisford, P., Poli, P., Kobayashi, S., … Vitart, F. (2011). The ERA-Interim reanalysis: Configuration and performance of the data assimilation system. *Quarterly Journal of the Royal Meteorological Society*, *137*(656), 553–597. https://doi.org/10.1002/qj.828

Doğan, M., Ciioglu, H. K., Sanli, D. U., & Ulke, A. (2015). Investigation of sea level anomalies related with NAO along the west coasts of Turkey and their consistency with sea surface temperature trends. *Theoretical and Applied Climatology*, *121*(1–2), 349–358.

ECMWF. (n.d.). ERA 5. Retrieved from https://www.ecmwf.int/en/forecasts/datasets/reanalysis-datasets/era5

EROL, O. (1990). Impacts of sea-level rise on Turkey. *Changing Climate and the Coast*, 183–200.

EROL, O. (1991). Turkey and Cyprus. *The World Coastline*, 491–500.

Goda, Y. (2000). *Random Seas and Design of Maritime Structures*. London: World Scientific.

Goda, Y. (2010). Random Seas and Design of Maritime Structures. In *Advanced Series on Ocean Engineering* (3rd ed., p. 732).

Goda, Y., & Kobune, K. (1990, May 27). Distribution Function Fitting for Storm Wave Data. *Coastal Engineering 1990*, pp. 18–31. https://doi.org/doi:10.1061/9780872627765.003

Gommenginger, C. P., Srokosz, M. A., Challenor, P. G., & Cotton, P. D. (2003). Measuring ocean wave period with satellite altimeters: A simple empirical model. *Geophysical Research Letters*, *30*(22), 1–5. https://doi.org/10.1029/2003GL017743

Karaca, M., & Nicholls, R. J. (2008). Potential Implications of Accelerated Sea-Level Rise for Turkey. *Journal of Coastal Research*, *242*(11), 288–298. https://doi.org/10.2112/07a-0003.1

Kumar, P., Min, S. K., Weller, E., Lee, H., & Wang, X. L. (2016). Influence of climate variability on extreme ocean surface wave heights assessed from ERA-interim and ERA-20C. *Journal of Climate*, *29*(11), 4031–4046. https://doi.org/10.1175/JCLI-D-15-0580.1

Kutupoğlu, V., Akpınar, A., Bingölbali, B., & Çakmak, R. E. (2018). *Spatial Distributions of Maximum Significant Wave Heights over the Sea of Marmara*. 617–628.

Mackay, E. B. L., Retzler, C. H., Challenor, P. G., & Gommenginger, C. P. (2008). A parametric model for ocean wave period from Ku band altimeter data. *Journal of Geophysical Research: Oceans*, *113*(3), 1–16. https://doi.org/10.1029/2007JC004438

Neural Network Concepts. (n.d.). Retrieved from https://missinglink.ai/guides/neural-network-concepts/complete-guide-artificial-neural-networks/

Özhan, E., & Abdalla, S. (1999). Wind and Wave Climatologhy of Turkish Coasts and The Black Sea: An Overview of the NATO TU_WAVES Project. *MEDCOAST Conference on Wind and Wave Climate of the Mediterranean and the Black Sea*, 1–20. Antalya.

Özhan, E., & Abdalla, S. (2002). *Wind & Deep Water Wave Atlas for Turkish Coast* Ankara: TMK/MEDCOAST.

Özyurt, G., & Ergin, A. (2009). Application of Sea Level Rise Vulnerability Assessment Model to Selected Coastal Areas of Turkey Application of Sea Level Rise Vulnerability Assessment Model Selected Coastal Areas of Turkey. *Journal of Coastal Research*, *56*(56), 248–251.

Özyurt, G., Ergin, A., & Baykal, C. (2010). Coastal Engineering 2010 Coastal Vulnerability Assessment To Sea Level Rise Integrated With. *Proceedings of the Coastal Engineering 2010 Conference*, 1–8.

Patra, A., & Bhaskaran, P. K. (2017). Temporal variability in wind–wave climate and its validation with ESSO-NIOT wave atlas for the head Bay of Bengal. *Climate Dynamics*, *49*(4), 1271–1288. https://doi.org/10.1007/s00382-016-3385-z

Poli, P., Hersbach, H., Dee, D. P., Berrisford, P., Simmons, A. J., Vitart, F., … Fisher, M. (2016). ERA-20C: An atmospheric reanalysis of the twentieth century. *Journal of Climate*, *29*(11), 4083–4097. https://doi.org/10.1175/JCLI-D-15-0556.1

Poli, P., Hersbach, H., Tan, D., Dee, D., Thépaut, J.-N., Simmons, A., … Fisher, M. (2015). *ERA report series: The data assimilation system and initial performance evaluation of the ECMWF pilot reanalysis of the 20th-century assimilating surface observations only (ERA-20C)*. 1–62.

Quilfen, Y., Chapron, B., Collard, F., & Serre, M. (2004). Calibration/validation of an altimeter wave period model and application to TOPEX/Poseidon and Jason-1 altimeters. *Marine Geodesy*, *27*(3–4), 535–549. https://doi.org/10.1080/01490410490902025

Scharroo, R., Lillibridge, J., Oceanic, N., Byrne, D., Oceanic, N., & Naeije, M. (2013). *RADS : Consistent multi-mission products RADS : Consistent Multi-Mission Products*. (January), 2–6.

Simav, Ö., Şeker, D. Z., & Gazioğlu, C. (2013). Coastal inundation due to sea level rise and extreme sea state and its potential impacts: ??ukurova Delta case. *Turkish Journal of Earth Sciences*, *22*(4), 671–680. https://doi.org/10.3906/yer-1205-3

Ulaştırma Kıyı Yapıları Master Plan Çalışması. (2010).

Young, I. R., Zieger, S., & Babanin, A. V. (2011). Global trends in wind speed and wave height. *Science*, *332*(6028), 451–455. https://doi.org/10.1126/science.1197219

APPENDIX A

EXTREME WAVE STATISTICS RESULTS

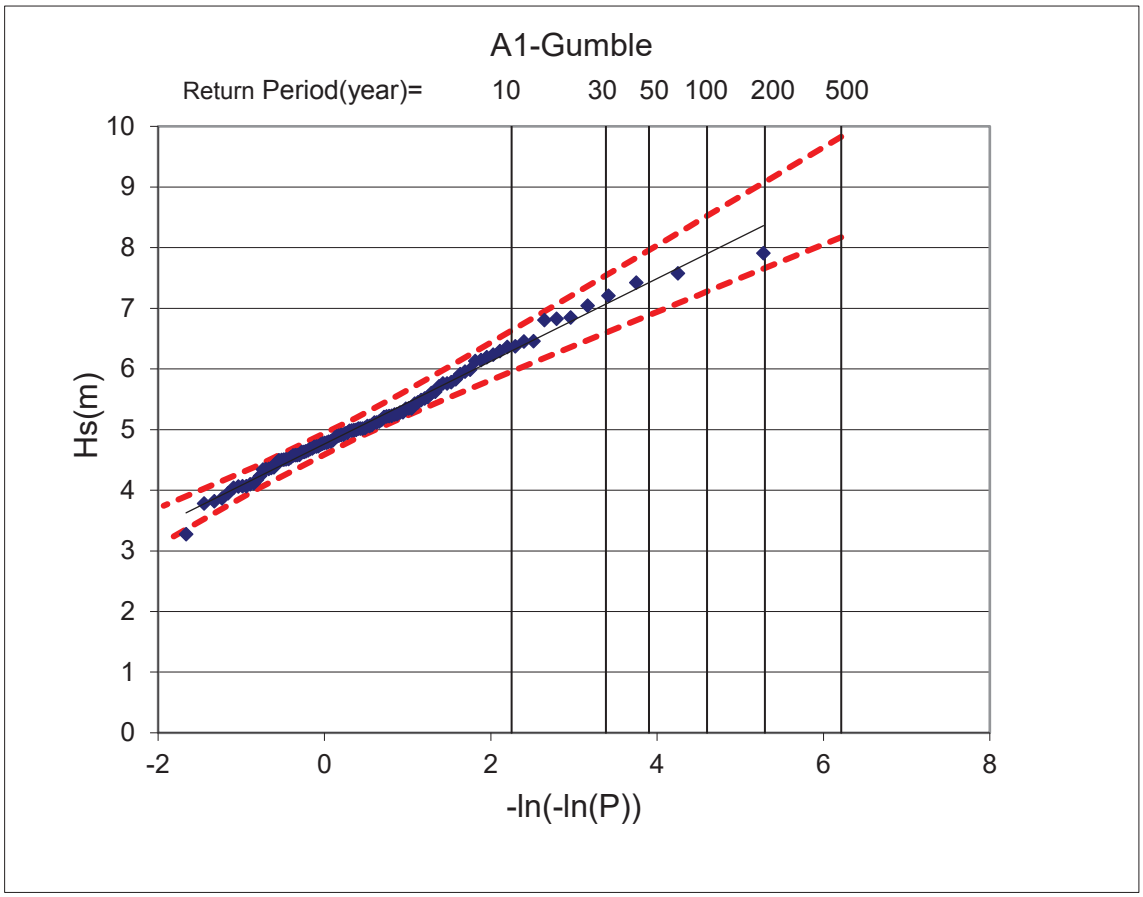

Figure 37. Extreme wave statistics results for A1

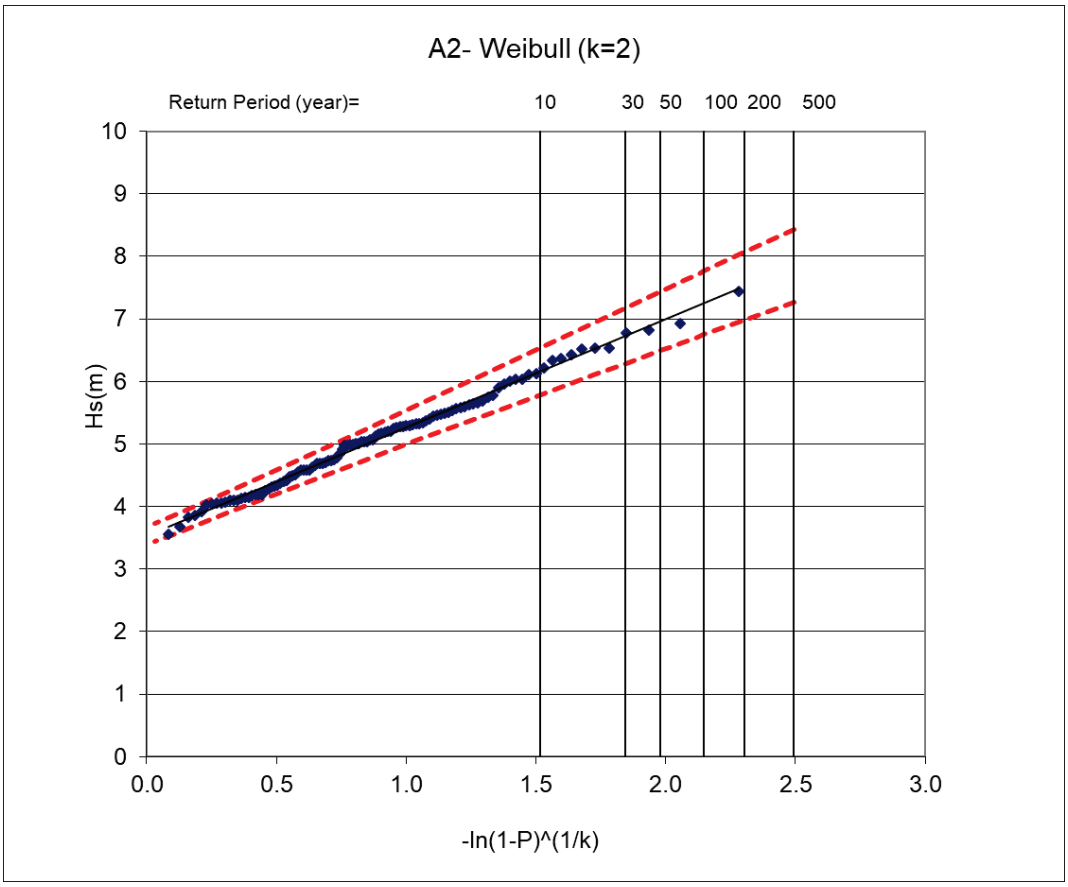

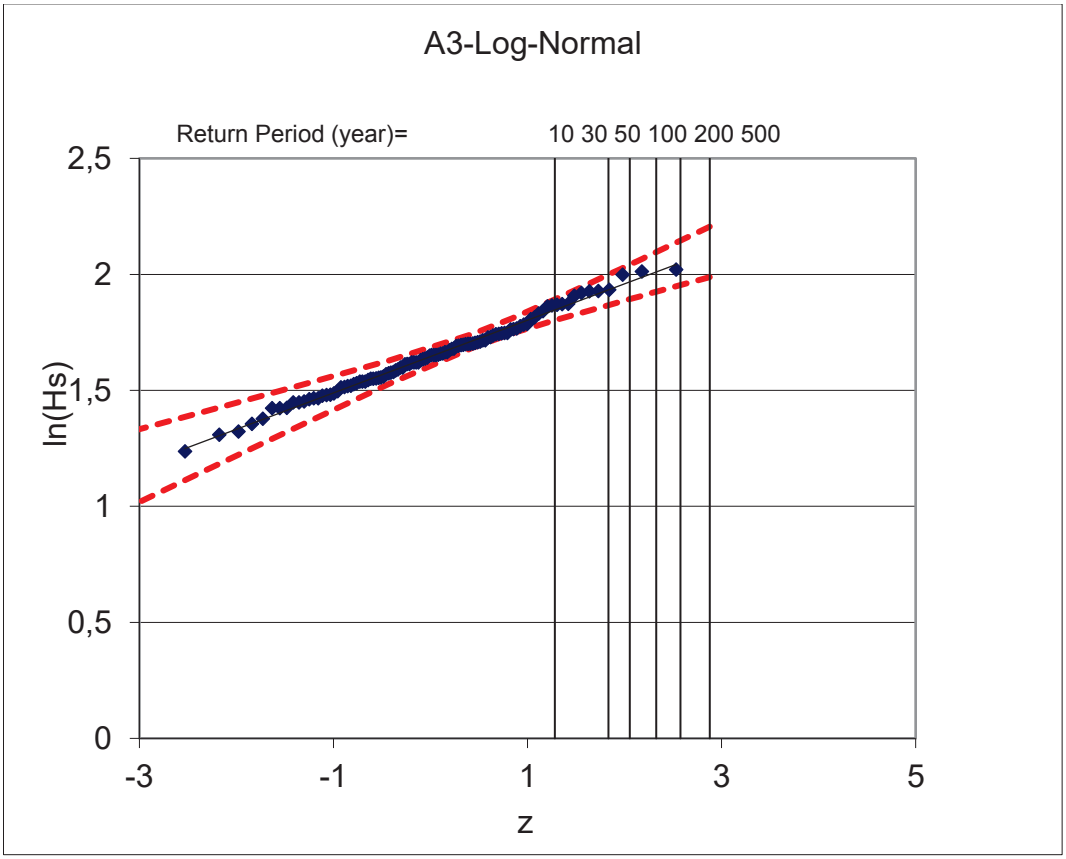

Figure 38. Extreme wave statistics results for A2 and A3

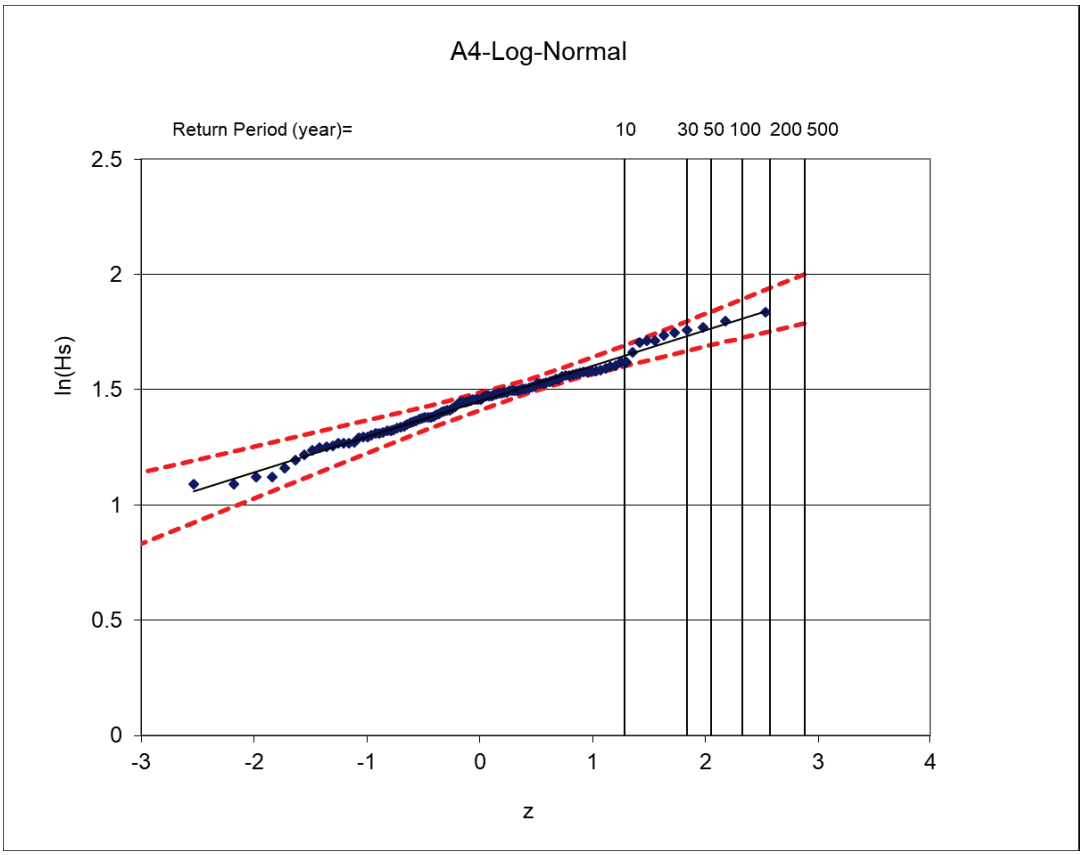

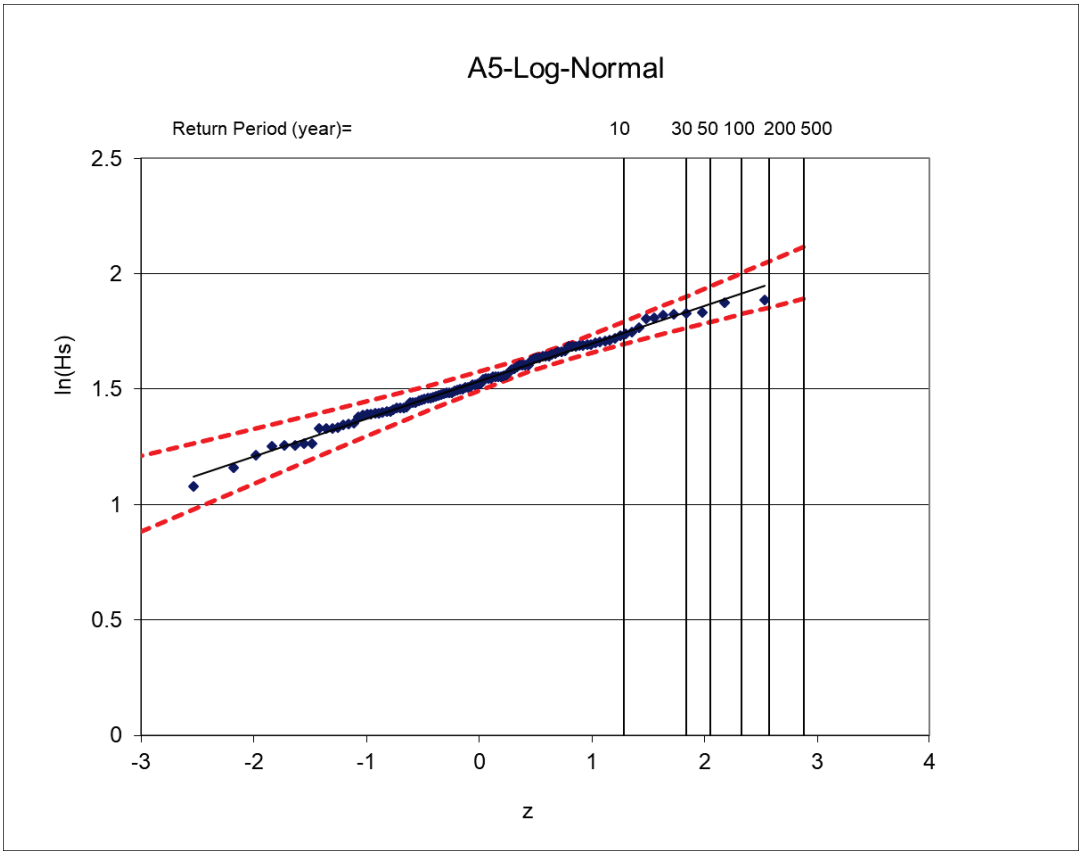

Figure 39. Extreme wave statistics results for A4 and A5

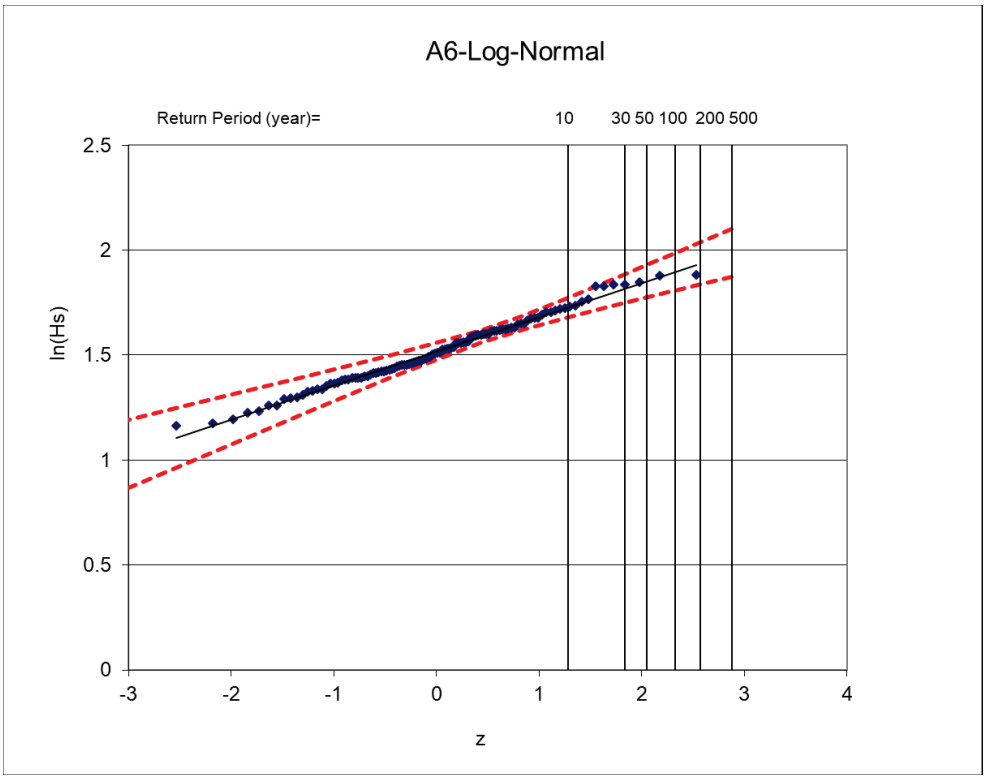

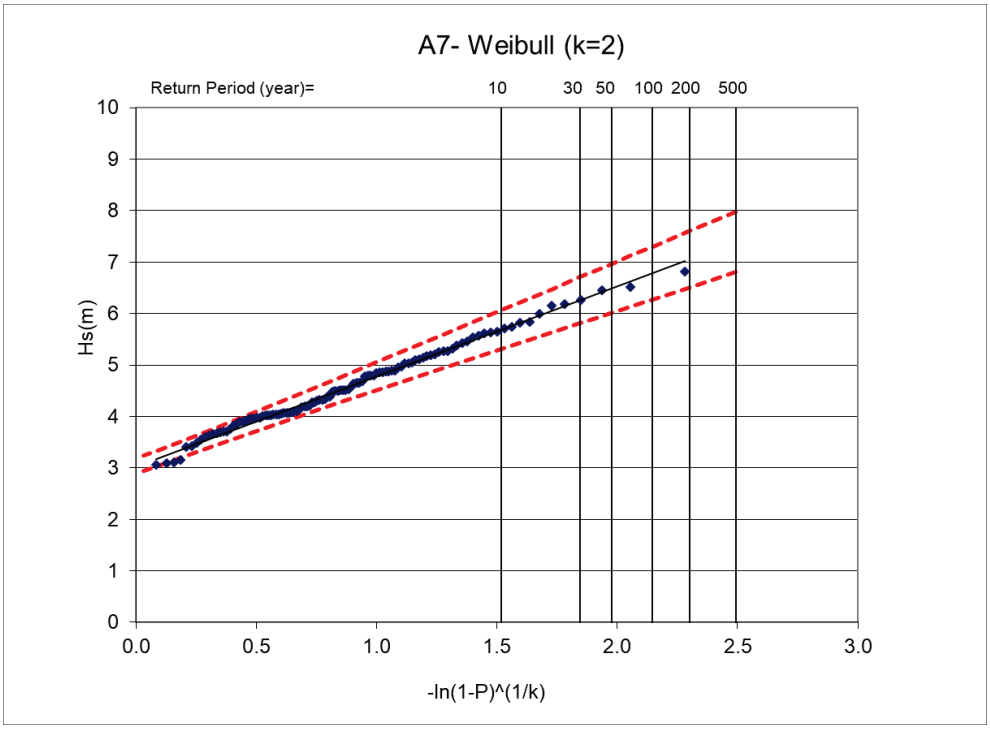

Figure 40. Extreme wave statistics results for A6 and A7

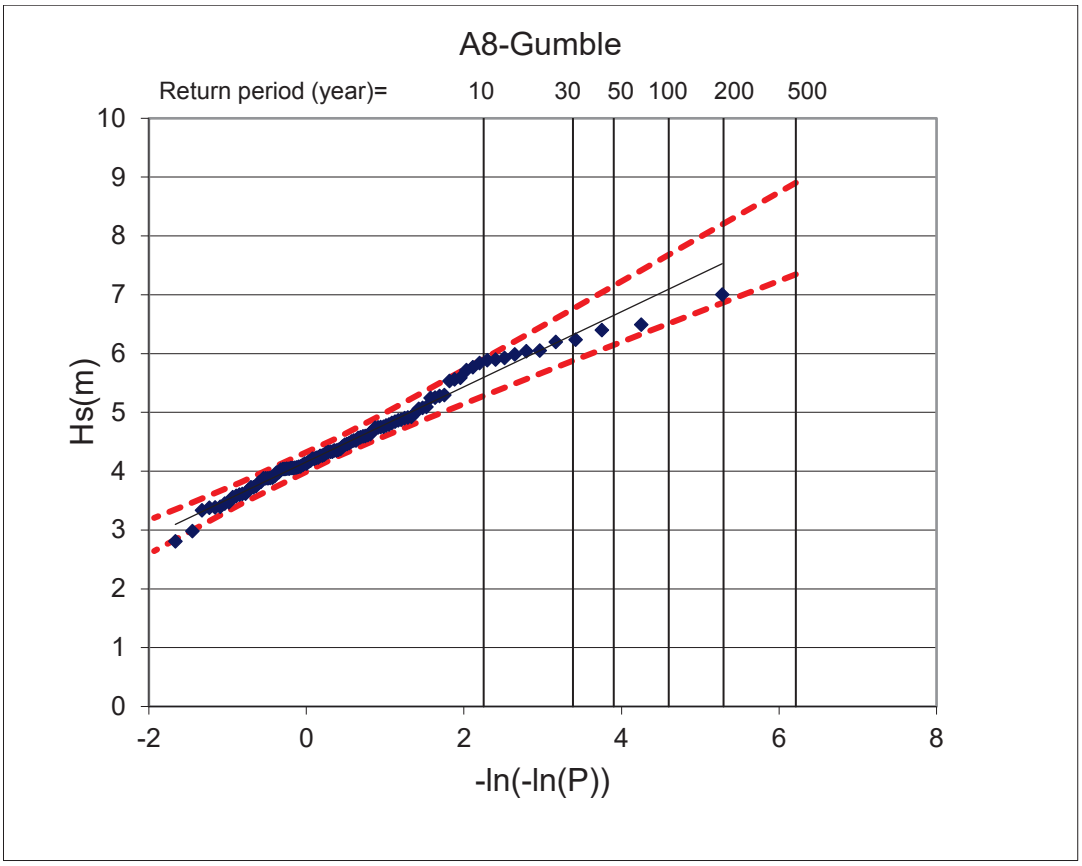

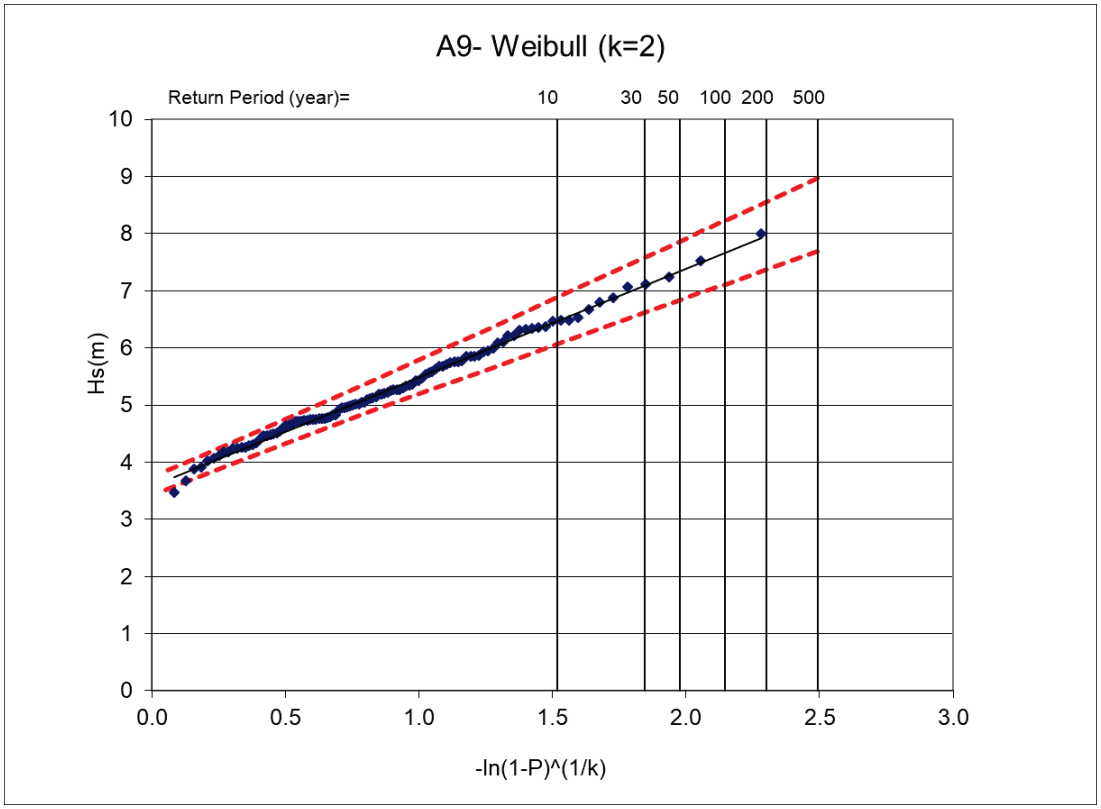

Figure 41. Extreme wave statistics results for A8 and A9

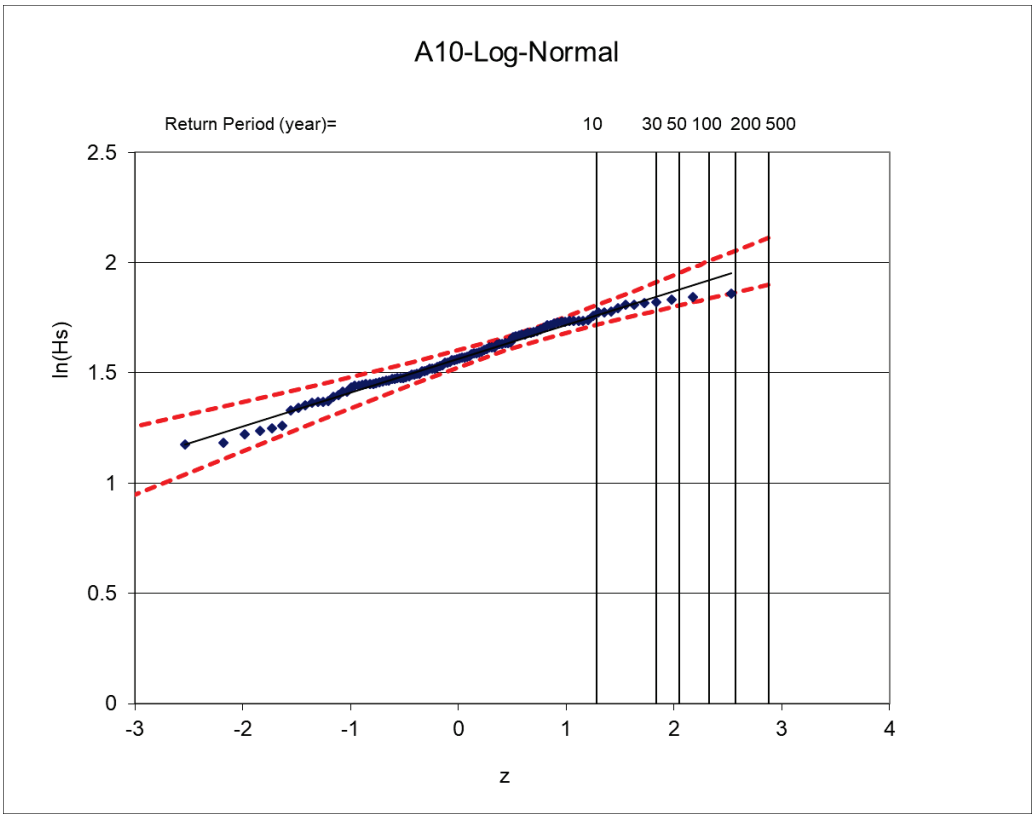

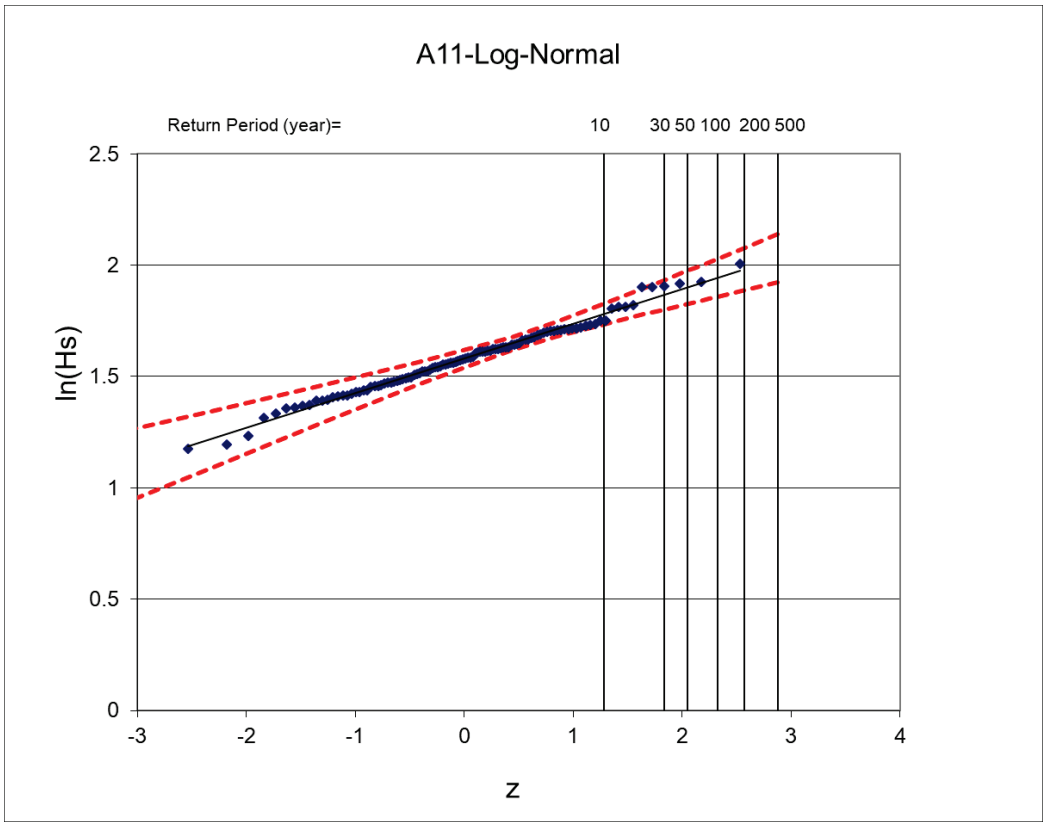

Figure 42. Extreme wave statistics results for A10 and A11

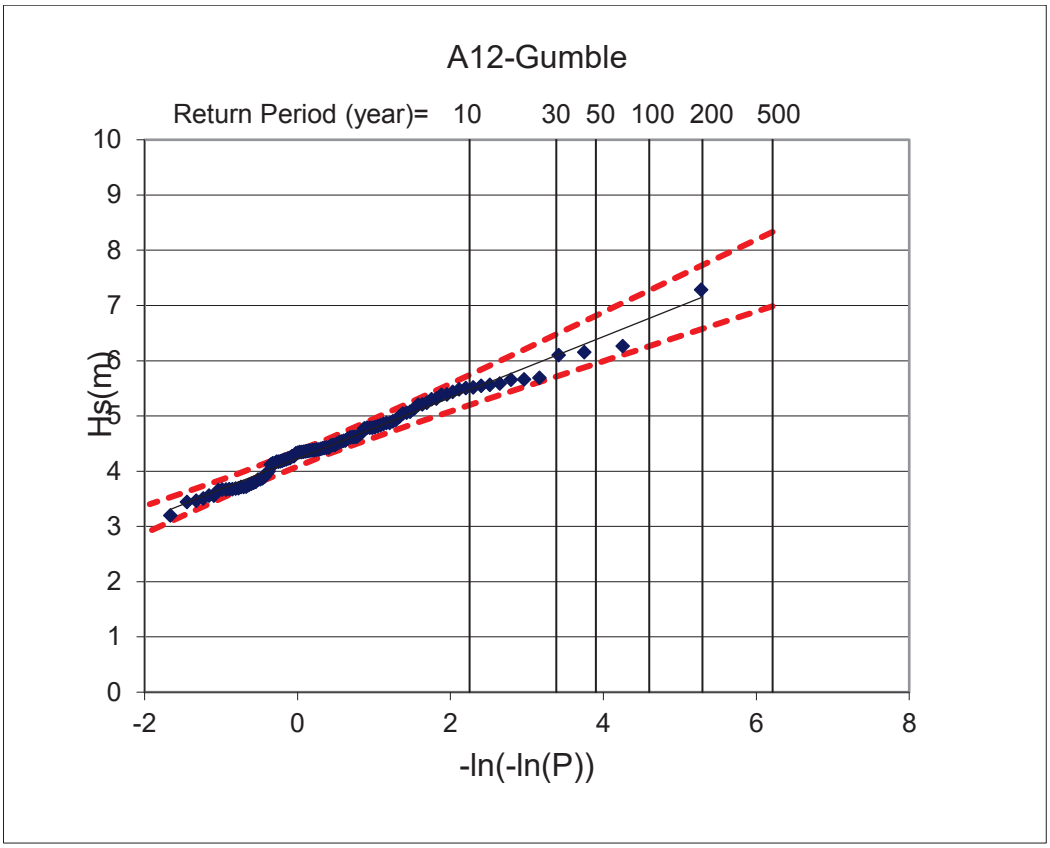

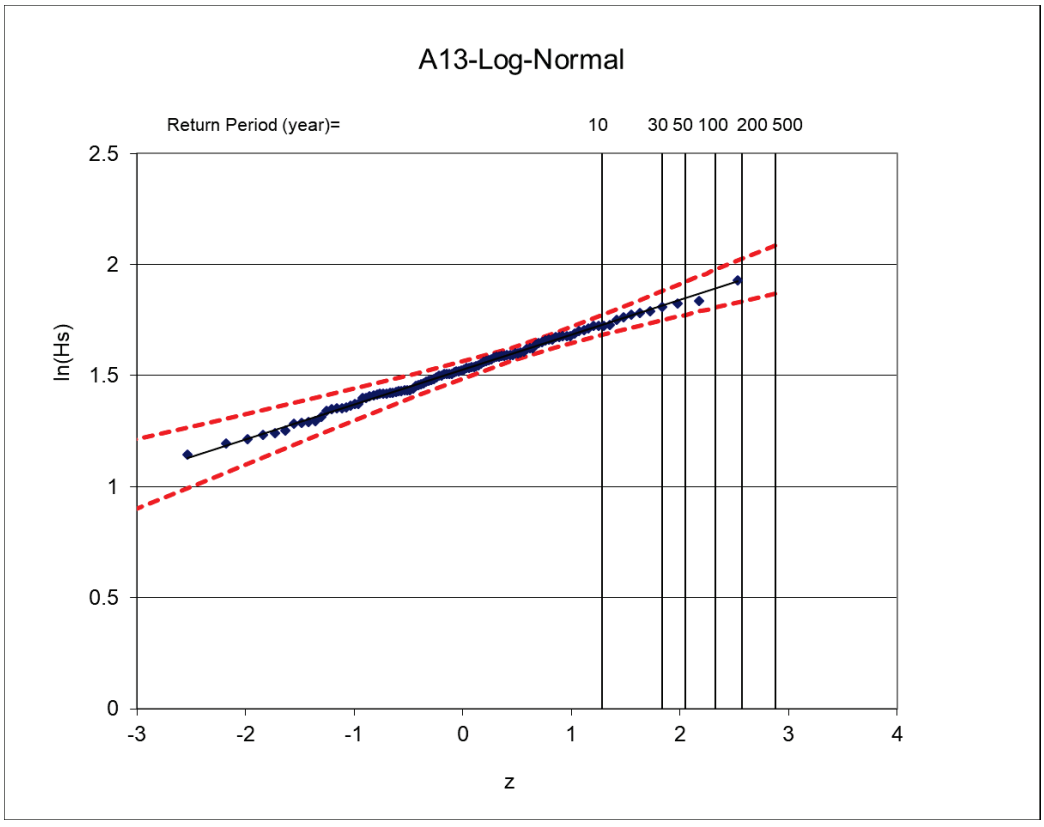

Figure 43. Extreme wave statistics results for A12 and A13

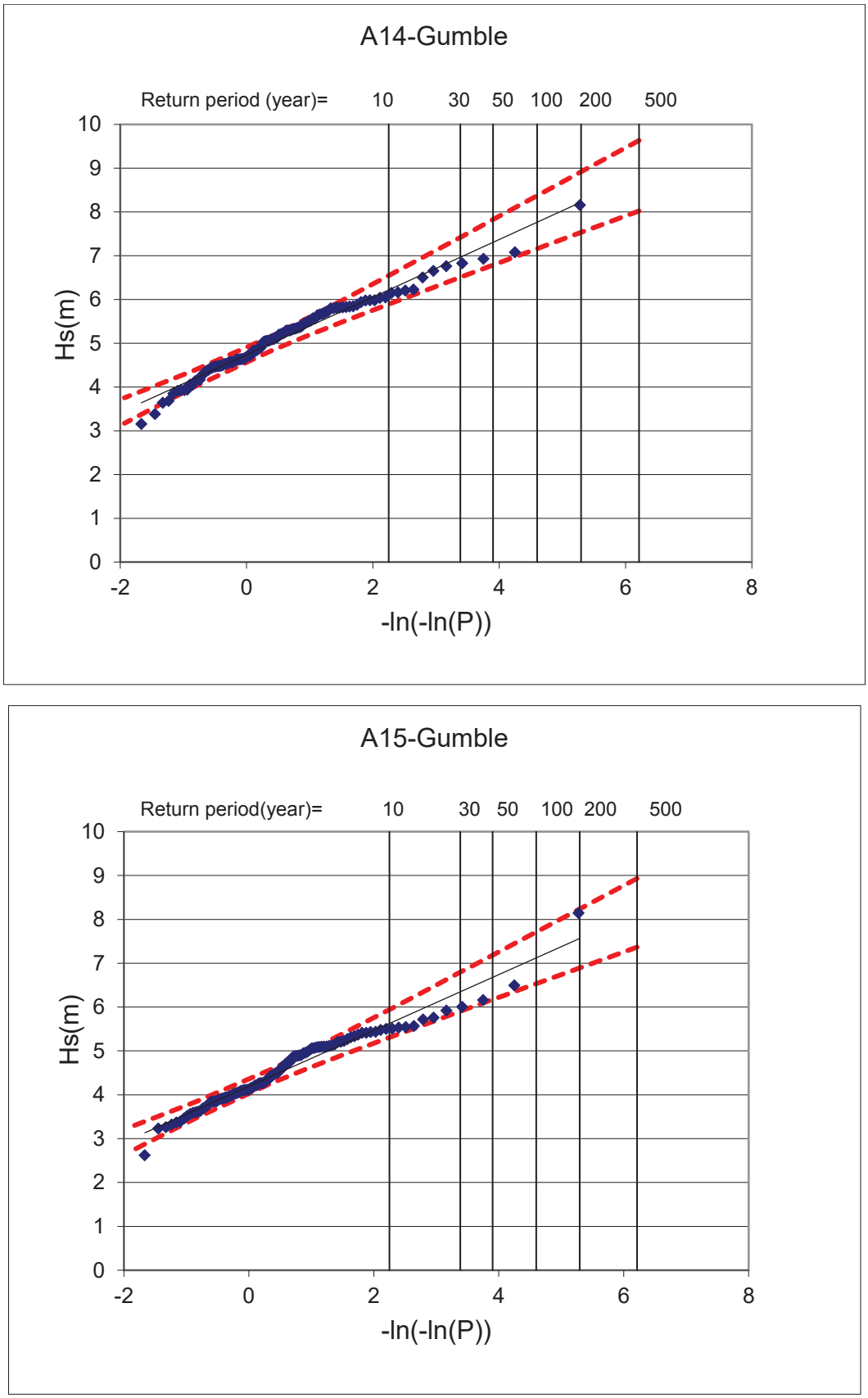

Figure 44. Extreme wave statistics results for A14 and A15

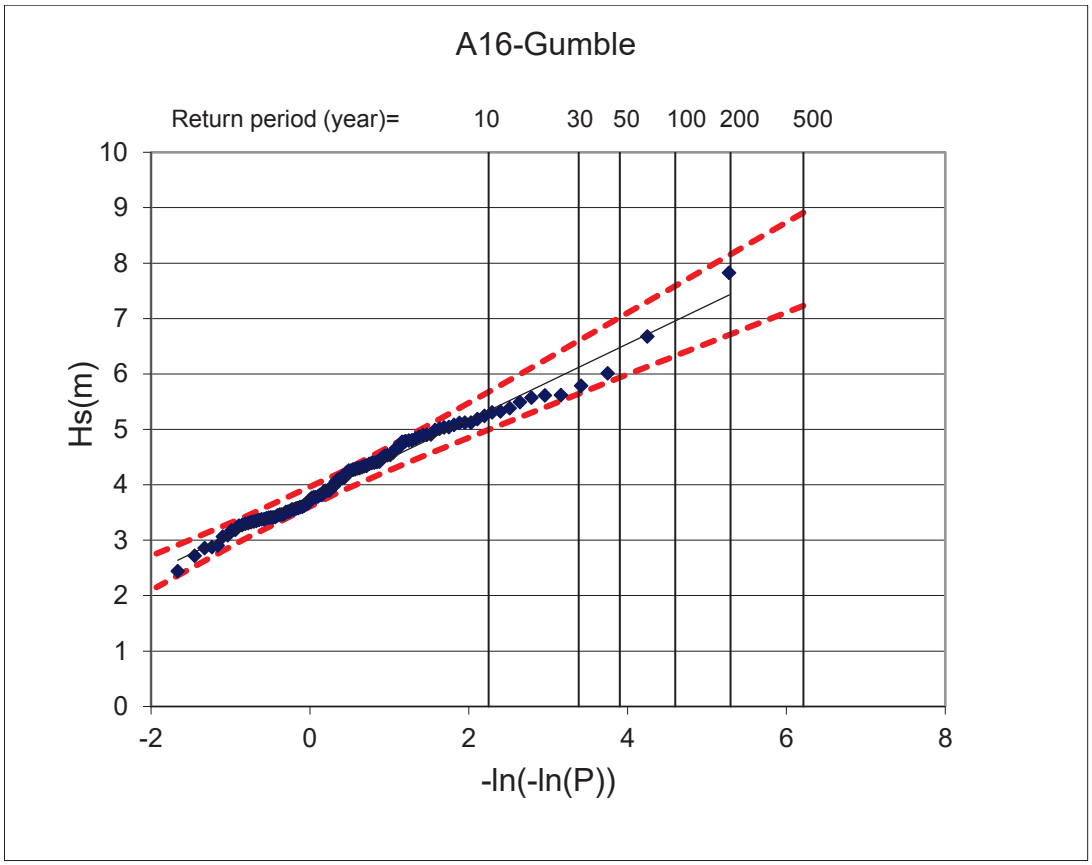

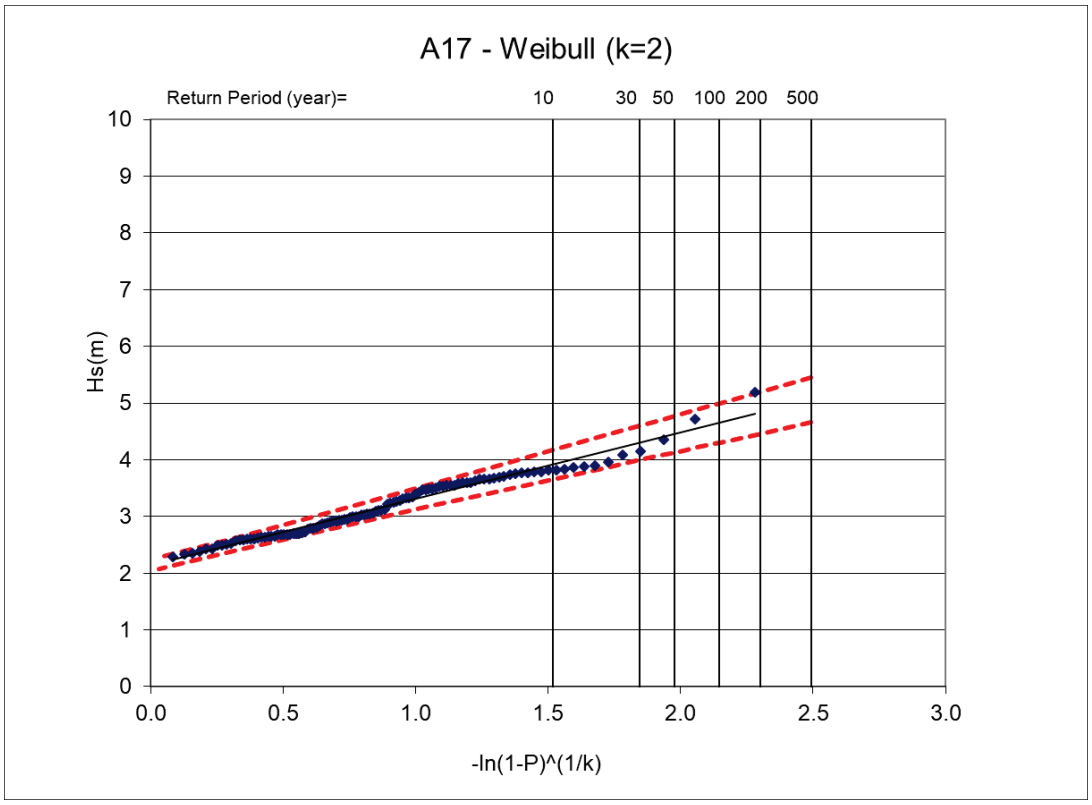

Figure 45. Extreme wave statistics results for A16 and A17

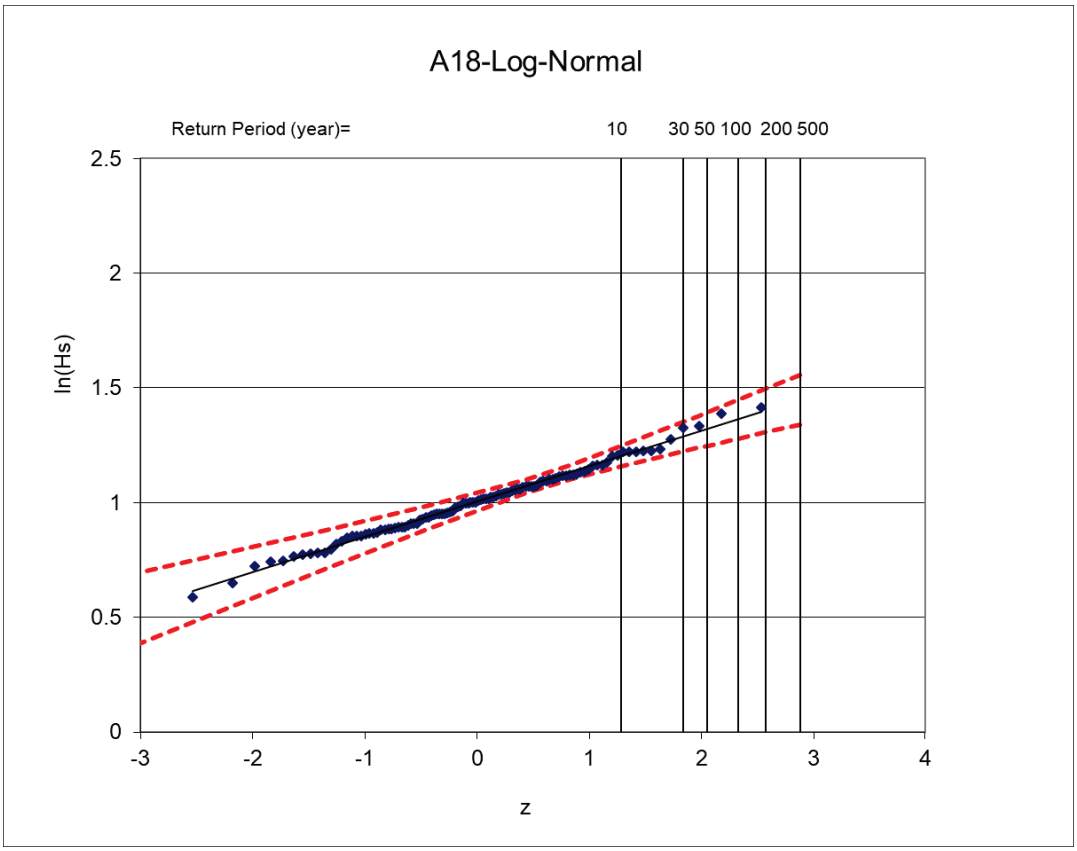

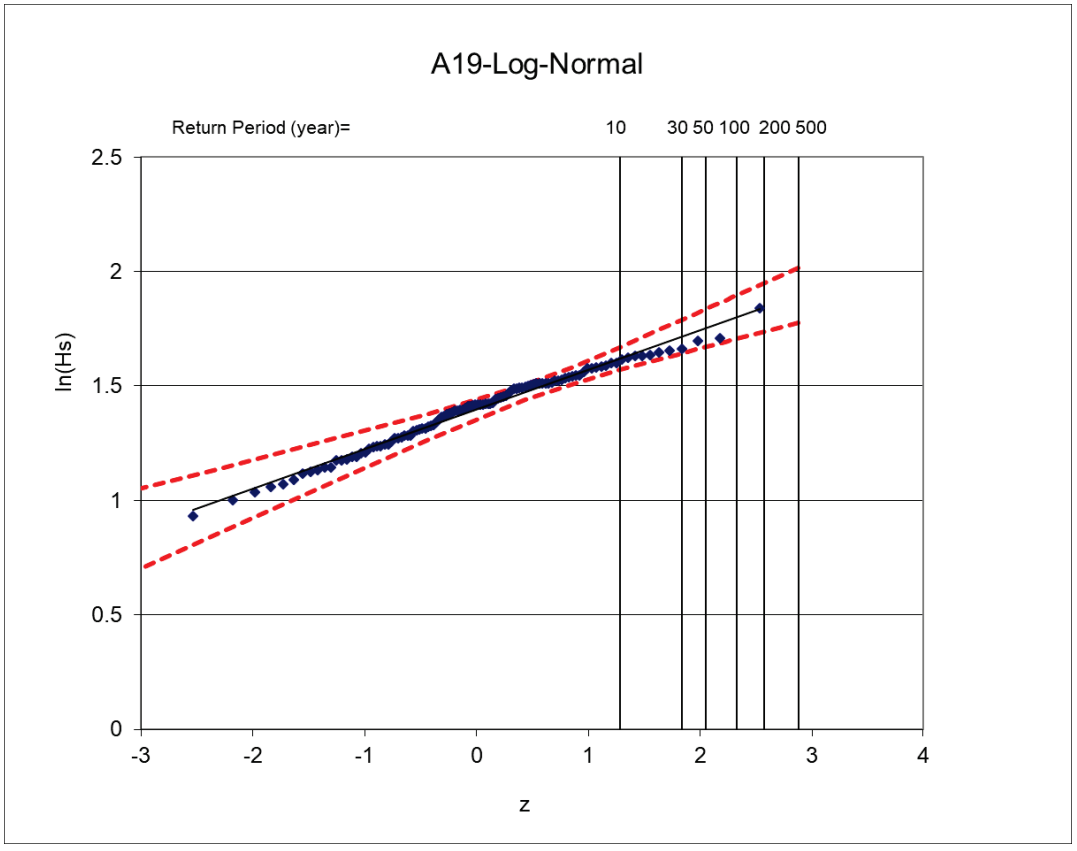

Figure 46. Extreme wave statistics results for A18 and A19

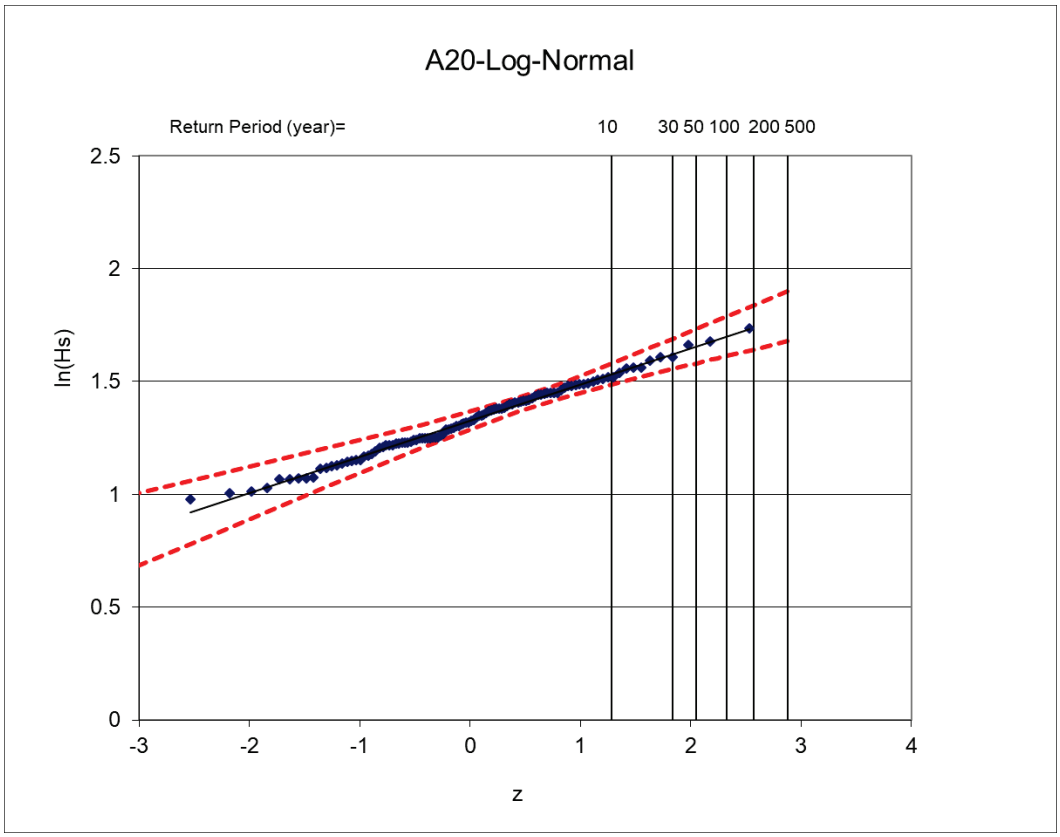

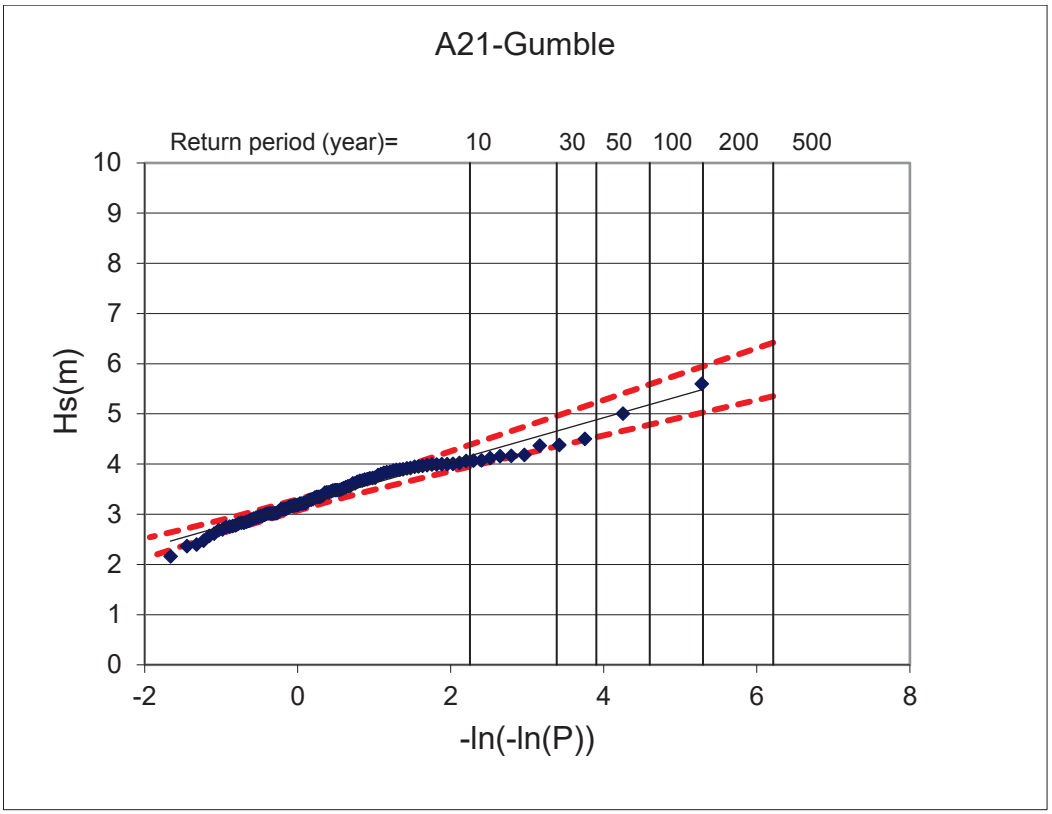

Figure 47. Extreme wave statistics results for A20 and A21

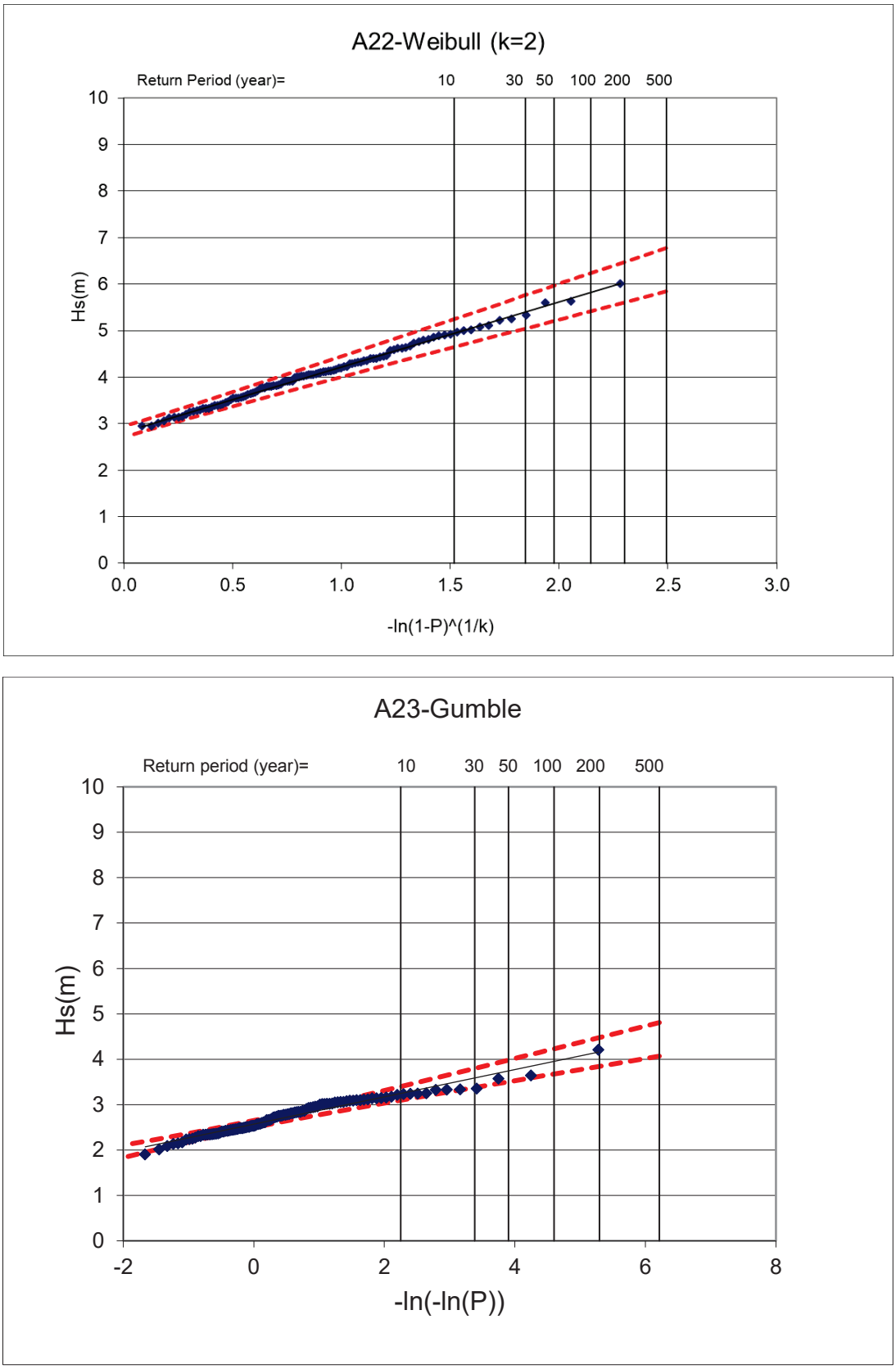

Figure 48. Extreme wave statistics results for A22 and A23

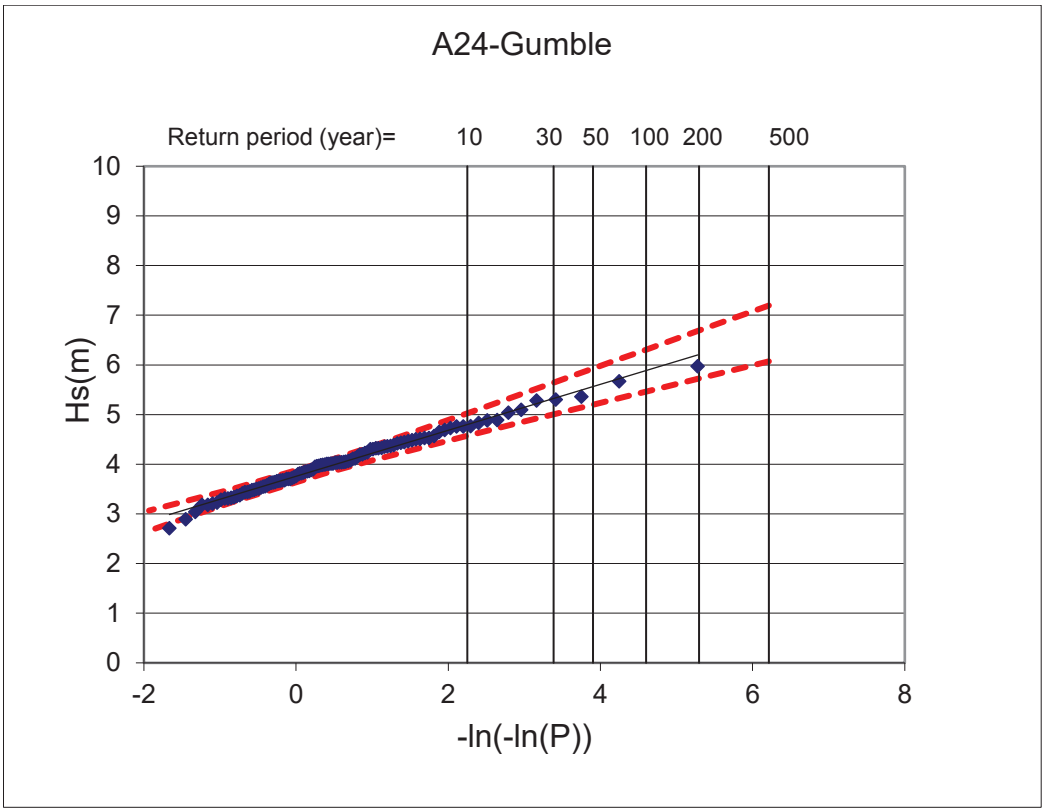

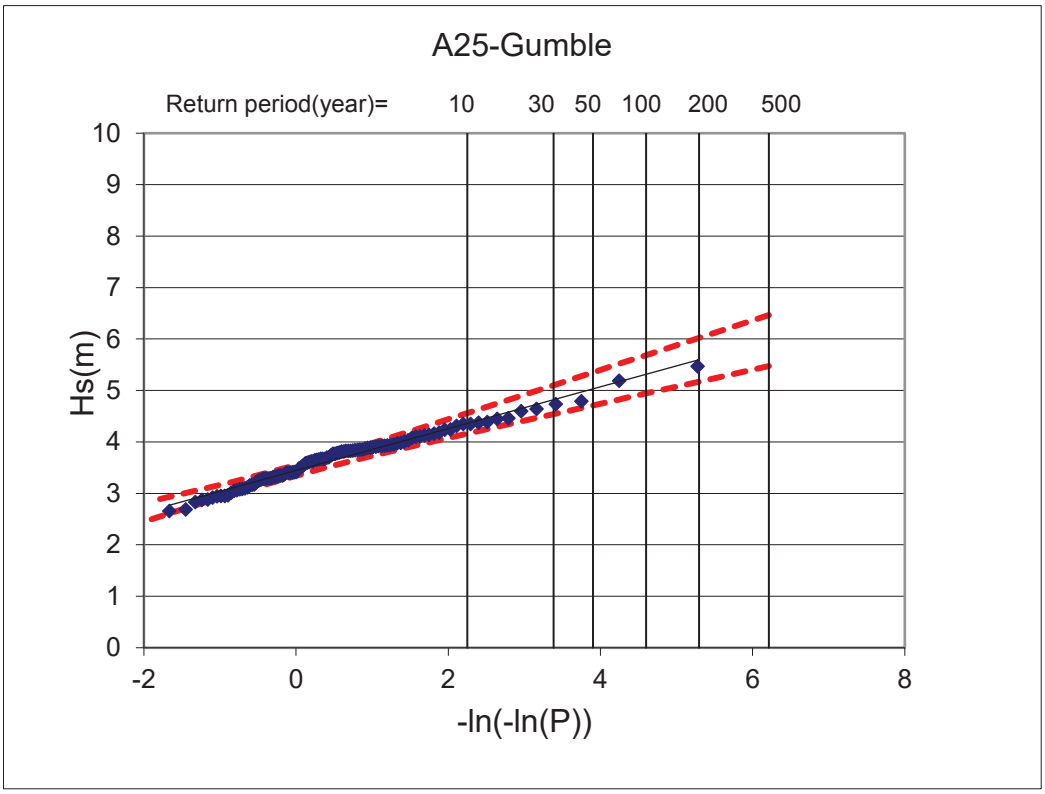

Figure 49. Extreme wave statistics results for A24 and A25

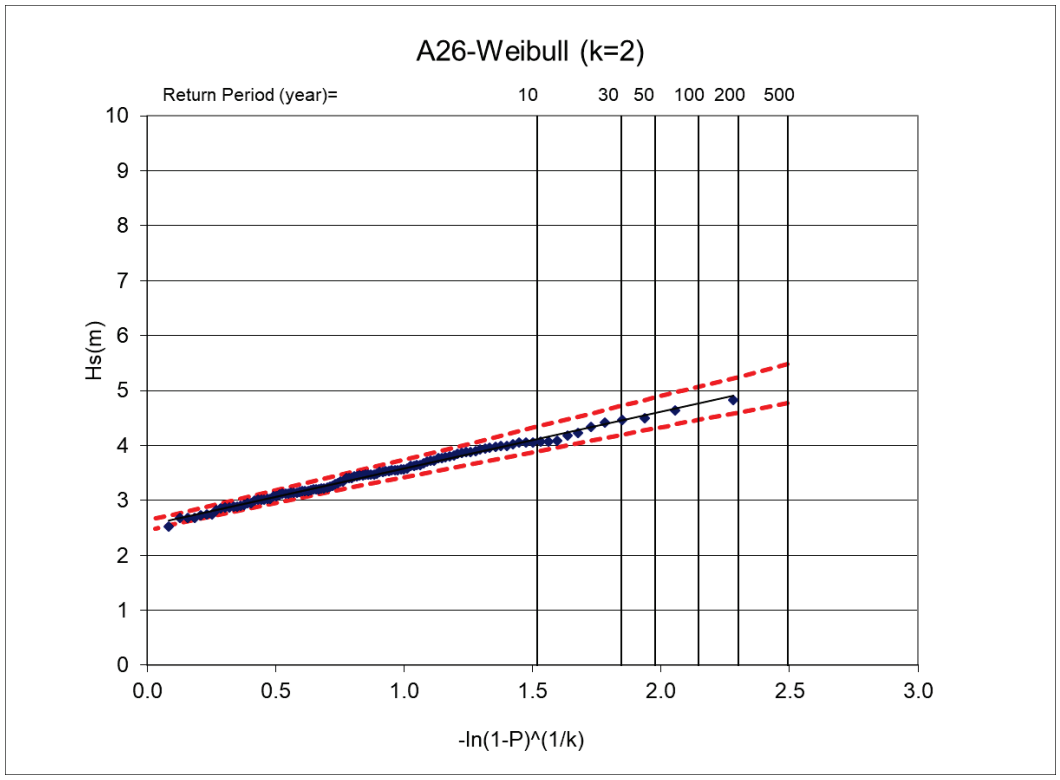

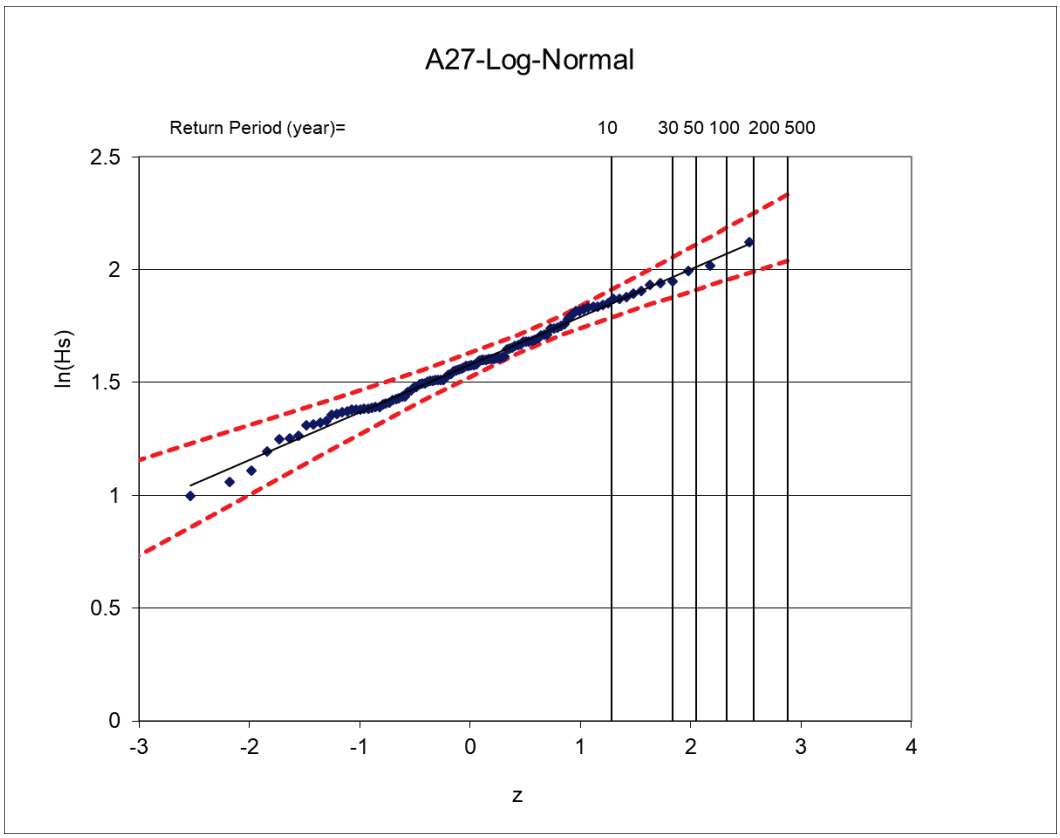

Figure 50. Extreme wave statistics results for A26 and A27

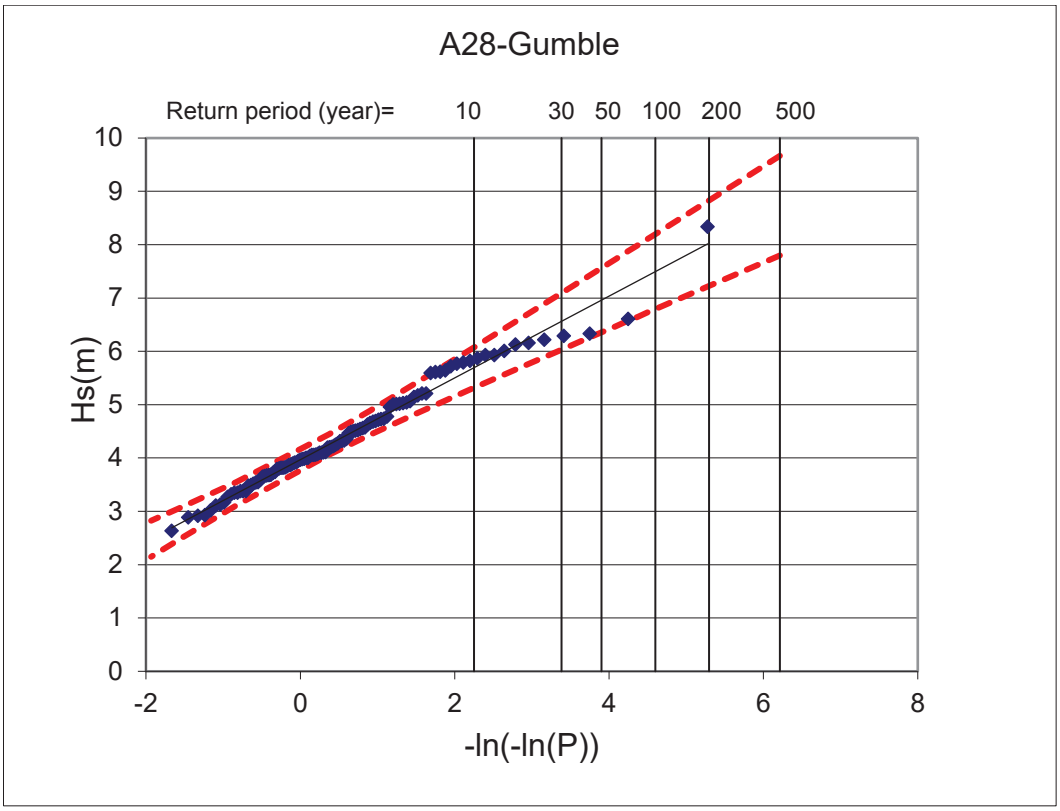

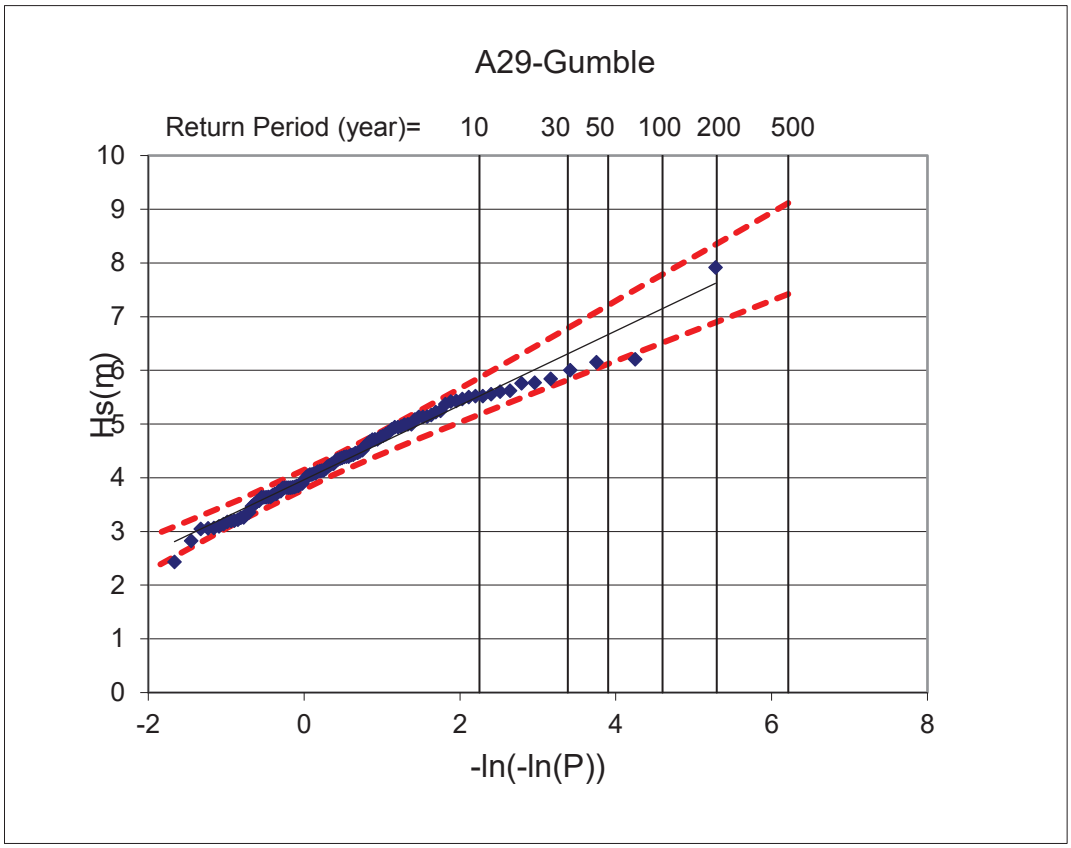

Figure 51. Extreme wave statistics results for A28 and A29

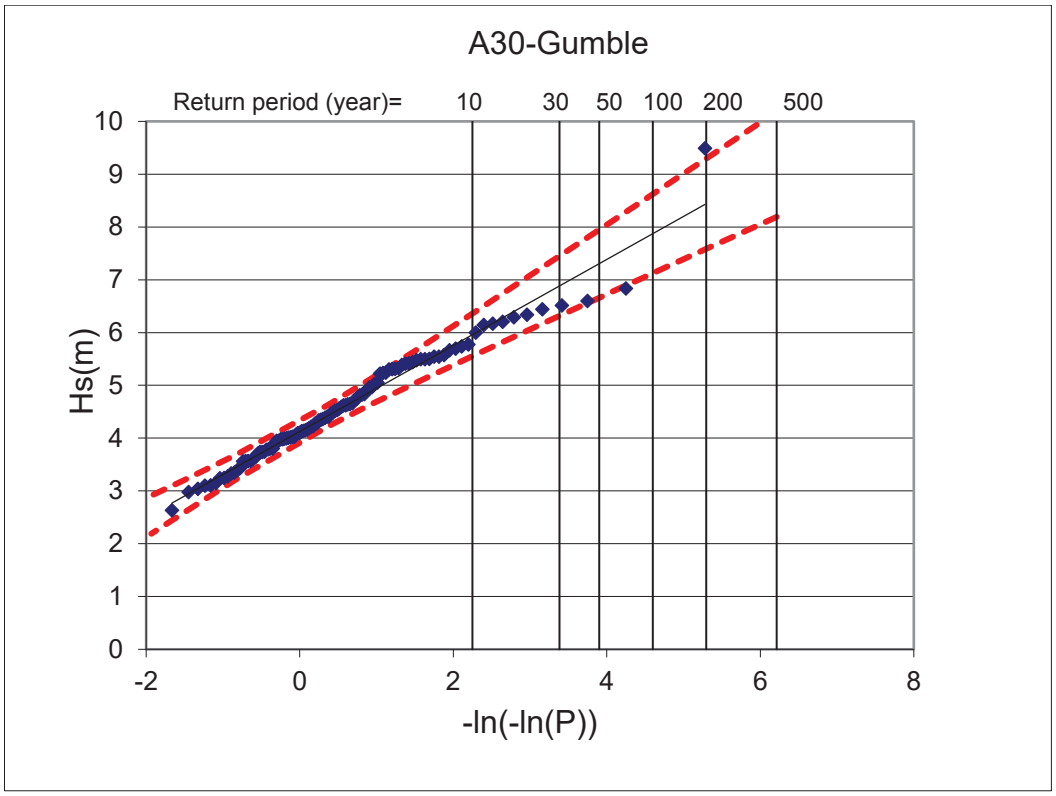

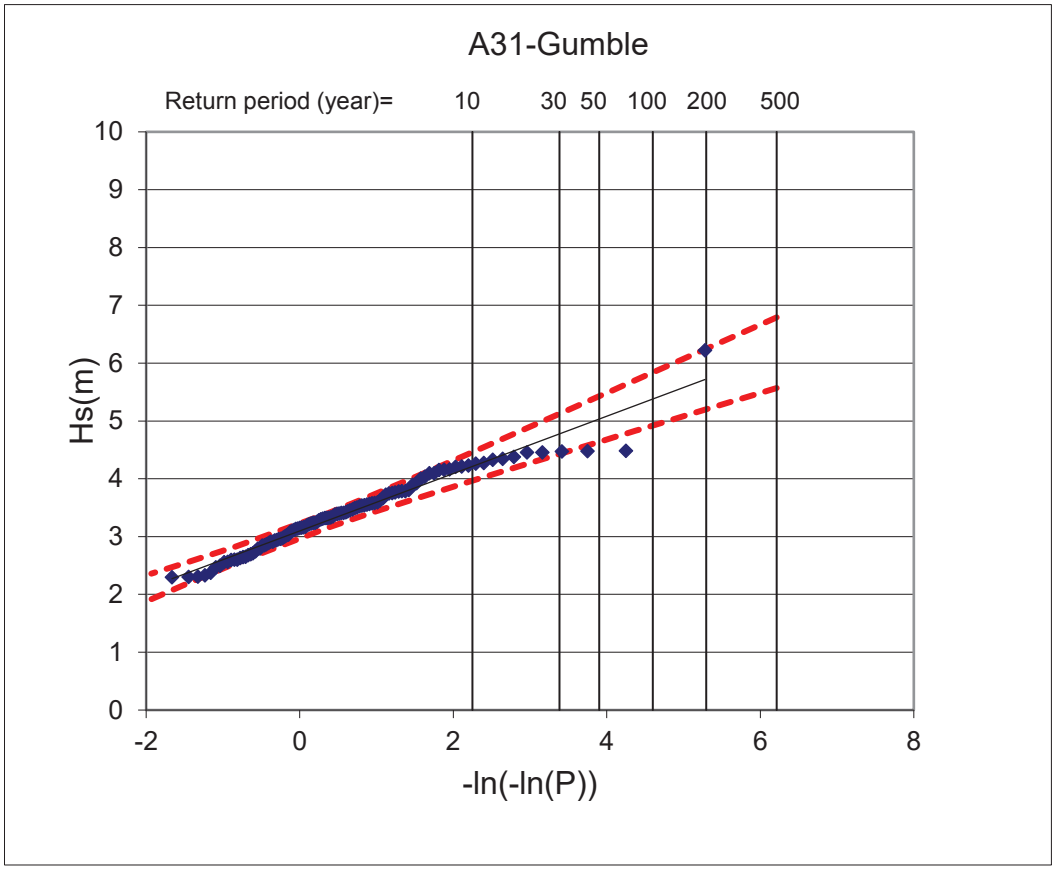

Figure 52. Extreme wave statistics results for A30 and A31

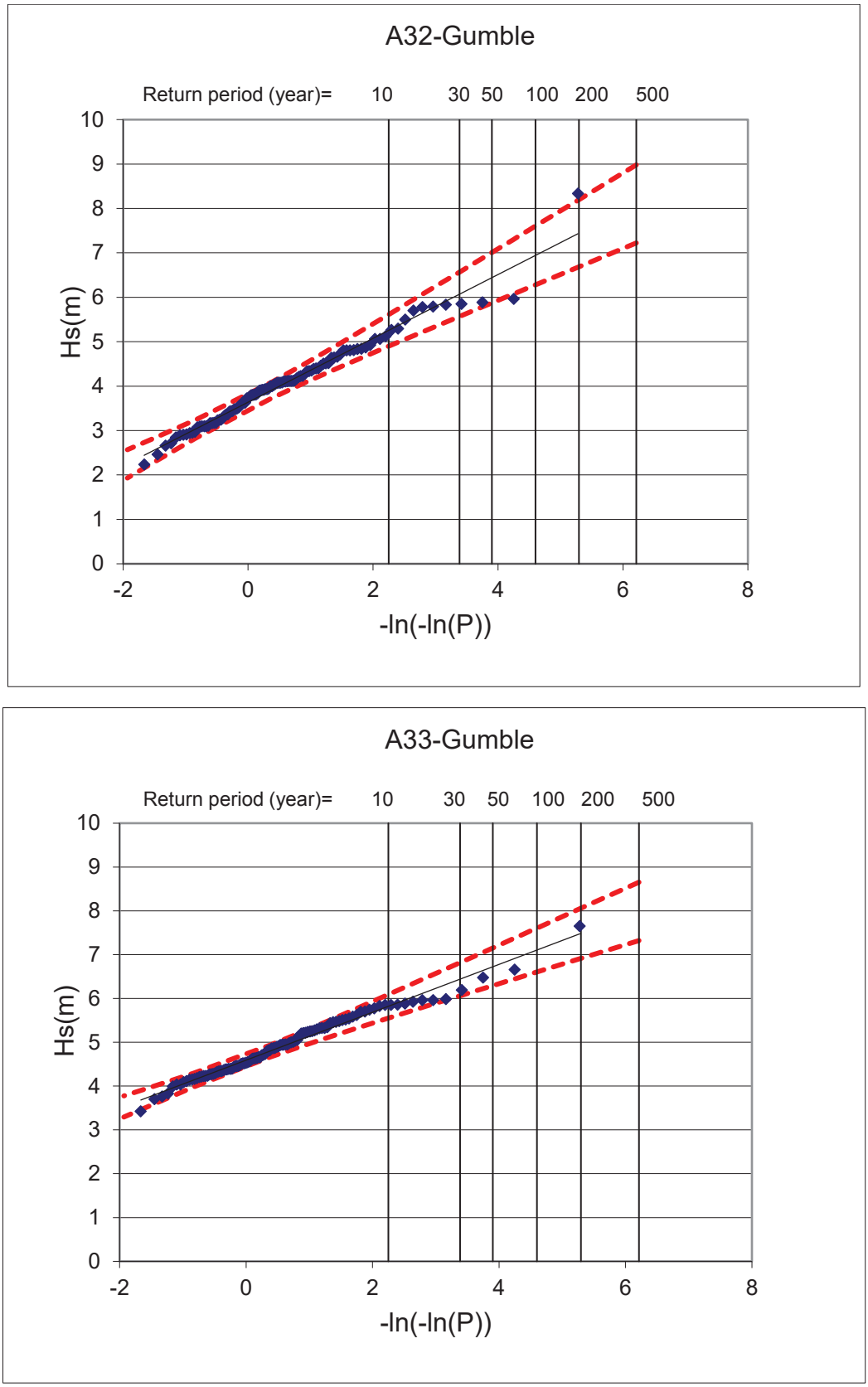

Figure 53. Extreme wave statistics results for A32 and A33

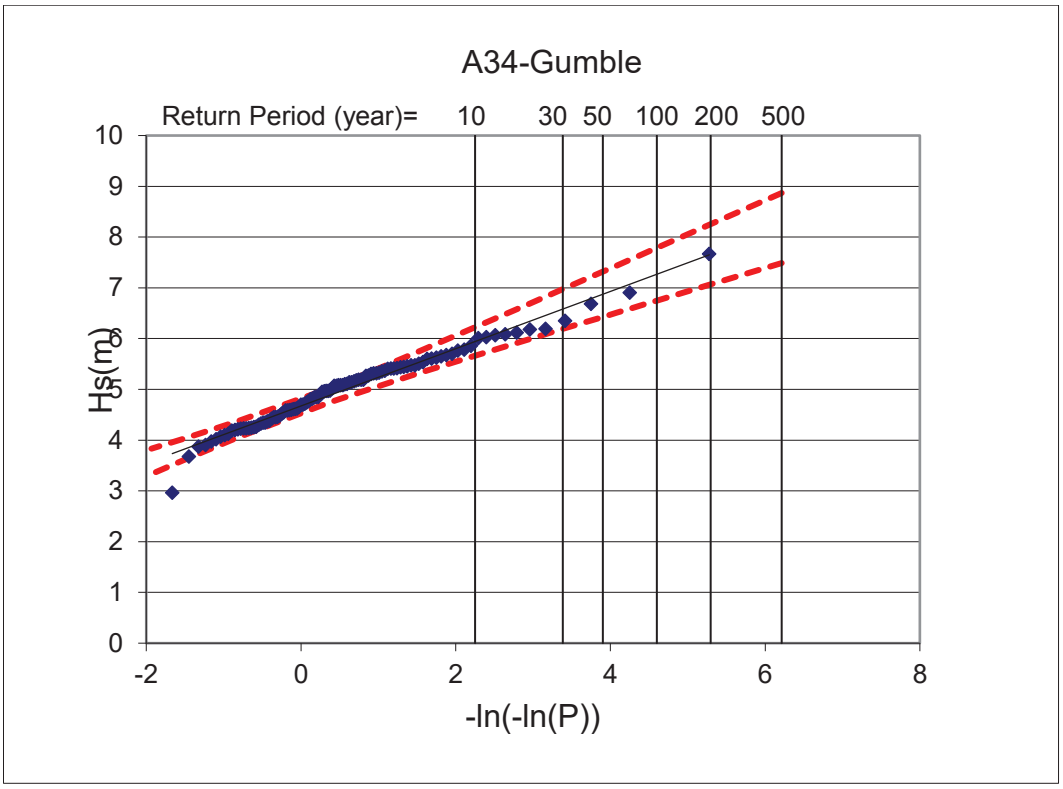

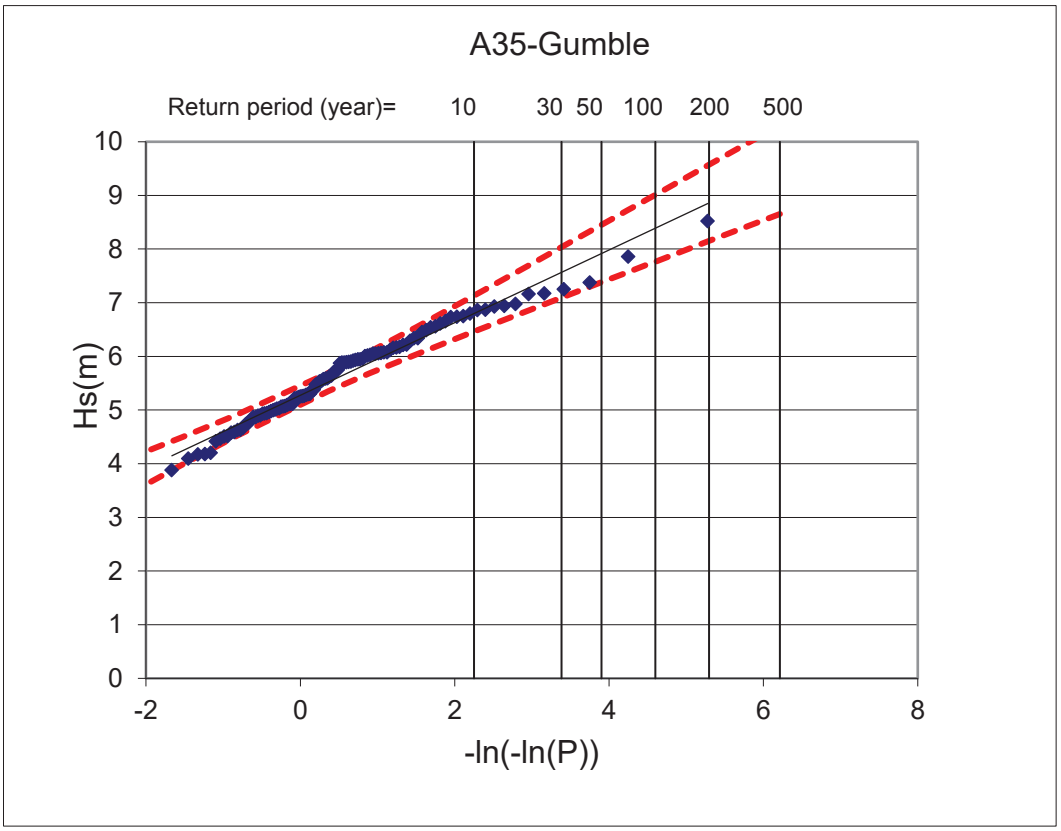

Figure 54. Extreme wave statistics results for A34 and A35

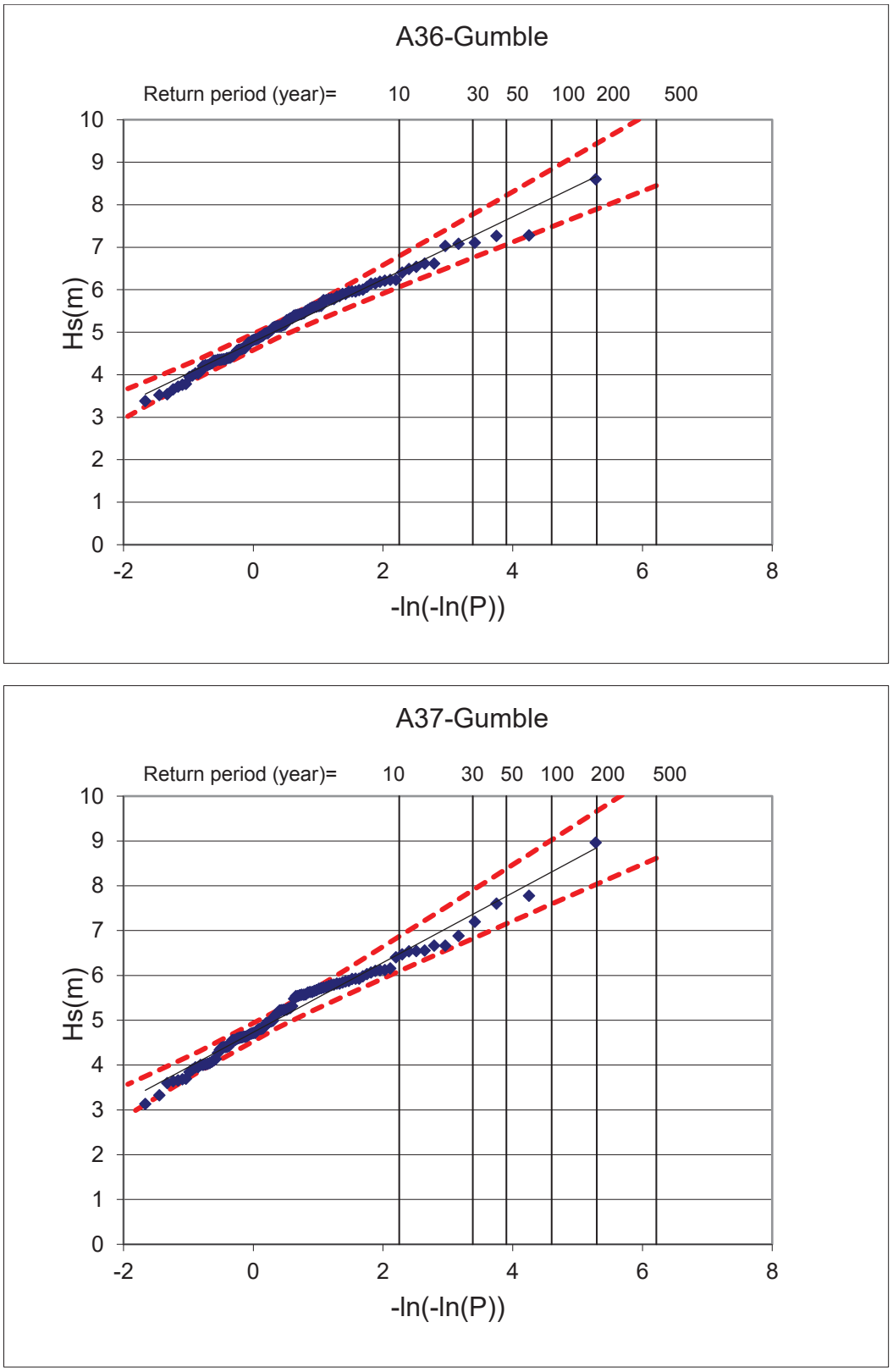

Figure 55. Extreme wave statistics results for A36 and A37

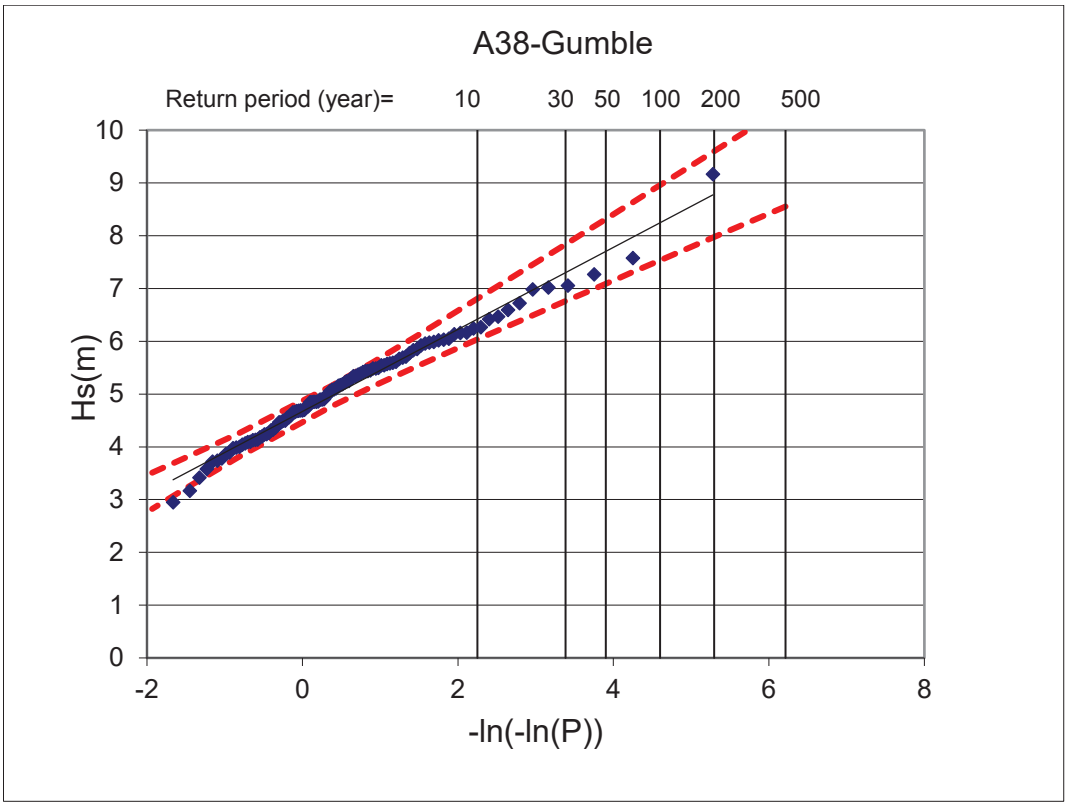

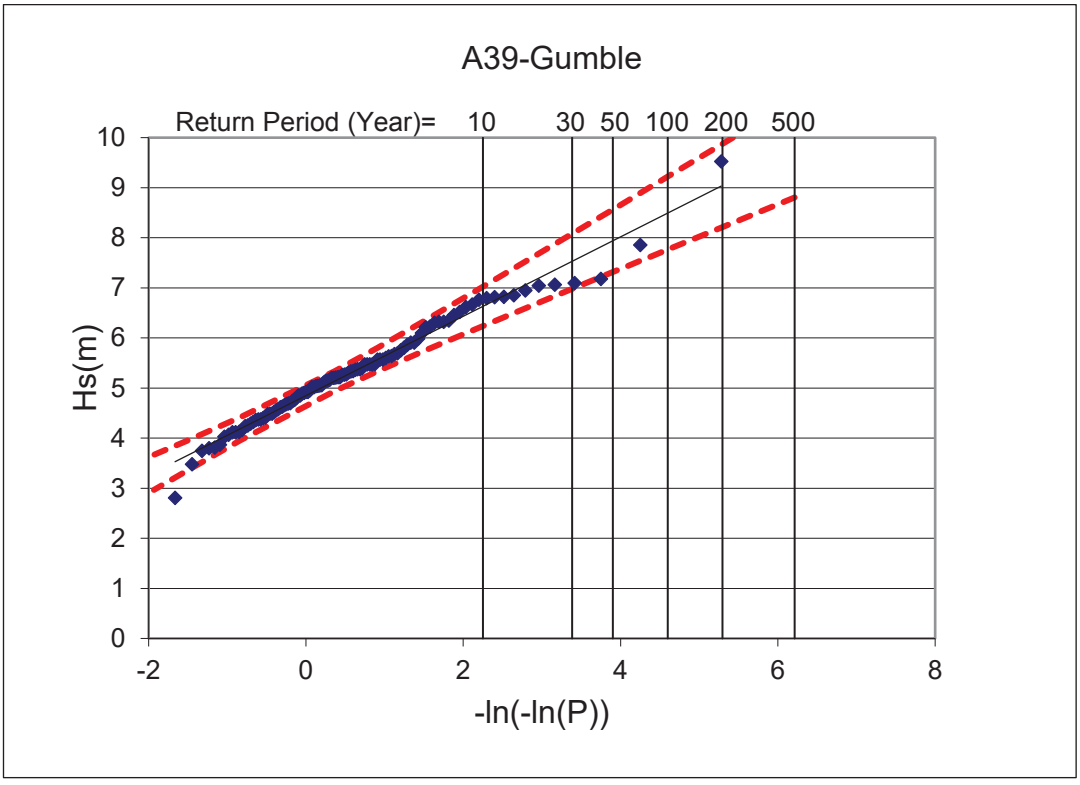

Figure 56. Extreme wave statistics results for A38 and A39

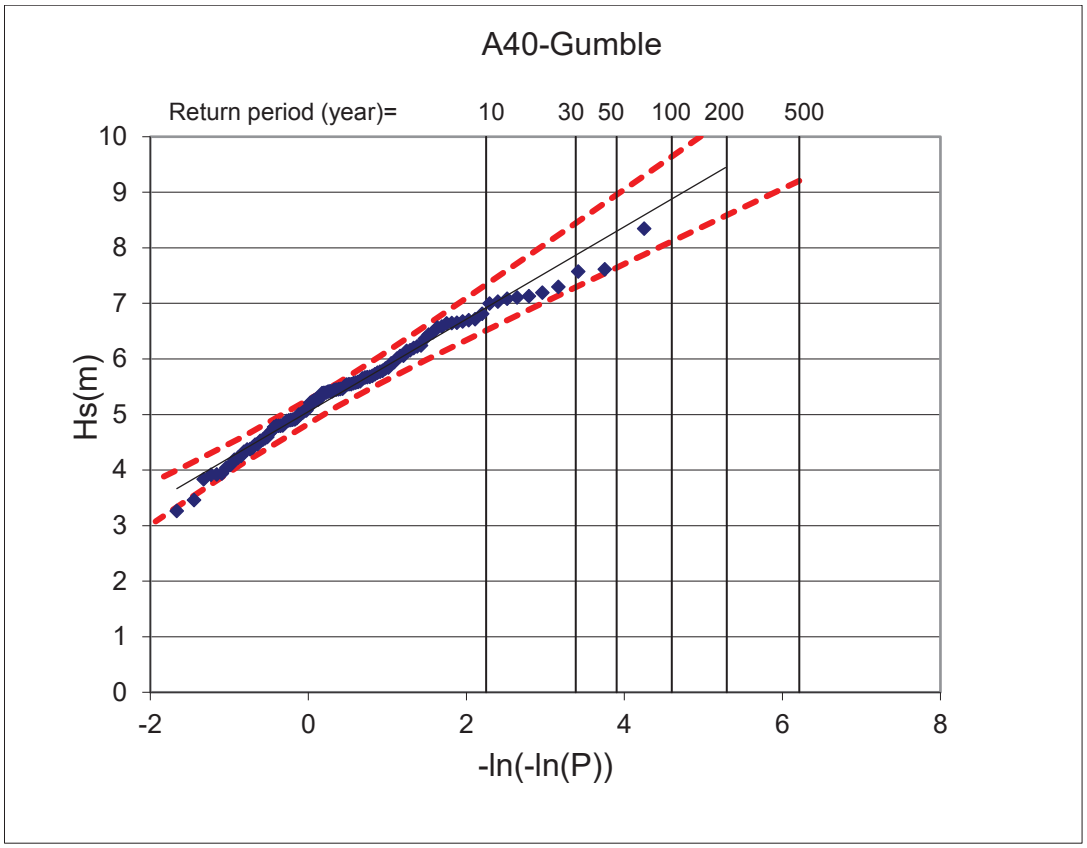

Figure 57. Extreme wave statistics results for A40